Isolation, Structure Characterization and Cytotoxicity Assessment of Alkaloids from *Ficus fistulosa* var. *tengerenisis (Miq.) Kuntze*

A THESIS SUBMITTED IN FULFILMENT OF THE

REQUIRMENTS FOR THE DEGREE OF

MASTER OF PHILOSOPHY

FACULTY OF SCIENCE

SCHOOL OF PHARMACY

UNIVERSITY OF NOTTINGHAM MALAYSIAN CAMPUS

2017

BY

AMJAD AYAD QATRAN AL-KHDHAIRAWI

ACKNOWLEDGEMENTS

First and foremost, I would like to express my most sincere gratitude to my supervisor, Dr. Lim Kuan Hon, for his patience, motivation and enthusiasm throughout the course of this research and the time of writing this thesis. His guidance made this project a success and as a postgraduate researcher I could not have wished for a better advisor and mentor.

This research would have been impossible without the aid and support of my senior colleague, Premanad Krishnan, and the rest of my fellow friends and colleagues in the natural products research group, namely Margret Chinoso Ezeoke, Lee Fong Kai, Cho Eun Seon and Chan Zi Yang. I want to thank each one of them for providing a supportive and friendly working environment. The assistance from the staff at the Faculty of Science, University of Nottingham Malaysian Campus is also greatly appreciated.

I would also like to thank Dr. Low Yun Yee and Miss Dawn Sim form Department of Chemistry, University of Malaya for performing the required NMR and X-ray diffraction experiments for many of my fractions and compounds. I would like to express my appreciation to Dr. Mai Chun Wai and Prof. Leong Chee Onn from School of Pharmacy, International Medical University for carrying out the biological assay reported in this thesis.

My sincere thanks also go to my two brothers and my sister for always being there when I need them. Last but not least, I would like to extend my deepest gratitude to my parents, for having faith in me and for their invaluable support emotionally and financially. Without them, I would not have been able to get such an amazing opportunity to pursue higher education in a foreign country.

ABSTRACT

The alkaloidal content from the leaves of a local Malaysian plant, *Ficus fistulosa* var. *tengerensis* (Miq.) Kuntze was investigated following a preliminary screening which revealed the presence of alkaloids in the plant. However, the bark material was devoid of alkaloids and was thus not investigated. The leaves of *F. fistulosa* var. *tengerensis* were collected in large scale, dried, ground and extracted with 95% ethanol. Acid-base treatment of the ethanolic crude extract followed by numerous chromatographic processes resulted in the isolation of five alkaloids. The pure alkaloids were subjected to spectroscopic analysis (NMR, UV, IR, X-ray and ECD) for structure elucidation. Of the five alkaloids isolated, two were novel alkaloids, namely, (±)-tengerensine (**1**) and (±)-tengechlorenine (**2**). (±)-Tengerensine (**1**), was isolated as a pair of racemic enantiomers and they represent a pair of rare unsymmetrical cyclobutane dimers and the first dimeric benzopyrroloisoquinoline alkaloids to be discovered. (±)-Tengechlorenine (**2**), was isolated as a scalemic mixture with a slight excess of the dextrorotatory enantiomer. (±)-Tengechlorenine (**2**) represents the first chlorinated phenanthroindolizidine alkaloid to be isolated. In addition to the two new alkaloids, three known alkaloids were also isolated and characterized, *viz.*, (±)-fistulosine (**3**) a benzopyrroloisoquinoline alkaloid, (*S*)-(+)-antofine (**4**) a phenanthroindolizidine alkaloid, and (*R*)-(–)-*seco*antofine (**5**) a septicine-type alkaloid. *In vitro* antiproliferation assay was carried out on alkaloids (±)-**1**, (+)-**1**, (–)-**1** and **3** on a small panel of breast cancer and normal cell lines, including MCF-7, MDA-MB-231 and MDA-MB-468 (human breast adenocarcinoma cells), and MCF-10A (non-tumorigenic breast epithelial cell breast epithelial cells). (+)-Tengerensine **1** was found to display a selective cytotoxic effect against MDA-MB-468 cells (IC_{50} 7.4 μM), while (±)-**1**, (–)-**1** and **3** were found to be generally ineffective against all the cell lines tested.

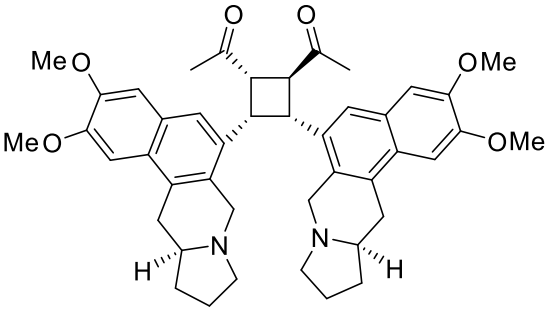

(±)-Tengerensine (**1**)

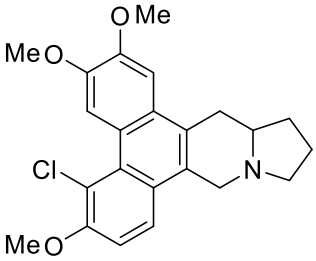

(±)-Tengechlorenine (**2**)

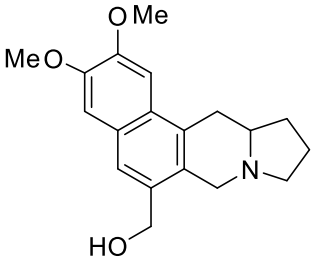

(±)-Fistulosine (**3**)

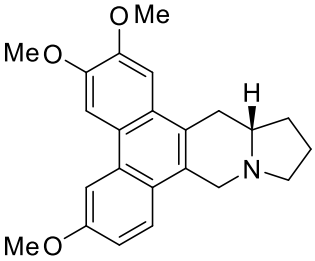

(*S*)-(+)-Antofine (**4**)

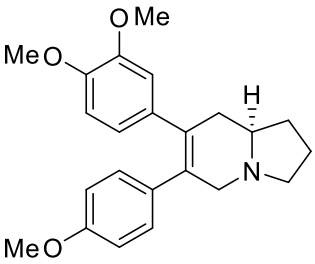

(*R*)-(–)-Seco-antofine (**5**)

Table of Contents

Chapter One

Introduction

1.1 Natural Products and Drugs Discovery

Drugs of plant origin have been around since the beginning of recorded history. Ancient civilizations are known for their use of plants to make medical remedies. The oldest known written evidence for the use of plants as medicines is approximately 5000 years old.[1] It was found on a Sumerian clay slab near Nagpur based in modern day Iraq. Twelve remedies were made by combining over 250 various plants, some of which contain alkaloids, such as *Hyoscyamus niger, Mandarke mandragora* and *Papaver somniferum.*[2]

Emperor Shen Nung "the father of Chinese medicine" wrote a similar book in *ca*. 2500 BC. The Chinese book of roots and grasses "Pen T'sao" contains about 365 different formulations, many of which are still used today including; ginseng, jimson weed, cinnamon and ephedra.[3,4]

Like other ancient civilizations the ancient Egyptians were known for their medicine and pharmacology and they documented the use of plants as drugs. The Ebers Papyrus has more than 800 remedies of 700 different plant species such as castor oil, aloe, senna, garlic, fig and onion.[5] Other ancient Egyptian known texts include the Edwin Smith Papyrus (1800 BC), the Hearst Papyrus (1600 BC) and the London Medical Papyrus (1300 BC).

Greeks developed the use of medicinal plants and herbs. Theophrastus (c*a*. 300 BC) studied the pharmacology of plants, and wrote one of the most important books of ancient natural history "Historia Plantarum" or "history of plants". In this book, Theophrastus studied the anatomy of plants along with their pharmacological use. Another influential western scientist is Dioscorides, who is arguably the most prominent writer of ancient medicinal plants and the father of pharmacognosy. He studied plants and herbs as he travelled with the Roman army in the "known world" around 75 AD and wrote his famous book "De Materia Medica" containing over 900 plant medical formulations along with detailed description of the plant's appearance, distribution, cultivation, preparation and pharmacological use. Galen (130–200 AD), a Roman physician, pharmacist, surgeon and philosopher, published at least 30 books on the subjects of anatomy, physiology and neurology.

Much of the Greco-Roman medicine knowledge was lost during the Middle Ages, but the Arab and the Islamic scholars in Andalusia and the Middle East managed to save and upgrade most of the expertise of that era. They improved it by adding their own sources and knowledge of their local

plants together with the knowledge of Indian and Chinese medicine. Arabs were also the first in history to have private drug stores regulated by the state, where formulations and remedies were sold directly to patients. It was around that Islamic golden age where pharmacy flourished and advanced as a science.

This advancement in medicine took place between the 9th and 12th centuries, after which the renaissance era started and science began to be studied and developed more in the western world (after the fall of the Caliphate Empire in the Middle East). For thousands of years the crude extracts of plants were used to treat ailments. This was the case until early 19th century when pharmaceutical companies started to commercially sell pure naturally derived compounds as medicines.[6] The past 200 years had witnessed the discovery, isolation and structure elucidation of thousands of natural products, of which, hundreds were found to possess tremendous biological activities, and made it to the pharmaceutical market for medical use.[7] For instance, the first natural product to be isolated and used commercially was morphine (**6**) (potent analgesic) discovered by the German pharmacist Friedrich Sertürner from *Papaver somniferum*.[8]

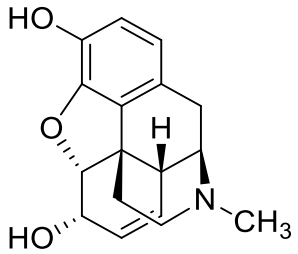

6

Useful biological activity in organic molecules is considered as a rare property. Therefore, no chemist can predict whether any randomly given molecule possess any biological activity. Thus, screening as much structures as possible is the only way to determine whether molecules have an effect on biological systems or not.[9] The extraction of pure natural products and then subjecting them to biological assay became the standard process for drug discovery in the early 20th century. In the year 1928 the first true antibiotic penicillin (**7**) was extracted from the fungus *Penicillium notatum* by the Scottish pharmacologist Alexander Fleming.[7] This discovery revolutionized medicine and the treatment of bacterial infection in the 1940s.[7,10] Pharmaceutical companies then continued their pursue of antibacterial agents discovery from natural sources and managed to discover streptomycin

(**8**), gentamicin (**9**) and tetracycline (**10**) in the following years.[7] After the discovery of penicillin and other antibiotics of natural origin, natural products were the main research focus of big pharmaceutical companies.

The focus was not limited to anti-infective agents but also expanded to other pharmacological targets. In the 1970s, mevastatin (**11**) was isolated from the fungus *Penicillium citrinum* which led to the establishment of the statin group as an extremely effective antihyperlipidemic agents that work by inhibiting cholesterol biosynthesis and is still used today.[11]

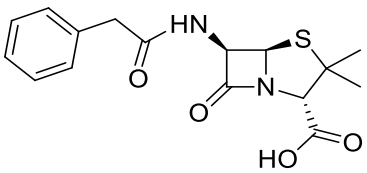

7

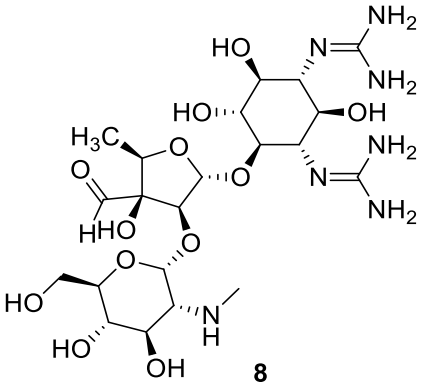

8

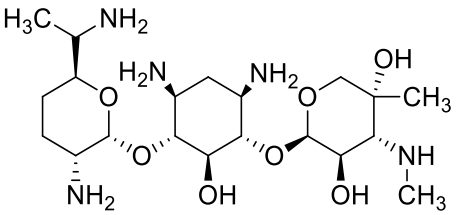

9

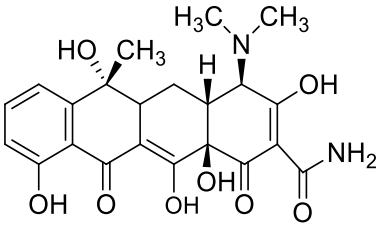

10

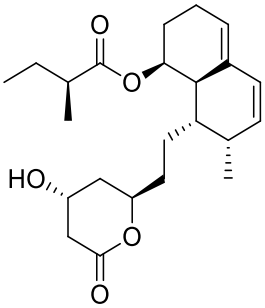

11

During the 1980s about 62% of antineoplastic agents approved were natural products or related to natural products in some ways. In some cases, the original lead compound exhibited high toxicity profile and chemists had to modify parts of the structure to arrive at a more tolerated semi-synthetic compound that can be used as a drug.[11] Good examples of effective natural products for the treatment of cancer are the vinca alkaloids, vinblastine (**12**) and vincristine (**13**). Simple modifications of these new alkaloids gave the synthetic analogue, vinorelbine (**14**), which was approved for use shortly after.[11, 7]

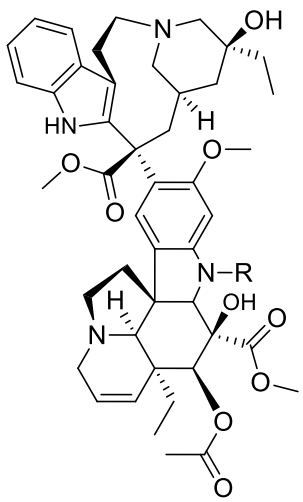

12 R = Me
14 R = CHO

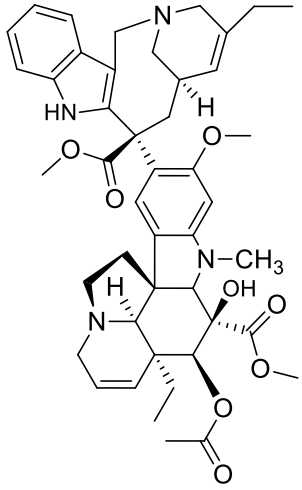

13

Before the beginning of the 1990s drug discovery was a serendipitous process where scientists usually used whole extracts or pure compounds and screened them for biological activity without thorough understanding of their molecular biological target (mechanism of action). This process was called phenotypic drug discovery or classical pharmacology.[12, 13]

Recent advancement in the sequencing of the human genome led to a rapid cloning and synthesis of purified proteins. New techniques were developed to use the isolated synthesized protein targets. High-throughput screening where millions of compounds are tested on a specific protein target for receptor/ligand chemical interaction is practiced by big pharmaceutical companies. Candidates that show a promising affinity to a target are then modified for maximum affinity minimum toxic profile

and then tested *in vivo* on animal and then onto human clinical trials.[12,11,14] This new approach is known as target based drug discovery or reverse pharmacology (Figure 1.1).[12,14]

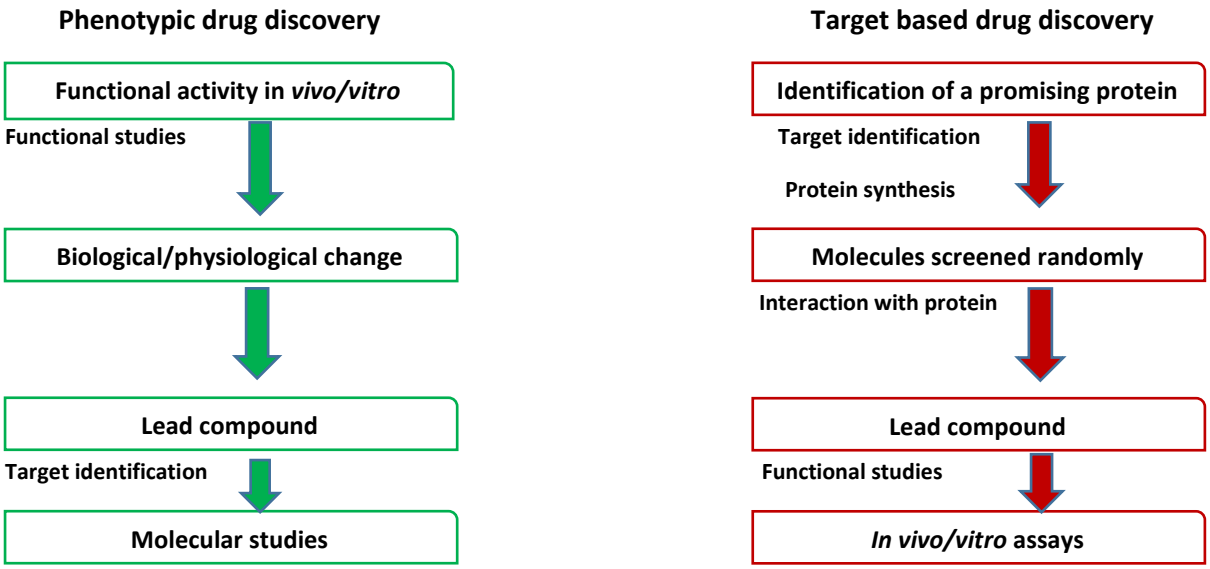

Figure 1.1 - Comparison between classical and reverse pharmacology

The new drug discovery approach however did not inhibit natural products research and the discovery of new lead compounds of natural origin. A study that examined all new approved drugs from 1981 to 2014 found that a total number of 1211 new drugs were approved worldwide, of which 320 drugs were natural products or their derivatives. That is 32.7% of all medicines approved for the past three decades (see Figure 1.2).[15]

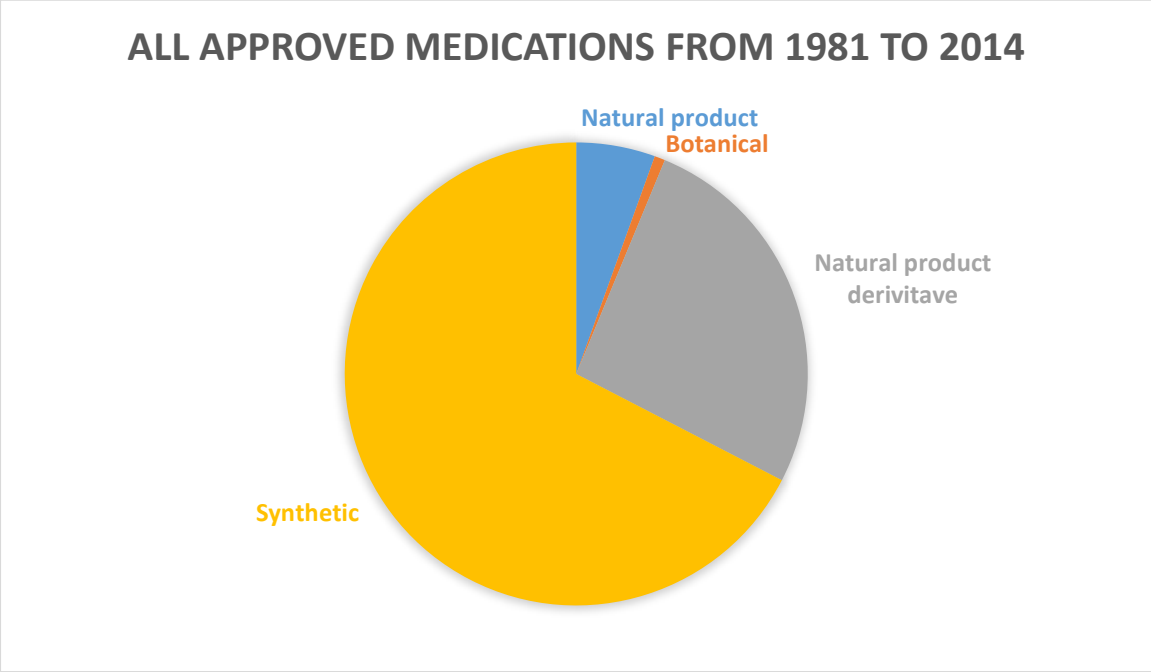

Figure 1.2 – All approved medicines between 1981-2014

The latest milestone in natural products drug discovery was the extraction and isolation of artemisinin (**15**), an extremely potent anti-malarial agent isolated from *Artemisia annua* by the Chinese scientist Tu Youyou. Artemisinin has become the lead compound in the development of new anti-malarial agents to overcome the multi-drug resistance strain and was subsequently modified to produce semi-synthetic analogues with higher potency. Tu Youyou was awarded half of the 2015 Nobel Prize in Medicine. Artemisinin and its derivatives are now the first line treatment against *Plasmodium falciparum* malaria.[16,17,18]

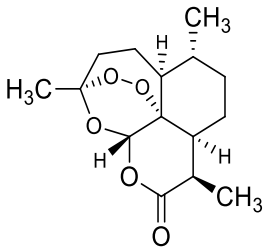

15

1.2 The Alkaloids

1.2.1 General

Alkaloids are a class of naturally occurring organic molecules produced by a variety of organisms including bacteria, fungi, plants and animals.[19] The German pharmacist Carl Friedrich Wilhelm Meissner introduced the term 'alkaloid' in 1819. He defined it as "a substance derived from plants that react like alkalis". However, this definition was regarded to be not sufficiently broad to encompass all substances that are readily perceived as alkaloids. Over the years the term 'alkaloid' was redefined many times and today the most widely accepted definition is "alkaloids are naturally occurring nitrogen-containing organic compounds which have a greater or lesser degree of basic character".[20, 21]

Alkaloids constitute one of the most diverse classes of secondary metabolites. They are biosynthesized by unique metabolic pathways involving amino acid precursors and show a broad spectrum of pharmacological activity.[22] Secondary metabolites are molecules that are produced in minute amounts by a unique biosynthetic pathway in each specific organism, where in many instances genetic and enzymatic evidence have proven the proposed pathway.[23] On the other hand, other natural molecules produced by these organisms such as carbohydrates and proteins are referred to as primary metabolites.[22,23,24] There is an extreme variation in the structures of different alkaloids. A comparison between coniine (**16**) a plant toxin and batarachotoxin (**17**) produced by the golden poison frog can show the difference in structure complexity between alkaloids.[25, 26]

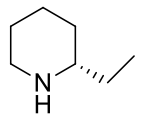

16

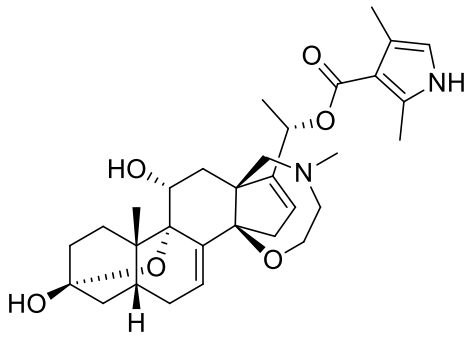

17

Due to the vast number of alkaloids that needs to be classified into meaningful and convenient groups, the most widely used classification of alkaloids is based on their nitrogen-containing structural features. Therefore, alkaloids are classified into five major groups (Table 1.1):

1) Heterocyclic alkaloids
2) Alkaloids with an exocyclic nitrogen atom
3) Polyamine alkaloids
4) Peptide alkaloids
5) Terpene and steroidal alkaloids.[20,21]

Table 1.1 – Selected examples of each group of alkaloids

1- Heterocyclic alkaloids These are alkaloids that have nitrogen as part of their cyclic ring system. They are the most common group of alkaloids in nature. An example of heterocyclic alkaloids is cocaine (**18**).[21]	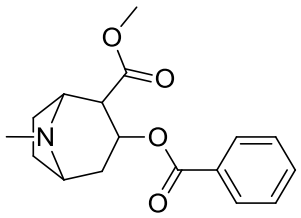 **18**
2- Alkaloids with exocyclic nitrogen atom Also called proto alkaloids or biological amines, these alkaloids have nitrogen that is not part of any ring system. They are less common in nature. An example of this group is ephedrine (**19**).[21]	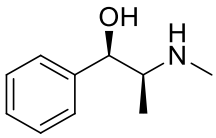 **19**
3- Polyamine alkaloids These are aliphatic molecules with one or more amino groups. An example of polyamines is putrescine (**20**).[27]	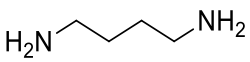 **20**

4- Peptide alkaloids Peptide alkaloids are composed of amino acid monomers linked by peptide bonds. An example of peptide alkaloids is ergotamine (**21**). [21]	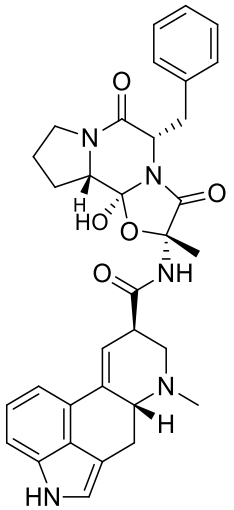 **21**
5-Terpene and steroidal alkaloids Terpene alkaloids are made of a mono-, sesqui-, di-, and tri-terpenoid skeleton while steroidal alkaloids as the name indicates have a steroid skeleton. An example of steroidal alkaloid is solasodine (**22**). [21]	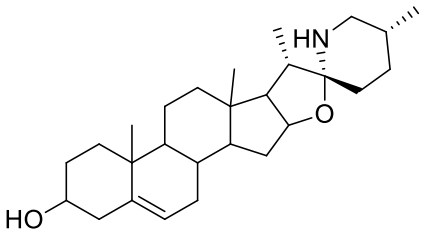 **22**

1.2.2 Occurrence and distribution

Alkaloid occurrence in the plant kingdom is predominant in higher plants (angiosperms including both mono- and di-cotyledons). Alkaloids may be found in the flowers, fruits, leaves and seeds. However, there are some lower non-flowering plants that produce alkaloids, e.g., paclitaxel (**23**) from *Taxus brevifolia.* Some fungi are also known to produce alkaloids such as ergotamine (**21**).[28] Alkaloids are also produced by the animal kingdom. For example the toxic steroidal alkaloid samandarin (**24**) secreted by the fire frog *Salamandra salamandra.*[29] Table 1.2 shows some selected examples of plants alkaloids.

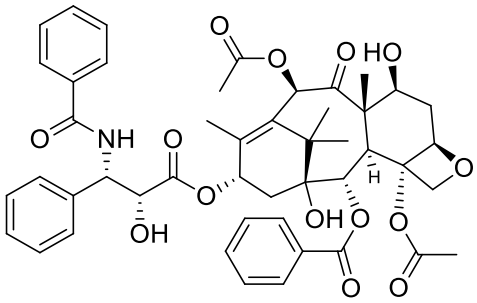

23

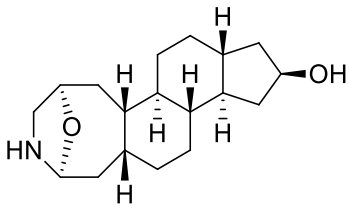

24

Table 1.2 – Distribution of selected alkaloids in selected families within the plant kingdom.[30]

Family	Plant genus	Alkaloid
Amaryllidaceae	*Amaryllis*	Lycorine
	Galanthus, Narcissus	Galanthamine
Ancistroclaceae	*Ancistrocladus*	Michellamine B
Apiaceae	*Conium*	Coniine
Apocynaceae	*Alstonine*	Alstonia
	Rauvolfia	Ajmalicine
	Rauvolfia	Ajmaline
	Aspidosperma	Anspidospermine
	Holarrhena	Conessine
	Ochrosia	Ellipticine
	Rauwolfia	Reserpine
	Catharanthus	Vinblastine
		Vincristine
	Yohimbe	Yohimbine
Arecaceae	*Areca*	Arecoline
Aristolochiaceae	*Aristolochia*	Aristolochic acid
Asteraceae	*Senecio*	Senecionine
Berberidaceae	*Berberis*	Berberine
	Mahonia	Berberine
Boraginaceae	*Heliotropium*	Indicine *N*-oxide

Cactaceae	*Lophophora*	Mescaline
Celastraceae	*Catha*	Cathine
		Cathinone
Chenopodiaceae	*Anabasis*	Anabasine
Colchicaceae	*Colchicum*	Colchicine
Convolvulaceae	*Calystegia*	Calystegines
Dioncophyllaceae	*Triphyophyllum*	Dioncophylline C
Ephedraceae	*Ephedra*	Ephedrine
Equisetaceae	*Equisetum*	Palustrine
Erythroxylaceae	*Coca*	Cocaine
Fabaceae	*Castanospermum*	Canstanospermine
	Anagyris	Anagyrine
	Laburnum	Cytisine
	Crotalaria	Monocrotaline
	Physostigma	Physostigmine
	Cytisus	Sparteine
	Swainsona	Swainsonine
Fumariaceae	*Dicentra*	Chelerythrine
Melanthiaceae	*Schoenocaulon*	Cevadine
	Veratrum	Rubijervine
Loganiaceae	*Strychnos*	Strychnine
Lycopodiaceae	*Lycopodium*	Lycopodine
Menispermaceae	*Chondrodendron*	Tubocurarine
Moraceae	*Morus*	Calystegines
Nyssaceae	*Camptotheca*	Camptothecin
Orchidaceae	*Dendrobium*	Dendrobine
Papaveraceae	*Papaver*	Morphine
		Codeine
		Papaverine
		Narcotine
Peganaceae	*Peganum*	Harmaline

Ranunculaceae	*Aconitum*	Aconitine
	Delphinium	Ajaconine
Rubiaceae	*Coffea*	Caffeine
	Psychotria	Emetine
	Cinchona	Quinine
		Quinidine
Rutaceae	*Acronychia*	Acronycine
	Zanthoxylum	Canthine-6-one
	Pilocarpus	Pilocarpine
Solanaceae	*Capsicum*	Capsaicin
	Atropa	Scopolamine
	Datura	
	Duboisia	
	Hyoscyamus	
	Mandragora	Hyoscyamine
	Solanum	Solanine
	Nicotiana	Nicotine
Sterculiaceae	*Theobroma*	Theobromine
Taxaceae	*Taxus*	Paclitaxel
		Baccatin III
Theaceae	*Camellia*	Caffeine

1.2.3 Properties of alkaloids

Alkaloids are found in plants as solid colourless crystals or amorphous. They exist in plants in three different forms, i.e., free-state, acidic salts, or N-oxides. There are coloured alkaloids although it is less common, e.g., sanguinarine is copper-red alkaloid. Beside carbon and nitrogen atoms, most alkaloids have oxygen atom, and less commonly sulfur atoms.[31]

Solubility is a crucial physical property for alkaloids used as medicines. Most alkaloid-based drugs are delivered in solution form. A simple modification from free-state to salt or vice-versa can affect the solubility of an alkaloid greatly.[31]

Alkaloid presence in plants can be tested by the use of Dragendorff's reagent (potassium iodide-bismuth nitrate) which when reacts with alkaloids gives an orange colour.

1.2.4 Physiological importance of alkaloids in plants

There are several hypotheses about the true physiological functions of alkaloids, some of which are presented below:

1) end product of metabolic processes – they serve no function.[32]
2) synthesized and used by plants as weapons and toxins to defend against predation
3) as growth regulators
4) as storage reservoir for nitrogen
5) as substitutes for minerals in plants

The first and fifth hypotheses are widely discredited now due to overwhelming evidence of the usefulness of alkaloids within the species that produce them.[33]

1.2.5 Classifications of heterocyclic alkaloids

Heterocyclic alkaloids are subdivided into fifteen distinct groups based on their heterocyclic ring system (Table 1.3).[21]

Table 1.3 – Classification of alkaloids according to their C-N skeleton.[21]

Class	Description
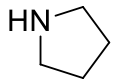 Pyrrolidine	• Also known as tetrahydropyrrole • Is a cyclic secondary amine • Saturated heterocycle
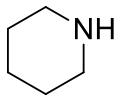 Piperidine	• Mostly found in the genus *Piper* • Saturated heterocyclic secondary amine

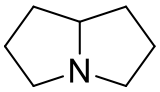 pyrrolizidine	• Fusion of two 5-membered rings
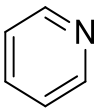 Pyridine	• Closely related to benzene with one methine replaced by a nitrogen atom
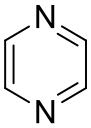 Pyrazine	• Symmetrical di-substituted benzene ring
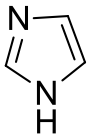 Imidazole	• A planar five-membered ring. • Exist in two tautomeric forms
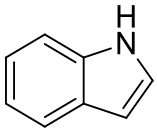 Indole	• Bicyclic alkaloids constituting fused benzene and pyrrole rings

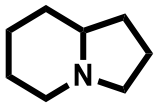 **Indolizidine**	• Bicyclic alkaloids with a six-membered ring fused to a five-membered ring with one of the ring junction atoms being a nitrogen atom.
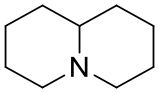 Quinolizidine	• Bicyclic alkaloids with two six-membered rings fused together with one of the ring junction atoms being a nitrogen atom.
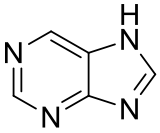 Purine	• Fusion of pyrimidine and imidazole rings.
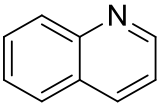 Quinoline	• Fusion of pyridine and benzene rings
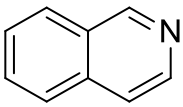 Isoquinoline	• Isomer of quinoline
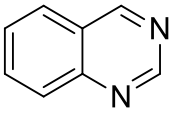 Quinazoline	• Fusion of benzene and pyrimidine rings.

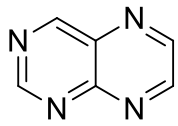 Pteridine	• Fusion of pyrimidine and pyrazine rings.
 Tropane	• Class of bicyclic alkaloids with tropane ring. • Mostly found in the plant family of Solanaceae.

1.2.6 Indolizidine alkaloids

One of the fifteen groups of heterocyclic alkaloids is indolizidine alkaloids, which can be found in a myriad of species across the plant kingdom. They are also found on the skin of some amphibians, in ants, and microorganisms.[34] However, many of these compounds are assigned under different classifications due to their biosynthetic origin or structural complexity that favours another heterocyclic classification. Indolizidine alkaloids are found in a number of different plant families, i.e., Orchiaceae, Asclepidaceae, Moraceae and Convolvulaceae. This research will focus on two sub-classes of indolizidine alkaloids, namely, phenanthroindolizidine and the less common benzopyrroloisoquinoline, which were isolated from Asclepidaceae and Moraceae (see Figure 1.3).[35]

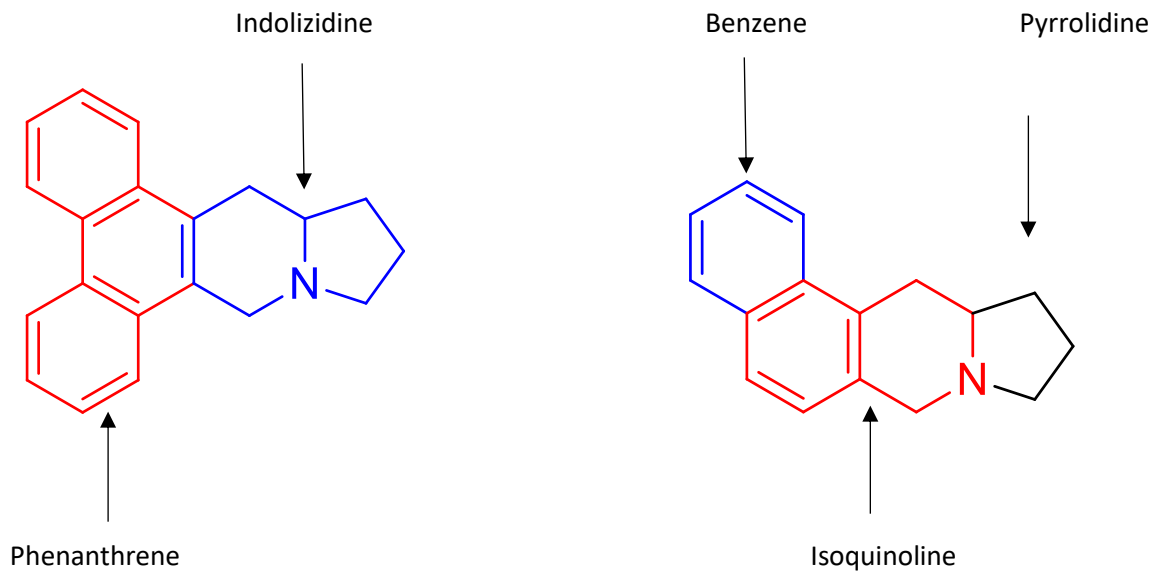

Figure 1.3 - The phenanthroindolizidine and benzopyrroloisoquinoline (naphthaloindolizidine) skeletons

1.3 Phenanthroindolizidine Alkaloids

1.3.1 - General

Phenanthroindolizidine alkaloids are a subgroup of indolizidine alkaloids. As the name indicates phenanthroindolizidines are a group of organic molecules where a phenanthrene ring system is fused with an indolizidine moiety. The first phenanthroindolizidine to be discovered was tylophorine (**28**) isolated from *Tylophora asthmatica.* Phenanthroindolizidines attracted much attention from scientists in the 1960s with their extremely potent anti-tumor, anti-inflammatory, anti-viral and ameobicidal activities.[36] Nonetheless, there were few drawbacks for their use as potential therapeutic agents such as low availability in nature, CNS toxicity and low *in vivo* anticancer toxicity.[37] These major drawbacks however did not stop the interest in phenanthroindolizidines and their unique chemistry and bioactivity. A large number of studies were carried out later and Table 1.4 lists all the phenanthroindolizidine alkaloids discovered until the present day.

Table 1.4 – A list of all naturally occurring phenanthroindolizidine alkaloids isolated to date.

Plant	Alkaloid	Structure	Reference
Albizzia julibrissin	Antofine	**25**	[36]
Antitoxicum funebre	Antofine	**25**	[35]
Cynanchum komarovii	Antofine	**25**	[36]
	14-Hydroxyantofine	**26**	[36]
	7-Demethoxytylophorine N-oxide	**27**	[38]
Cynanchum vincetoxicum	Antofine	**25**	[39]
	Tylophorine	**28**	[35]
	(-)-10β-Antofine N-oxide	**29**	[40]
	(-)-10β,13aα-14β-Hydroxyantofine N-oxide	**30**	[40]
	(-)-10β,13aα-*Seco*antofine N-oxide	**31**	[40]
	(-)-(*R*)-13aα-6-O-Desmethylantofine	**32**	[41]
	*Seco*antofine	**33**	[41]
	(-)-(R)-13aα-6-O-Desmethyl*seco*antofine	**34**	[41]
Ficus fistulosa	Tylophorine	**28**	[42]

	Antofine	**25**	43
	14-Hydroxyantofine	**26**	42
	*Seco*antofine	**33**	42
	Tylocrebrine	**35**	42
	Septicine	**36**	42
	Fistulopsine A	**37**	42
	Fistulopsine B	**38**	42
	3,6-Didemethylisotylocrebrine	**39**	42
Ficus hispida	O-Methyltylophorinidine	**40**	44
	Hispiloscine	**41**	45
Ficus septica	Antofine	**25**	46, 47
	Tylophorine	**28**	46
	Tylocrebrine	**35**	46
	Dehydrotylophorine	**42**	35
	Isotylocrebrine	**43**	46
	Septicine	**36**	46
	10*R*,13a*R*-Tylophorine N-oxide	**44**	47
	10*R*,13a*R*-Tylocrebrine N-oxide	**45**	47
	10*S*,13a*R*-Tylocrebrine N-oxide	**46**	47
	10*S*,13a*R*-Isotylocrebrine N-oxide	**47**	47
	10*S*,13a*S*-Isotylocrebrine N-oxide	**48**	47
	Ficuseptine A	**49**	48

	Ficuseptine B	**50**	47
	Ficuseptine C	**51**	47
	Ficuseptine D	**52**	47
	Ficuseptine E	**53**	49
	Ficuseptine F	**54**	49
	Ficuseptine G	**55**	49
	Ficuseptine H	**56**	49
	Ficuseptine I	**57**	49
	Ficuseptine J	**58**	49
	Ficuseptine K	**59**	49
	Ficuseptine L	**60**	49
	Ficuseptine M	**61**	49
	Ficuseptine N	**62**	49
	14α-Hydroxyisocrebrine N-oxide	**63**	46
	14-Hydroxy-3,4,6,7-tetramethoxypheanthroindolizidine	**64**	46
	14-Hydroxy-2,3,4,6,7-pentamethoxyphenanthroindolizidine	**65**	46
Hypoestes verticillaris	Hypoestestatin 1	**66**	36
	Hypoestestatin 2	**67**	36
Pergularia pallida	Tylophorine	**28**	35
	Tylophorinidine	**68**	35

	Tylophorinine	**69**	[35]
	Deoxytylophorinine	**70**	[35]
	14-Hydroxytylophorine	**71**	[35]
Typhlora asthmatica	Tylophorine	**28**	[39]
	Tylophorinidine	**68**	[39]
	O-Methyltylophorinidine	**40**	[39]
	Tylophorinine	**69**	[39]
	Isotylocrebrine	**43**	[39]
	Deoxytylophorinine	**70**	[39]
	Desoxytylophorinidine	**72**	[39]
Tylophora atrofolliculata	Tylophorinidine	**68**	[50]
	Tylophorinine	**69**	[50]
	Tylophoridicine C	**73**	[50]
	Tylophoridicine D	**74**	[50]
	Tylophoridicine E	**75**	[50]
	Tylophoridicine F	**76**	[50]
	11-Ketotylophorinidine	**77**	[51]
	13a*S*-2,6-Didemethyltylophorine	**78**	[51]
	2-Hydroxyltylophorinidine	**79**	[51]
	10R-3-O-Demethyltylophorinidine N-oxide	**80**	[51]
	10*R*-2-Hydroxyltylophorinine N-oxide	**81**	[51]

	10R-2-Methyl-O-methyltylophorindine N-oxide	**82**	51
	10R,13aS-Tylophorine N-oxide	**83**	51
	10R-Deoxytylophorinine N-oxide	**84**	51
	10S-2-Hydroxyl-6-demethyltylophorinine N-oxide	**85**	51
	13aR-2-Hydroxyltylophorinine	**86**	51
	11-keto-O-methyltylophorinidine	**87**	51
	3-O-demethyltylophorinidine	**88**	51
Tylophora hirsuta	Isotylocrebrine	**43**	36
	Tylophorine	**28**	36
	14-Hydroxyisotylocrebrine	**89**	36
	4-Demethylisotylocrebrine	**90**	36
	Tylohirsutinine	**91**	36
	Tylohirsutinidine	**92**	36
	13a-Methyhylohirsutine	**93**	36
	13a-Methyltylohirsutinidine	**94**	36
	13a-Tydroxysepticine	**95**	36
	14-Desoxy-13a-methyltylohirsutinidine	**96**	36
	5-Hydroxy-O-methyltylophorinidine	**97**	36
	Tylohirsuticine	**98**	36
	13a-Hydroxytylophorine	**99**	36
Tylophora indica	Tylophorine	**28**	36
	Tylophorinidine	**68**	36

	Tylophorinine	**69**	[36]
	Septicine	**36**	[36]
	Isotylocrebrine	**43**	[36]
	3-*O*-Demethyltylophorinidine	**88**	[36]
	4-Demethyltylophorine	**90**	[36]
	6-Demethyltylophorine	**100**	[36]
	5-Hydroxy-O-methyltylophorinidine	**97**	[36]
	Tyloindicine A	**101**	[36]
	Tyloindicine B	**102**	[36]
	Tyloindicine C	**103**	[36]
	Tyloindicine D	**104**	[36]
	Tyloindicine E	**105**	[36]
	Tyloindicine F	**106**	[36]
	Tyloindicine G	**107**	[36]
	Tyloindicine H	**108**	[36]
	Tyloindicine I	**109**	[36]
	Tyloindicine J	**110**	[36]
	4,6-Desdimethylisotylocrebrine	**111**	[36]
	14-Hydroxyisotylocrebrine	**89**	[36]
Tylophora ovata	Tylophorine	**28**	[52]
	O-Methyltylophorinidine	**40**	[52]
	Septicine	**36**	[52]
	6-Desmethyltylophorine	**100**	[52]

	Tylophovatine A	**112**	[50]
	Tylophovatine B	**113**	[50]
	Tylophovatine C	**114**	[50]
Tylophora tanakae	Tylophorine	**28**	[53]
	Isotylocrebrine	**43**	[53]
	6-Demethyltylocrebrine	**115**	[53]
	3-Demethylisotylocrebrine	**116**	[53]
	3-Demethyl-14α-hydroxyisotylocrebrin	**117**	[53]
	Isotylocrebrine N-Oxide	**118**	[53]
	14α-Hydroxyisotylocrebrine N-Oxide	**119**	[53]
	3-Demethyl-14α-Hydroxyisotylocrebrine N-Oxide	**120**	[53]
	Tylohorinine N-Oxide	**121**	[53]
	7-Demethyltylophorine	**122**	[53]
	Tylophorine N-Oxide	**83**	[36]
	7-Demethyltylophorine N-Oxide	**123**	[36]
	3,6-Diemethylisotylocrebrine	**124**	[36]
	14α-Hydroxy-3,6-didemethylisotylocrebrine	**125**	[36]
Vincetoxiucm hirundinaria	(+)-Antofine *N*-oxide	**29**	[36]

	(-)-Antofine *N*-oxide	**126**	[36]
Vincetoxicum officinale	Tylophorine	**28**	[35]
	Antofine	**25**	[35]

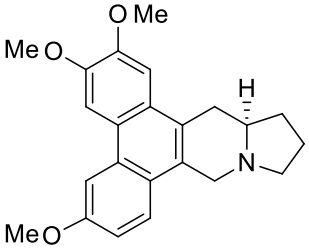

25

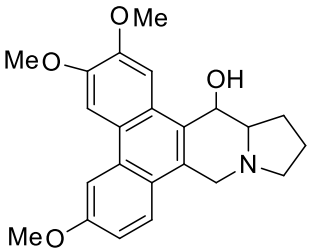

26

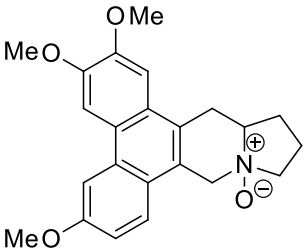

27

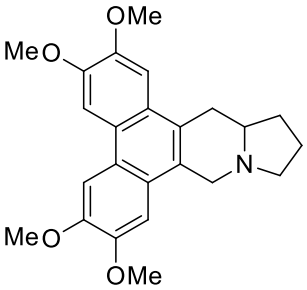

28

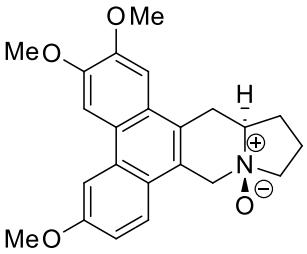

29

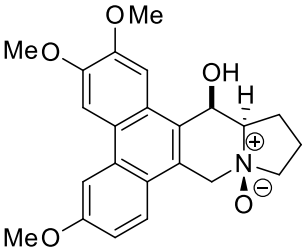

30

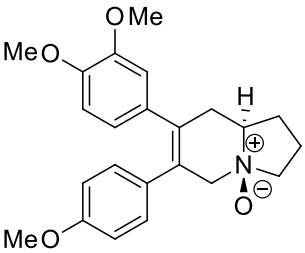

31

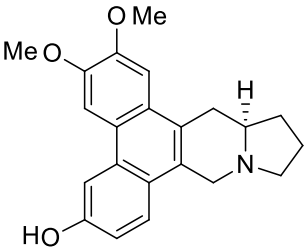

32

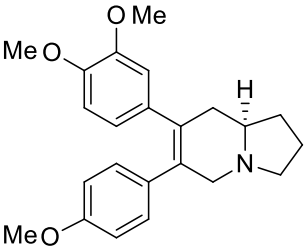

33

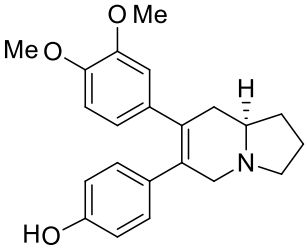

34

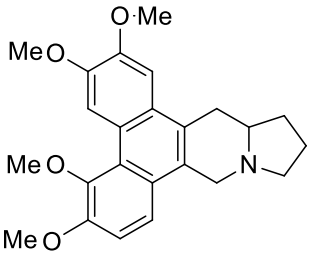

35

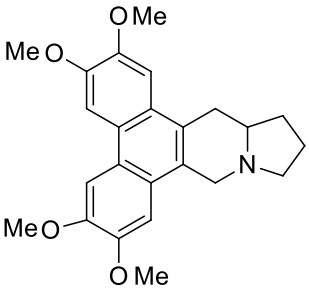

36

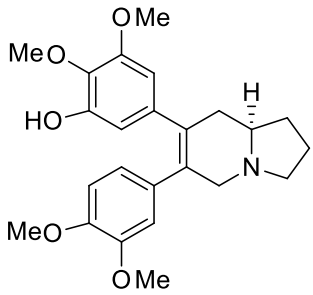

37

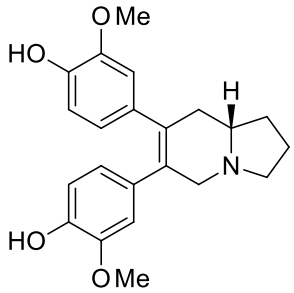

38

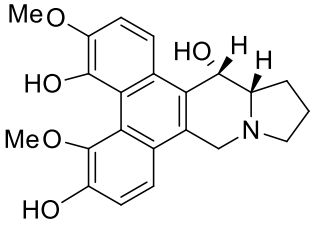

39

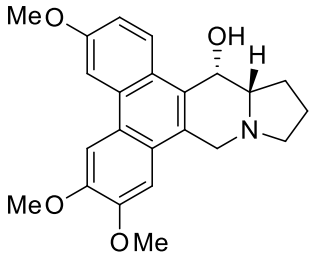

40

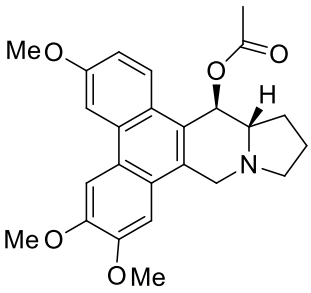

41

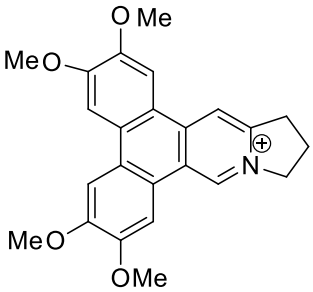

42

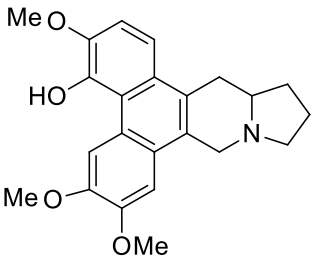

43

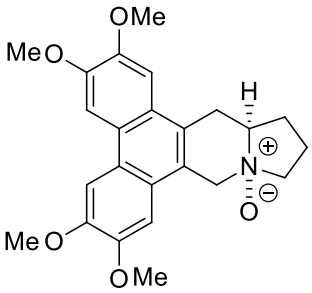

44

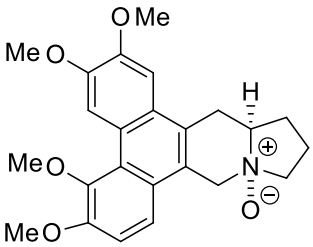

45

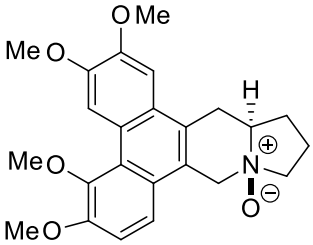

46

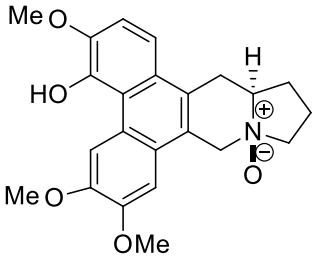

47

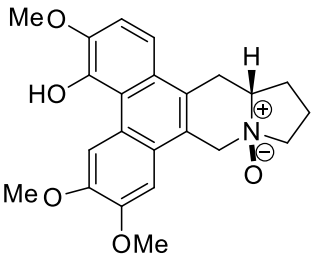

48

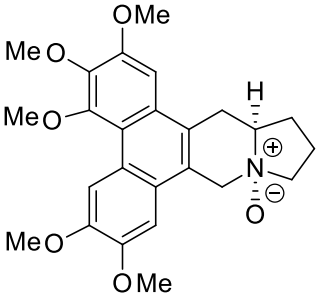

49

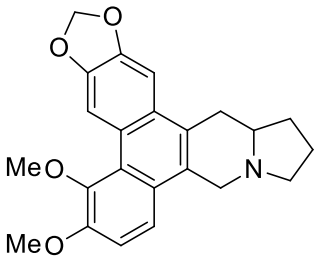

50

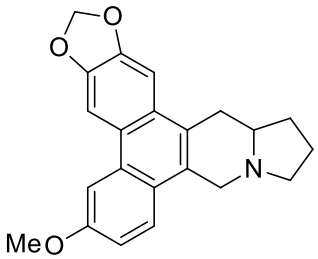

51

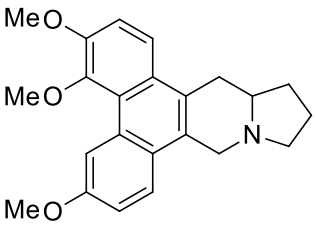

52

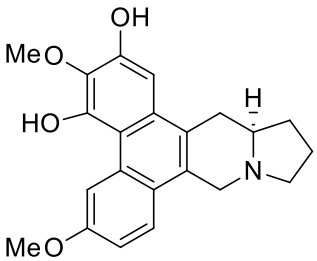

53

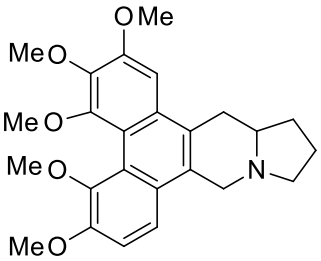

54

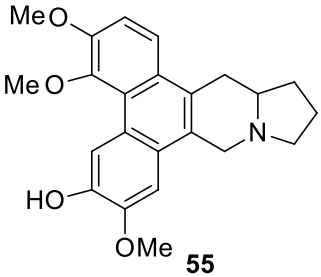

55

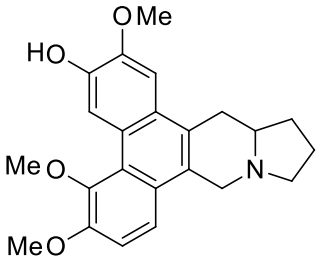

56

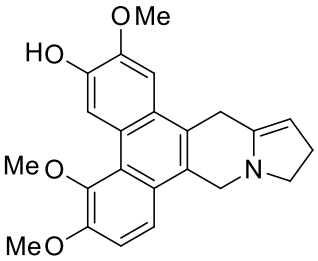

57

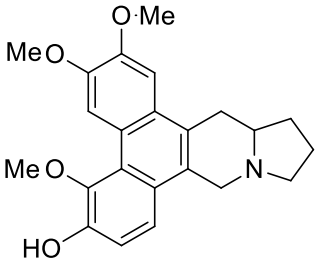

58

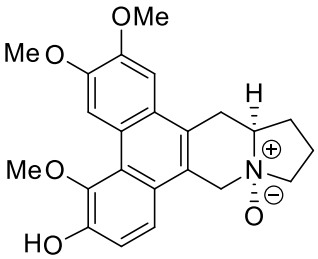

59

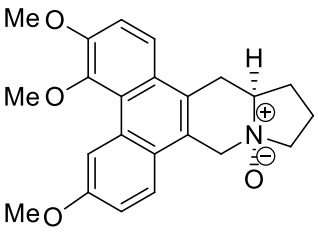

60

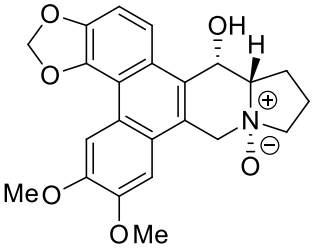

61

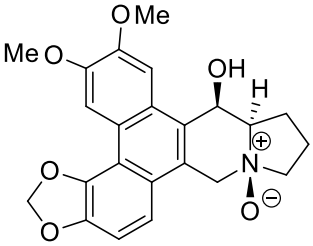

62

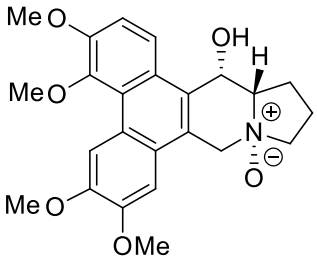

63

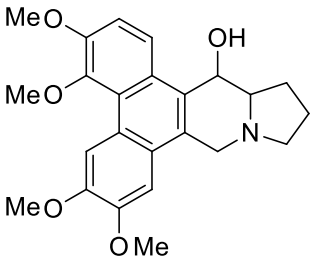

64

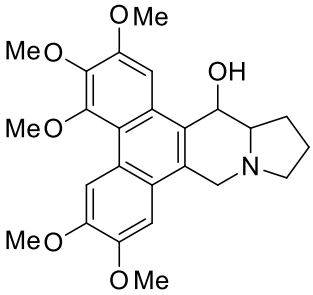

65

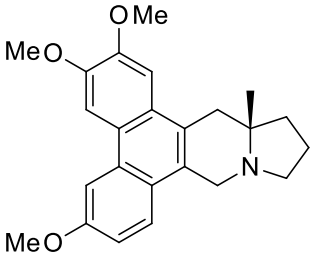

66

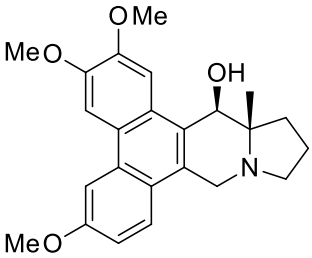

67

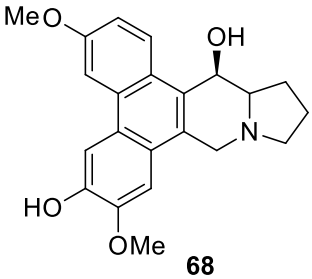

68

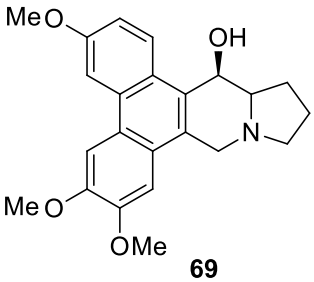

69

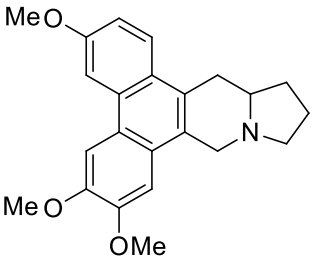

70

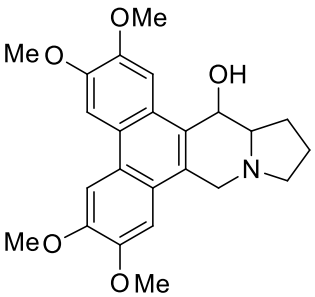

71

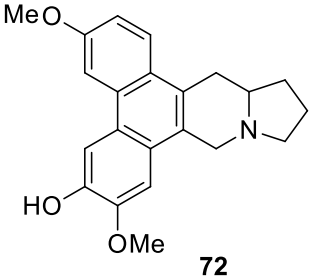

72

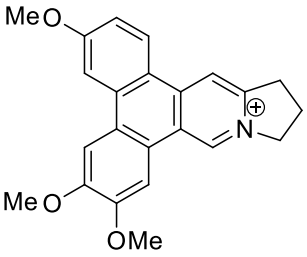

73

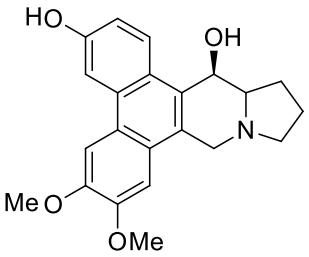

74

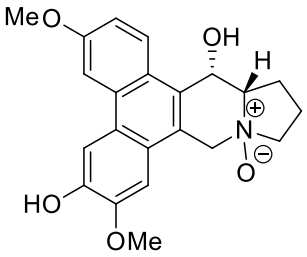

75

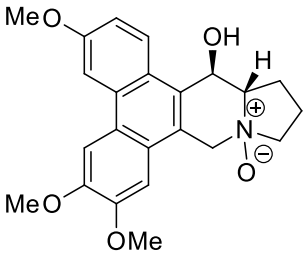

76

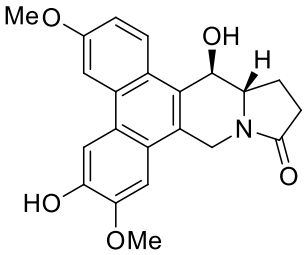

77

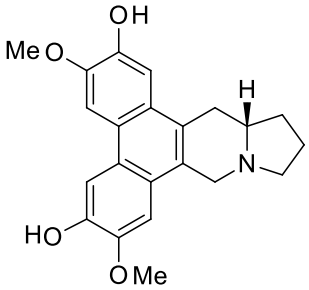

78

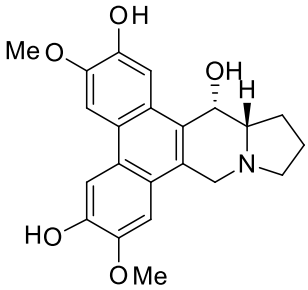

79

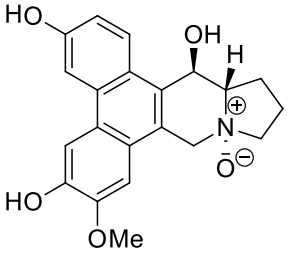

80

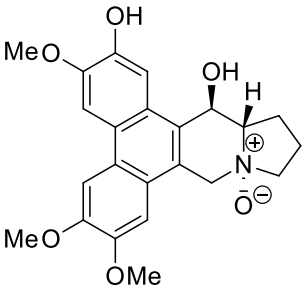

81

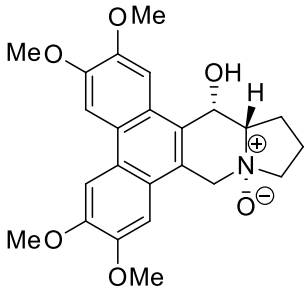

82

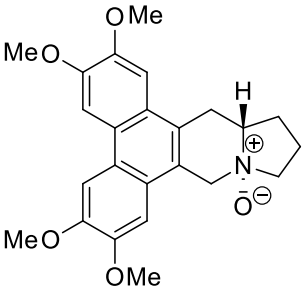

83

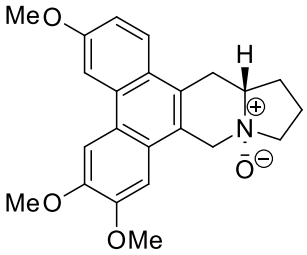

84

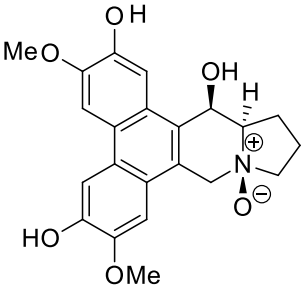

85

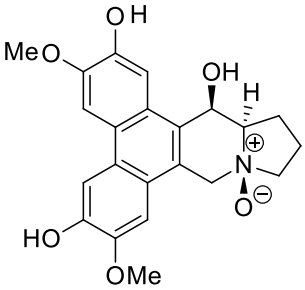

86

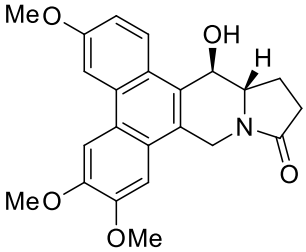

87

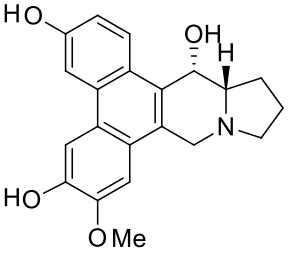

88

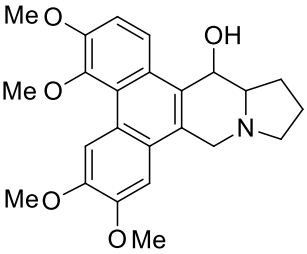

89

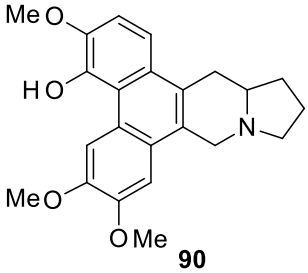

90

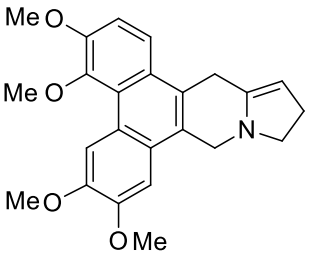

91

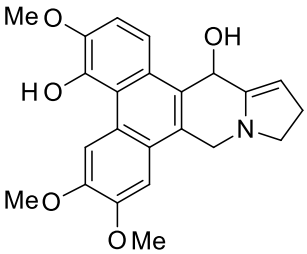

92

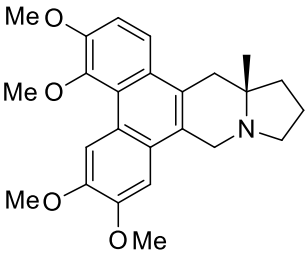

93

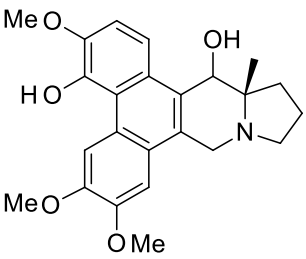

94

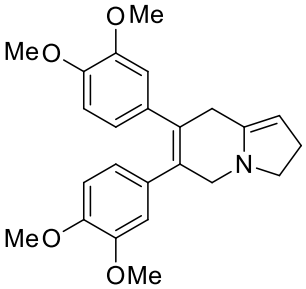

95

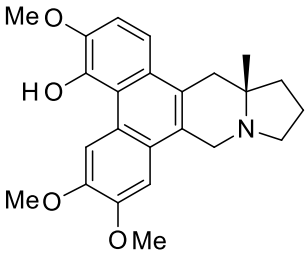

96

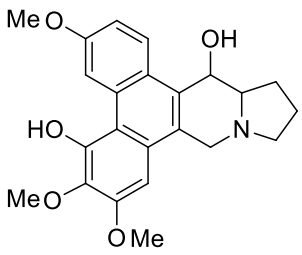

97

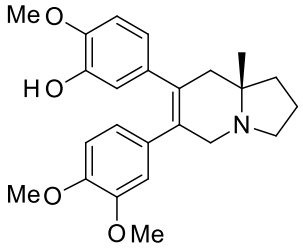

98

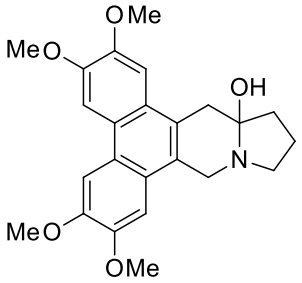

99

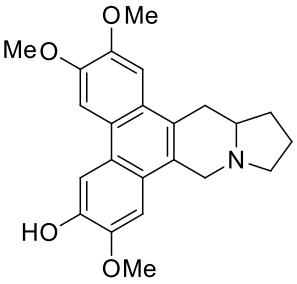

100

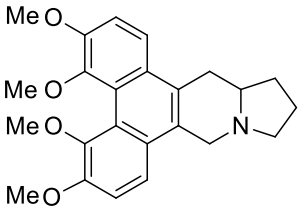

101

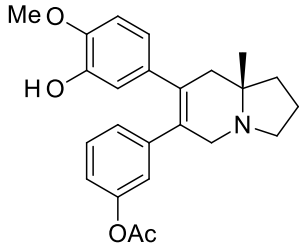

102

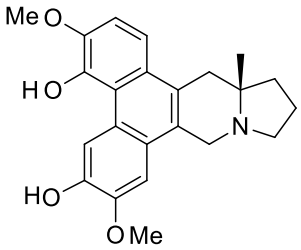

103

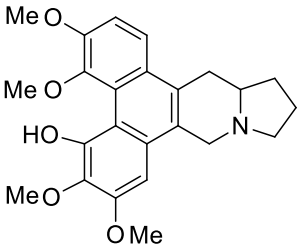

104

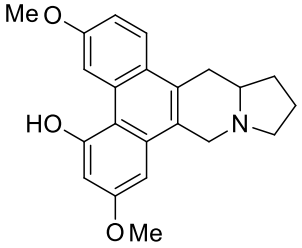

105

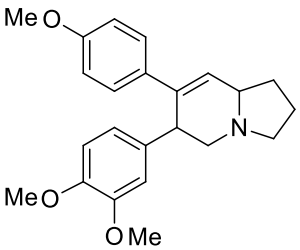

106

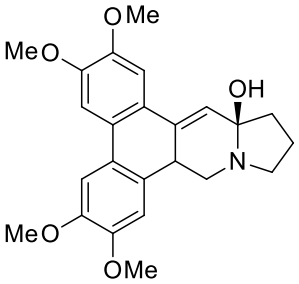

107

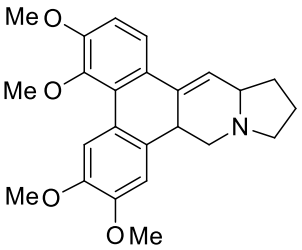

108

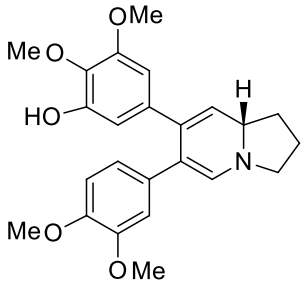

109

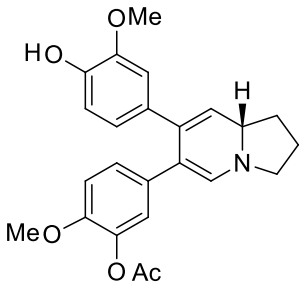

110

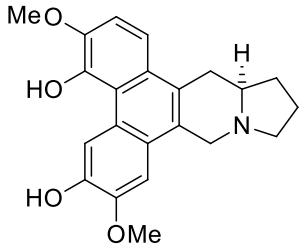

111

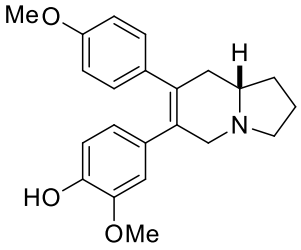

112

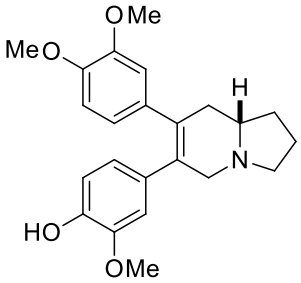

113

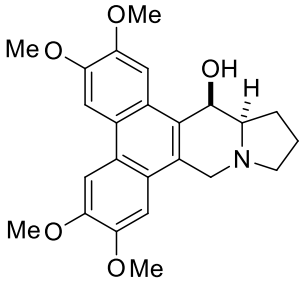

114

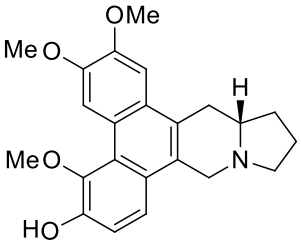

115

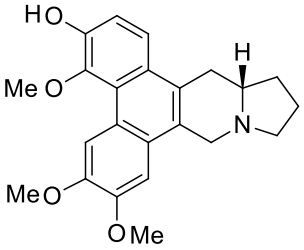

116

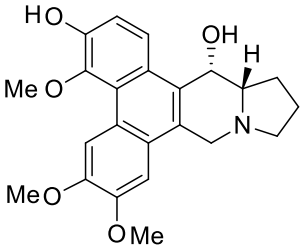

117

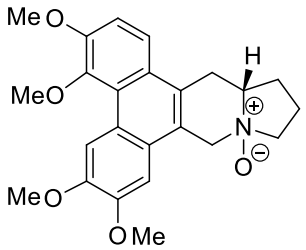

118

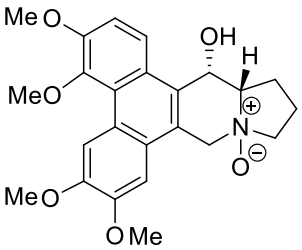

119

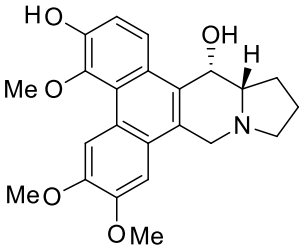

120

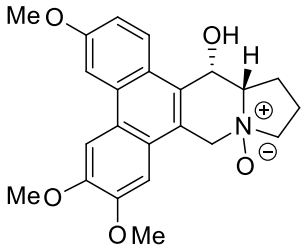

121

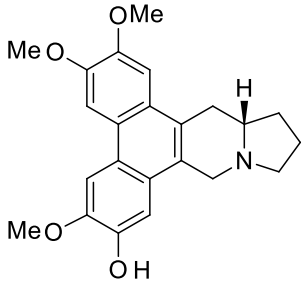

122

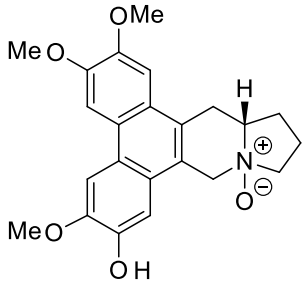

123

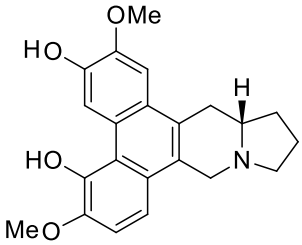

124

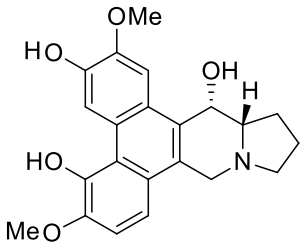

125

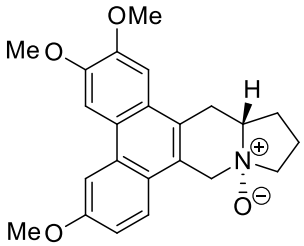

126

1.3.2 Biosynthesis of Phenanthroindolizidine Alkaloids

In 1984 a study was carried out to determine the biosynthetic pathway of phenanthroindolizidines. Phenylalanine and tyrosine were known to be the amino acid precursors to tylophorine and tylophorinidine, while ornithine is the amino acid that is responsible in providing the nitrogen-containing pyrrole ring in the indolizidine structure.[54]

To allow the elucidation of the biosynthetic pathway, radiolabelled 2-pyrrolidin-2-ylacetophenone and its oxygenated derivatives were used. The compounds were labelled with ^{14}C and ^{3}H radioisotopes that can be traced. The results of the study allowed the partial elucidation of the biosynthetic pathways to produce phenanthroindolizidine alkaloids (Figure 1.4).[54,55]

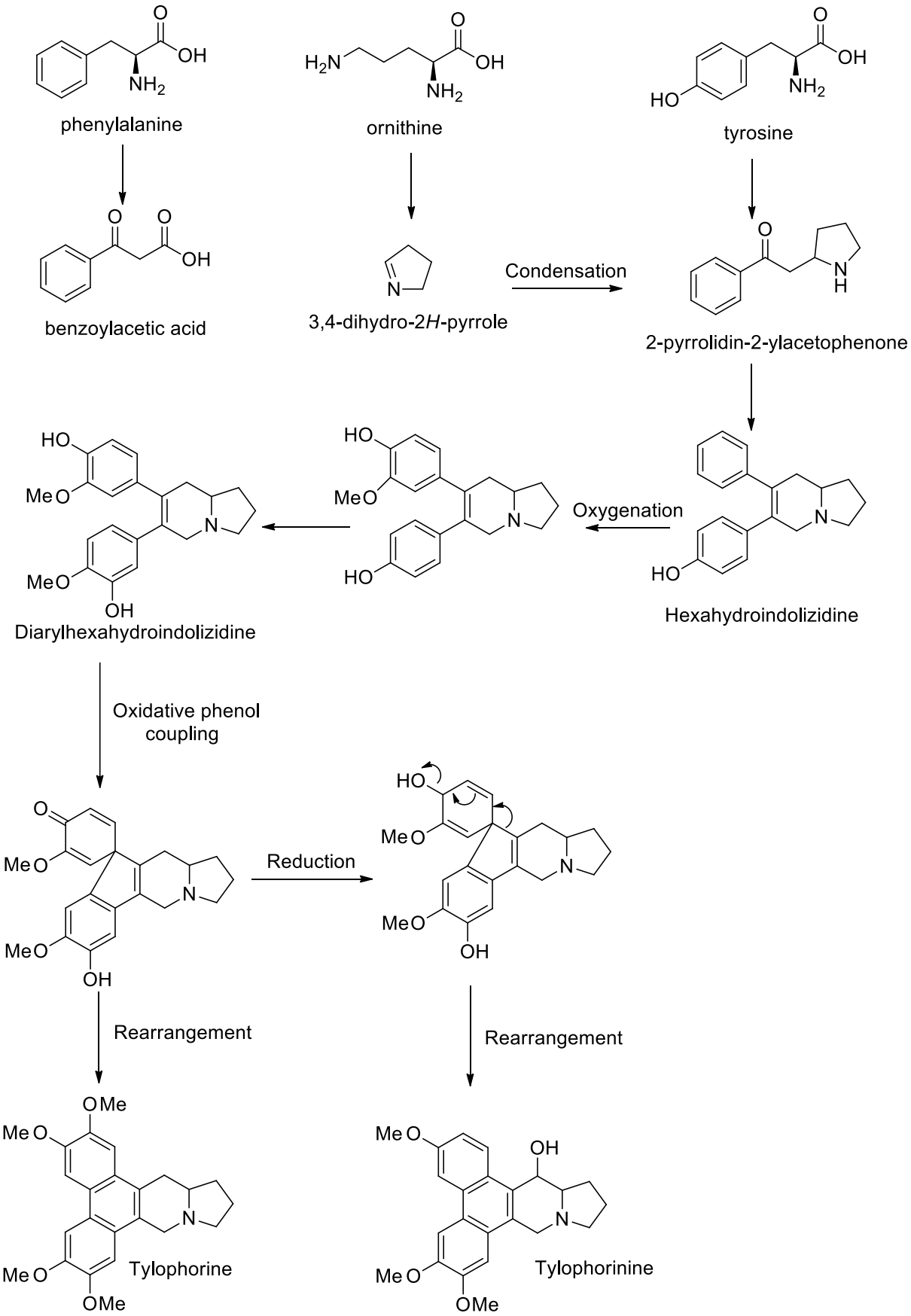

Figure 1.4 – Partial biosynthetic pathway to phenanthroindolizidines.[54]

1.3.3 Biological activity of phenanthroindolizidine alkaloids

The biological activities of phenanthroindolizidine alkaloids were studied extensively and they were found to possess tremendous anti-tumor, anti-viral, and anti-inflammatory activities. Initially the crude extract from *T. indica* was subjected to numerous biological tests, and it showed promising anti-inflammatory, immunosuppressive and cytotoxic activities. Due to its immense immunosuppressive activity, *T. indica* crude extract was later subjected to clinical studies for the treatment of asthma and showed noticeable efficacy over placebo. The immunosuppressive effect of the extract was attributed to an increase in the secretion of adrenal corticosteroids. *Tylophora indica* extract is currently marketed as a supplement in products such as T. Asthmatica plus®.[56]

Investigation of the pure alkaloids from *T. indica* was then carried out with specific focus on tylophorine, due to its relatively high abundance in the plant (0.015-0.035%) and ease of synthesis. Since the plant extract showed prominent anti-inflammatory, cytotoxicity and immunosuppression the pure alkaloids from the plant were expected to carry the same effect.

In vitro cytotoxicity assessment showed that phenanthroindolizidines possess remarkable cytotoxicity, established by a study carried out in 1997 by the NCI. The compounds used in this study inhibited the growth of all 60-cell lines used by the NCI in the low nanomolar range.[57] As can be seen in Table 1.5, phenanthroindolizidine alkaloids showed very little selectivity between the tested cell lines. For example, paclitaxel which was tested in the same study showed an IC_{50} range between 2-1000 nM, showing almost a 500-fold difference. Moreover, the compounds retained almost the same level of potency against the multi-drug resistant cancer cells. Phenanthroindolizidine alkaloids were studied thoroughly as potential anti-cancer lead compounds after the outcome of this study.

Table 1.5 - *In vitro* cytotoxicity of some phenanthroindolizidine alkaloids.[57]

Compound	60-cell line panel GI_{50} (nM)		Individual cell line GI_{50} (nM)		
	Mean	Range	A-549	MCF-7	HCT-116
Tylocrebrine (**35**)	29.5	10-126	25	50	25
Tylophorine (**28**)	17.5	10-400	10	10	10
Antofine (**25**)	ND	ND	10.4	12.4	9.9
Tylophorinine (**69**)	57.6	10-500	63	63	40
Tyloindicine F (**106**)	0.1	0.1-1	0.1	0.1	0.1

A549 = non-small cell lung carcinoma, MCF-7 = breast carcinoma, HCT 116 = colon carcinoma, ND = No data.

In vivo studies showed disappointing results as most phenanthroindolizidines tested were virtually inactive against sarcoma 180, adenocarcinoma 755, B16 melanoma, Lewis lung, P1534 leukemia and Walker 256 carcinosarcoma animal models. However, tylocrebrine (**35**) showed promising activity against lymphoid leukemia L1210 mouse models with 155% life extension at a dose of 20 mg/kg. This justified its entry into clinical trials for leukemia in 1965. Nevertheless, due to severe CNS toxicity and side effects, namely, ataxia and disorientation, the trials were aborted before the establishment of tylocrebrine's therapeutic value in humans. Until this day tylocrebrine is the only phenanthroindolizidine to have entered clinical trials.[56]

1.3.4 Mechanism of action of phenanthroindolizidine cytotoxicity

Studies have shown that phenanthroindolizidine alkaloids interact with multiple targets in the tumor cell. It is possible however that the cytotoxicity of these alkaloids is caused by a combination of drug-target interactions.

1) Protein, DNA and RNA biosynthesis inhibition

It is by far the most extensively studied mechanism of action for phenanthroindolizidine anti-cancer activity. Tylophorine and tylocrebrine were found to inhibit the biosynthesis of proteins in Ehrlich ascites-tumor cells while exerting no effect on RNA synthesis.[58] In addition, antofine has been reported to inhibit protein biosynthesis as well.[59] since the compounds exerted no similar effect on *E. coli* (bacterial prokaryotic 70s ribosomes) they were hypothesized to specifically target the eukaryotic 80s ribosomes protein biosynthesis.[58] On the other hand, tylocrebrine was shown to inhibit DNA synthesis in HeLa cells. It is worth mentioning that DNA and protein synthesis pathways are interdependent, consequently, protein synthesis inhibitors will in turn inhibit DNA synthesis as well. Thus indicating that inhibition of DNA synthesis is caused primarily by ribosomal inhibition.[56]

2) Apoptosis and cycle arrest

Compounds that inhibit protein synthesis will prevent proliferation, thus they are rather cytostatic. Although cytostatic agents can treat malignancies by stopping the accelerated proliferation in neoplastic growth, cancer cell death (apoptosis) is needed in order to achieve complete remission. *T. indica* extract was shown to completely inhibit cell multiplication at concentration of 0.1 μM. Interestingly, increasing the dose by ten-fold showed prominent apoptosis, however this can be attributed to synergistic effect, and the concentration is too high to be therapeutically practicable. Pure phenanthroindolizidines were tested and showed no

significant apoptosis indicating that phenanthroindolizidines are in fact cytostatic, with G1-Phase arrest linked to suppression of cyclin A2 expression. [56, 60]

3) Angiogenesis

Tumor cells have a very high oxygen demand for their basic sustenance, this demand is met by angiogenesis (the formation of new blood vessels) which is triggered by the release of VEGF growth factor and HIF-1. Targeting angiogenesis is an effective way to suppress tumor growth. Studies shows that phenanthroindolizidine alkaloids are potent inhibitors of HIF-1 and VEGF at low nanomolar concentrations.[61]

4) Cell differentiation

Due to their prominent effect as protein synthesis inhibitors it is not surprising that phenanthroindolizidines induce phenotypic changes in transformed cells. Tylophorine's effect on cell differentiation was investigated by monitoring the expression of two tumor biomarkers, albumin and alpha-fetoprotein (AFP). Tylophorine (1 μM) resulted in a suppression of AFP and an increase in albumin expression which is consistent with cell differentiation.[60]

5) Other molecular targets

Other targets have been proposed for the cytotoxicity of phenanthroindolizidine. Thymidylate synthase[62] and dihydrofolate reductase[63] have been observed at high concentrations (>30 μM) of tylophorinidine. However, it seems quite unjustifiable to explore these effects further since phenanthroindolizidines exert their effect at the nanomolar range.

1.3.5 Other biological activities of phenanthroindolizidines

As mentioned above, *T. indica* crude extract showed anti-inflammatory activity *in vitro* and *in vivo* (animal and human models). The activity of pure alkaloids as anti-inflammatory agents was then investigated. This was demonstrated in several studies that confirmed tylophorine anti-inflammatory effects *in vitro* and *in vivo.*[64, 65] It was shown that tylophorine significantly decreased the production of TNFα, iNOS and COX-2 at 3-10 μM without causing NF-κB inhibition.[56,64] Antiviral activity of phenanthroindolizidines have also been reported with antofine showing prominent anti-TMV activity in the nanomolar range.[56]

1.4 Benzopyrroloisoquinoline Alkaloids

1.4.1 – General

Benzopyrroloisoquinoline or naphthaloindolizidine alkaloids are very closely related to the phenanthroindolizidine alkaloids in terms of structure. However, they are far less common with only three benzopyrroloisoquinolines isolated from natural origin to date and in this research the fourth compound of this class is being reported. The three known benzopyrroloisoquinolines previously isolated are:

1. Vincetene (**127**)

   Vincetene was isolated from from *Cynanchum vincetoxicum. Cynachum* is a genus of about 300 species that belongs to the Apocynacaea family. The full NMR data was not provided in the paper published by the authors, instead they mentioned key proton signals only and the stereochemistry at C-11a stereocentre was not established.[66]

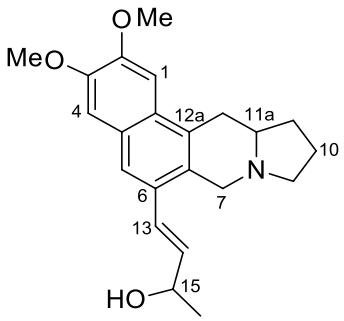

127

2. 2,3-Dimethoxy-6-[3-oxobutyl]-7,9,10,11,11a,12- hexahydrobenzo [f]pyrrolo[1,2-b] isoquinoline (**128**)

   Alkaloid **128** was isolated from another *Cynanchum* species *C. komarovii.* ^{1}H NMR data were fully reported. However, the stereochemistry of **128** was also not determined due to ^{1}H NMR signals involving H-11a and other hydrogens overlapped.[38]

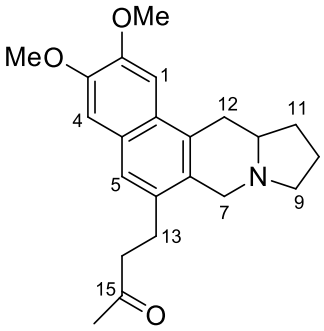

128

3. (–)-Fistulosine (**129**)

Fistulosine was isolated from the leaves of *F. fistulosa Reniw. ex Blume.* ^{1}H and ^{13}C NMR data were reported and the specific optical rotaion of **129** was reported as $[\alpha]_D$ -11 (*c 0.08,* MeOH). Relative stereochemistry of **129** was not established by NMR data due to signal overlapping involving H-11a. Nevertheless, (–)-fistulosine (**129**) was isolated together with three known phnanthroindolizidines all of which had negative optical rotation and *R* stereochemistry at the indolizidine ring junction carbon. (–)-Fistulosine (**129**) was thus assigned *R* at C-11a by anology.[43]

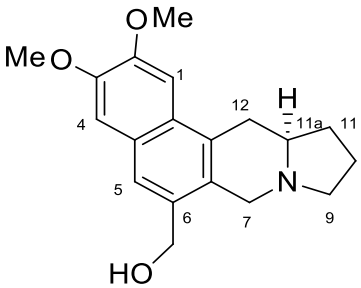

129

<u>1.4.2 – Biological activity of benzopyrroloisoquinoline alkaloids</u>

A study was performed to assess the cytotoxicity of synthetic benzopyrroloisoquinoline analogues of antofine and tylophorine. They however showed no apparent cytotoxicity.[67] Fistulosine (**129**) was previously tested for antifungal activity and it showed no activity.[43] Fistulosine isolated in the present study was tested for cytotoxic activity and was also found to be inactive. Nonetheless, the other natural benzopyrroloisoquinoline alkaloid (**128**) showed very modest activity against tobacco mosaic virus with 15% growth inhibition at 500 μg/mL.

1.5 The Genus *Ficus*

1.5.1 General

Ficus, commonly known as figs, is a pantropical genus of trees, vines and shrubs most of which are evergreen. *Ficus* is a massively diverse genus with over 800 species worldwide (Table 1.7). It is the largest of the 40 genera that make up the Moraceae family. Moraceae is divided into five tribes, specifically, Artocarpeae, Castilleae, Dorstenieae, Ficeae (which *Ficus* is part of) and Moreae.[68] *Ficus* is widely distributed around Peninsular Malaysia with about 99 species.[69]

Table 1.7 – Global distribution of the genus *Ficus.*[68]

Region	Number of subgenera	Number of species
Indo-Pacific	6	>500
Borneo	6	>160
Papua New Guinea	6	>150
Afrotropics	5	112
Neotropics	2	132
Global	7	>800

Ficus have a diverse range of botanical characteristics, many of which are common for tropical rainforest ecosystem such as hemi-epiphytes (including strangling figs and banyans), large woody climbers (e.g., *Ficus pumila*) and cauliflorous trees (e.g., *Ficus fistulosa Rienw ex Blume).* Figs support an astonishing 1200 species of vertebrate globally, some of which feed exclusively on figs.[68]

Figs have a distinctive and highly specific system for pollination. It depends to a great extent on specific wasps, namely, Agaoninae, Agaonidae and Chalcidoidae. Pregnant female wasps enter the fig fruit through a tiny hole in the bottom, which is highly selective and only allows the exact species of wasps that pollinates it to enter. The wasp loses its wings in the process of gaining entrance. The wasp pollinates the plant by brushing against uniovular female flowers with pollens it carries. Concurrently, the wasp lays its eggs on other ovules and then dies within the fig. Ovules with eggs laid within them are then triggered to form a gall; later on, the wasp larvae grow. After the wasp has fully grown within the gall it erupts and exits the fig. Simultaneously, the wasp gathers pollen from male flowers which have developed at the same time of the wasp to benefit from the egress of the

wasp. Once the wasp breaks free of the fig, the fig develops into a fruit. When female wasps leave the fig they have a limited time (hours to 2-3 days) to find a receptive fig fruit.[68,70]

Studies have shown that *Ficus* species have been cultivated for 11,000 years. Different species of figs were grown and used as a food source. Chinese and Indian traditional medicines are known to use *Ficus* for medicinal purposes. However, the use of *Ficus* was originally derived in the Middle East and are mostly found there.[71]

Recent studies on the biological activity of alkaloids from *Ficus* involved the isolation of pure compounds and assessing their biological activities for potential therapeutic uses. *Ficus carica* produces fig latex that was found to inhibit the growth of sarcoma *in vivo* (albino rats). Antofine (**25**), (+)-isotylocrebrine (**43**) and tylophorine (**28**) isolated from *Ficus septica,* showed potent cytotoxic activity against several tumour cell lines *in vitro* with GI_{50} values of 2 µM. Fistulopsines A (**37**) and B (**38**) isolated from the leaves of *Ficus fistulosa* exhibited *in vitro* cytotoxicity against HCT 116 and MCF 7 cell lines with GI_{50} ranging between 2-7 µM. Hispidacine (**130**) showed an appreciable vasorelaxant activity in rat isolated aorta with concentrations just above 1 µM.[42,45,48]

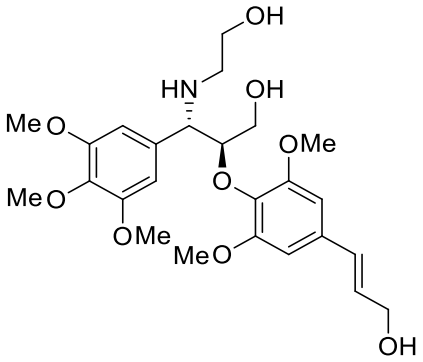

130

1.5.2 – Previous investigation of the genus *Ficus*

Ficus is one of the most under-investigated genera with only three species of *Ficus* reported the presence of alkaloids to the present day, namely, *Ficus hispida*, *Ficus fistulosa* and *Ficus septica*. Phenanthroindolizidine alkaloids make up the majority of the alkaloids isolated from the three *Ficus* species. They were found mainly in the leaves and bark of the investigated plants. Table 1.8 lists the alkaloids extracted from *Ficus* to date.

Table 1.8 – Alkaloids from *F. fistulosa, F. hispida* and *F. septica*.

Species	Source	Alkaloid Name	Structure	Reference
F. fistulosa	Bark and leaves	Antofine	**25**	[43]
		(–)-Fistulosine	**129**	[43]
		Fistulopsine A	**37**	[42]
		Fistulopsine B	**38**	[42]
		14β-Hydroxyantofine	**26**	[43]
		*Seco*antofine	**33**	[43]
		(–)-3,6-Didemethylisotylocrebrine	**39**	[42]
		Septicine	**36**	[42]
		Tylophorine	**28**	[42]
		Tylocrebrine	**35**	[42]
F. hispida	Bark and leaves	*O*-Methyltylophorinidine	**40**	[45]
		Hispiloscine	**41**	[45]
		Hispidacine	**130**	[45]
F. septica	Leaf	Tylophorine	**28**	[46]
		Isotylocrebrine	**43**	[46]
		Antofine	**25**	[46]
		Tylocrebrine	**35**	[46]
		14α-Hydroxyisocrebine *N*-oxide	**63**	[46]
		Septicine	**36**	[46]

		*Seco*antofine	**33**	[46]
		14-Hydroxy-3,4,6,7-tetramethoxypheanthroindolizidine	**64**	[46]
		14-Hydroxy-2,3,4,6,7-pentamethoxyphenanthroindolizidine	**65**	[46]
		Tylophorine *N*-oxide	**83**	[46]
		Norruspoline	**131**	[46]
		Phyllosterone	**132**	[46]
		Ficuseptamine A	**133**	[46]
		Ficuseptamine B	**134**	[46]
		Ficuseptamine C	**135**	[46]
	Bark	Tylophorine	**28**	[47]
		Tylocrebrine	**35**	[47]
		Isotylocrebrine	**43**	[47]
		Antofine *N*-oxide	**29**	[47]
		Ficuseptine A	**49**	[48]
		Ficuseptine B	**50**	[47]
		Ficuseptine C	**51**	[47]
		Ficuseptine D	**52**	[47]
		10*S*,13aR-Tylocrebrine *N*-oxide	**46**	[47]
		10*R*,13aR-Tylocrebrine *N*-oxide	**45**	[47]
		10*R*,13aR-Tylophorine *N*-oxide	**44**	[47]
		10*S*,13aR-Isotylocrebrine *N*-oxide	**47**	[47]
		10*S*,13aS-Isotylocrebrine *N*-oxide	**48**	[47]
	Root	Ficuseptine E	**53**	[49]
		Ficuseptine F	**54**	[49]
		Ficuseptine G	**55**	[49]
		Ficuseptine H	**56**	[49]
		Ficuseptine I	**57**	[49]
		Ficuseptine J	**58**	[49]
		Ficuseptine K	**59**	[49]

		Ficuseptine L	**60**	[49]
		Ficuseptine M	**61**	[49]
		Ficuseptine N	**62**	[49]

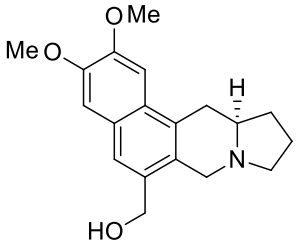

129

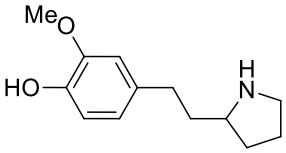

131

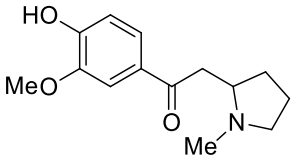

132

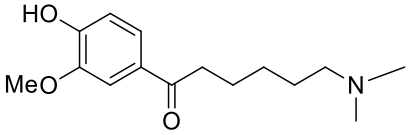

133

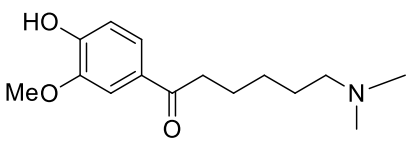

134

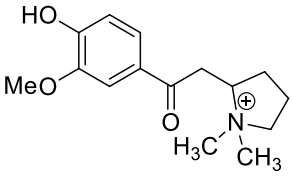

135

1.6.3 – *Ficus fistulosa* Reinw. ex Blume

F. fistulosa is an evergreen dioecious tree that can grow up to 10 m tall. It is distributed across India, South China, Taiwan and Malesia. *F. fistulosa* grows wildly in the forest at high altitudes up to 2000 m. The species is very variable in terms of morphology and position of the figs and thus it is further subdivided into at least 6 variations.[69] The focus of the present study was on *F. fistulosa* var. *tengerensis* (Miq.) Kuntze a variety of *F. fistulosa* found in Malesia.

1.6.4 *Ficus fistulosa* var. *tengerensis* (Miq.) Kuntze

The term tengerensis was first coined by the Dutch botanist Friedrich Anton Wilhelm Miquel in 1867 and it was assigned to a *Ficus* species (*Ficus tengerensis Miq.*).[72] In 1965, *Ficus tengerensis* was reduced to a variety under the species *Ficus fistulosa Reinw. ex Blume.* to become *Ficus fistulosa* var. *tengerensis*[73] and it was continued to be the accepted taxonomy of the species by later researchers such as Kochummen (1978). Berg and Corner in 2005 reclassified *Ficus fistulosa* var. *tengerensis* as a synonym to *Ficus fistulosa* without giving any further explanation.[69] However, in 2011 Berg published a paper titled "Corrective notes on the Malesian members of the genus *Ficus* (*Moraceae)*" in which he described both *Ficus fistulosa* and *Ficus fistulosa* var. tengerensis as two distinct varieties and gave a detailed description of the two plants.[74]

F. fistulosa var. *tengerensis* (Figure 1.6) is a small-leaved, ramiflorous (plants that have their fruits and flowers grow on branches and twigs) and evergreen tree. It is widely spread across the Malay Peninsula, Thailand, Sumatra, Java and Borneo. The tree can grow up to 20 m tall, and usually found on high altitudes up to 2000 m above sea level.[74]

Figure 1.6 – A) Foliage of *Ficus fistulosa* var. tengerensis. B) A close up of the fruit hanging from branches. C) A close up of the leaves with a hand to show relative size.

On the other hand, the other variety *F. fistulosa* is a large-leaved, cauliflorous (fruits and flowers grow on the main tree trunk) plant. It is distributed widely across South East Asia as well as mainland China, India, and Bangladesh. *F. fistulosa* is found on altitudes as high as 1700 m above sea level.[74]

Figure 1.7 – A) Fruits growing from the trunk of *Ficus fistulosa*. B) Profile shot of a leaf from *Ficus fistulosa* showing its shape and size.

The leaves and bark of *F. fistulosa* collected in Malaysia were previously investigated and resulted in the isolation of two new septicine-type alkaloids (i.e., fistulopsines A (**37**) and B (**38**)) and four known phenanthroindolizidine alkaloids, namely, septicine (**36**), tylophorine (**28**), tylocrebrine (**35**), and 3,6-didemethylisotylocrebrine (**39**).[42] However, an earlier investigation of *F. fistulosa* by Subramaniam et al. (2009) reported the isolation of a benzopyrroloisoquinoline alkaloid (i.e., (–)-fistulosine (**129**)) and three known phenanthroindolizidine and septicine-type alkaloids, namely, antofine (**25**), 14β-hydroxyantofine (**26**), and *seco*antofine (**33**).[43]

The previous investigation of *F. fistulosa* showed the potential of this un-investigated species to produce novel biologically active alkaloids. Thus, the closely related variety *F. fistulosa* var. tengerensis was chosen to be the focus of this study after a preliminary biological screening deemed the crude extract to possess cytotoxic activity. A large scale extraction was then performed with the intent of extensive chemical investigation of the alkaloidal content of the plant.

1.6 Research Objectives

The primary aim of the present research is to investigate the alkaloidal composition and biological activity of the alkaloids obtained from the leaves of *F. fistulosa* var. *tengerensis*, which was not previously investigated and was found to contain alkaloids. However, alkaloids were not detected in the bark material. The specific objectives of the present investigation are listed below:

- To extract the dried-ground leaf material with 95% ethanol and obtain crude alkaloid mixture from the bulk ethanolic extract using an acid-base method.
- To fractionate the crude alkaloid mixture into less complicated fractions using chromatography, and to isolate and purify alkaloids from semi-purified fractions using chromatography.
- To characterize and determine the structures of the pure compounds isolated via spectroscopic data analysis.
- To assess the biological activity of selected pure alkaloids *in vitro*.

Chapter Two

Results and Discussion

2.1 Overview

Investigation of the alkaloid content of *F. fistulosa* var. *tengerensis* leaves has provided five pure alkaloids. (±)-Tengerensine (**1**) and (±)-tengechlorenine (**2**) were obtained as novel alkaloids, while (±)-fistulosine (**3**), (+)-antofine (**4**) and (–)-*seco*-antofine (**5**) were known alkaloids. The dried leaves (15 Kg) were collected, extracted and eventually yielded 10.45g crude alkaloid mixture following the acid-base treatment. The yields of the alkaloids obtained from *F. fistulosa* var. *tengerensis* are shown in Table 2.1.

Table 2.1 – Alkaloid contents of *F. fistulosa* var. *tengerensis*

Alkaloid	Yield (mg/kg^{-1})
(±)-Tengerensine (**1**)	1.44
(±)-Tengechlorenine (**2**)	0.80
(±)-Fistulosine (**3**)	1.25
(S)-(+)-Antofine (**4**)	0.14
(*R*)-(-)-*Seco*antofine (**5**)	1.22

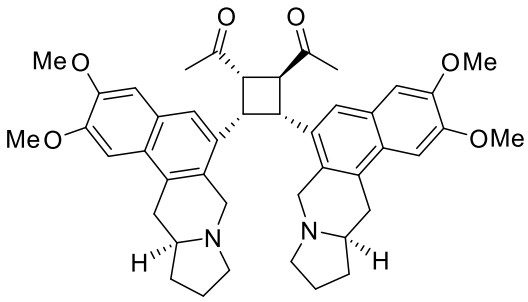

(±)-Tengerensine (**1**)

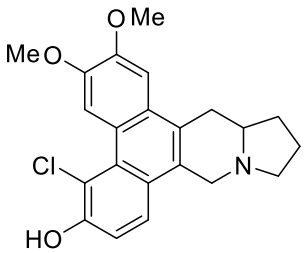

(±)-5-Chlorotylocrebrine (**2**)

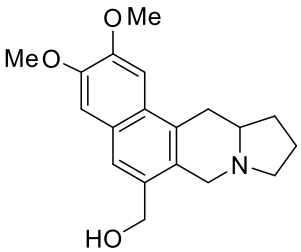

(±)-Fistulosine (**3**)

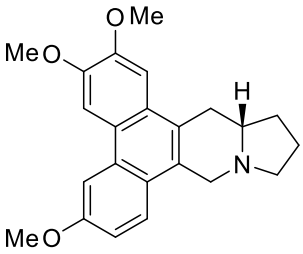

(*S*)-(+)Antofine (**4**)

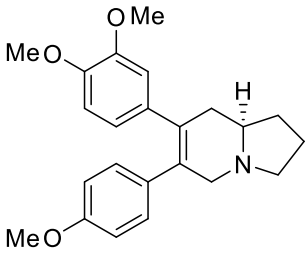

(*R*)-(–)-Seco-antofine (**5**)

During the isolation process of alkaloids from *F. fistulosa* var. *tengerensis*, chloroform was used as an eluting solvent for the fractionation of the main alkaloidal crude extract using vacuum column chromatography. The use of chloroform might have caused degradation of some alkaloids in the collected fractions. Phenanthroindolizidine alkaloids are extremely sensitive to light when they are in chloroform solution, due to the formation of isoquinolinum salts that can be recognised by their yellow appearance (Figure 2.1).[75]

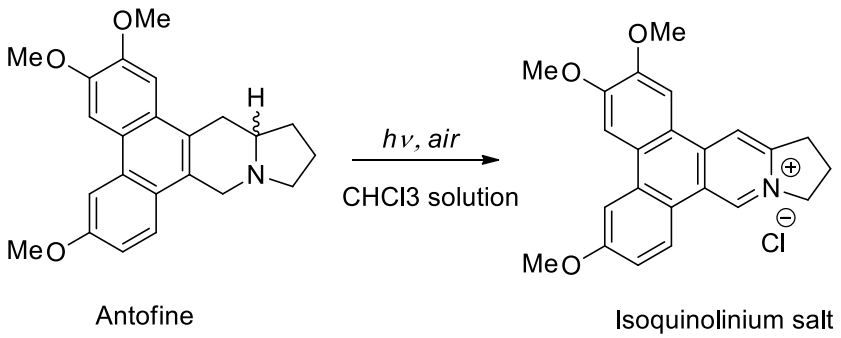

Figure 2.1 – The degradation of phenanthroindolizidines in $CHCl_3$ solution.

The isoquinolinuim salts of phenanthroindolizidines are highly stable under normal sample handling conditions. The reversal of the achiral isoquinolinium salt to give a racemic mixture of antofine for instance requires a very strong reducing agent such as, sodium borohydride, thus eliminating the possibility of artefact formation, due to chloroform use.[39] On the other hand, the highly polar isoquinolinium salts of phenanthroindolizidine affected the isolation process, with many fractions becoming too polar to be separated on the silica using normal phase chromatography. This effect was most prominent when performing TLC on those fractions where the salts showed virtually no separation and no movement on the normal phase silica even with highly polar mobile phase. Another effect could be attributed to the isoquinolinium salts is the extreme 'tailing' effect that could not be overcome with the addition of ammonia.

2.2 Structure Elucidation

2.2.1 Tengerensine (**1**)

Tengerensine (**1**) was obtained as light yellowish needles, $[\alpha]_D$ -0.7 (c 0.30, $CHCl_3$). The UV spectrum showed characteristic phenanthrene maxima at 239.0 and 331.8 nm (log ε 4.70 and 4.04 respectively). The IR spectrum showed a peak at 1702.2 cm^{-1}, which is characteristic of ketone function. HRESIMS measurements yielded the molecular formula $C_{44}H_{50}N_2O_6$ (21 degrees of unsaturation) with a protonated ion peak detected at m/z 703.37580 corresponding to ($C_{44}H_{50}N_2O_6$+H^+) (see appendix A).

The ^{13}C NMR spectrum (Table 2.2) accounted for 39 carbon signals out of the 44 determined by HRESIMS, indicating that five signals are overlapping. ^{13}C NMR data together with HSQC established the carbons in the structure as follows, six methyls, ten methylenes, six aliphatic methines, six aromatic methines, four oxygenated aromatic carbons, ten quaternary carbons and two carbonyls. The ^{13}C NMR spectrum suggested tengerensine to be a dimeric compound as most signals appearing in pairs.

The ^1H NMR spectrum (Table 2.2) showed the presence of six aromatic singlets (δ 6.55, 6.94, 6.95, 6.96, 7.04 and 7.51) suggesting the aromatic rings are substituted and fused together (naphthalenyl). This was also confirmed by the presence of 20 aromatic carbon signals indicating the presence of two naphthalenyl moieties. Furthermore, four distinct proton signals were observed as triplets at δ 4.02, 4.37, 4.54 and 4.84, an observation suggesting the presence of a tetra-substituted cyclobutane ring. The suggestion was verified by COSY and HSQC correlations. In addition, six methyl singlets were observed in the ^1H NMR spectrum, four of which are characteristic of *O*-methyl singlets at δ 3.76, 3.91, 3.94 and 3.98. The other two methyl singlets at δ 1.65 and 2.31 were assigned to the acetyl groups from the observed HMBC ^3J correlations with the two carbonyls at δ_C 206.27 and 207.82, respectively.

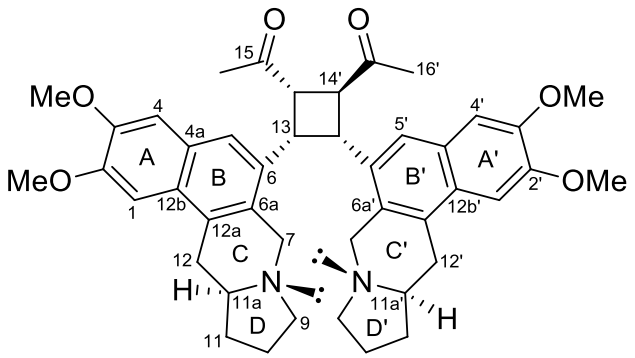

Figure 2.2 – Gross structure of tengerensine (**1**)

Table 2.2 – ^{1}H, ^{13}C NMR and HMBC data of tengerensine (**1**)

Position	^{1}H	^{13}C	HMBC	
			^{2}J	^{3}J
1	6.96 s	101.51	C-2	C-3, C-4a
2	-	149.36		
3	-	148.59		
4	6.55 s	106.98		C-5, C-2, C-12b
4a	-	128.98[c]		
5	6.94 s	124.84		C-4, C-13
6	-	129.26		
6a	-	126.94[c]		
7	3.47 m	55.51[a]		C-11a
	4.37 d (13.7)			
9	2.33 m	55.51[a]	C-10	C-11, C-11a
	3.43 m			
10	1.82 m[d]	21.55	C-11	C-11a
	1.92 m[d]			
11	1.70 m	31.14	C-10	C-12
	2.19 m			
11a	2.16 m	60.05	C-12	C-10
12	2.74 m	33.51	C-11a	C-11
	3.16 dd (15, 2)			
12a	-	128.67[c]		
12b	-	126.53		
13	4.54 t (10)	39.42		C-5, C-14’, C-15
14	4.02 t (10)	50.60	C-14’	C-6, C-15’
15	-	206.27		
16 (CH_3)	1.65 s	28.43	C-15	C-14
2-OMe	3.94 s	55.69[b]		C-2
3-OMe	3.76 s	55.75[b]		C-3
1’	6.96 s	101.85	C-12b’	C-3’
2’	-	149.19		
3’	-	148.79		
4’	7.04 s	106.73		C-2’, C-5’, C-12b’
4a’	-	129.67[c]		
5’	7.51 s	123.02		C-4’, C-13’
6’	-	130.87		
6a’	-	127.38[c]		
7’	2.75 d (14.5)	53.70		C-11a’
	4.16 d (14.5)			
9’	2.16 m	55.16[a]		C-11’, C-11a’
	3.34 m			
10’	1.95 m[d]	21.55	C-11’	
	2.04 m[d]			
11’	1.58 m	31.14		C-9’, C-12’
	2.05 m			
11a’	1.83 m	60.05		C-7’
12’	2.64 m	33.14	C-11a’	C-11’
	3.04 d (15)			
12a’	-	128.87[c]		
12b’	-	126.63		
13’	4.39 m	40.88	C-6’, C-13	C-5’, C-15’
14’	4.84 t (10)	47.78		C-6’, C-15
15’	-	207.82		
16’ (CH_3)	2.31 s	29.05	C-15’	C-14’
2’-OMe	3.91 s	55.75[b]		C-2’
3’-OMe	3.98 s	55.81[b]		C-3’

[a-d] signals are interchangeable. $CDCl_3$, 600 MHz (^{1}H), 150 MHz (^{13}C)

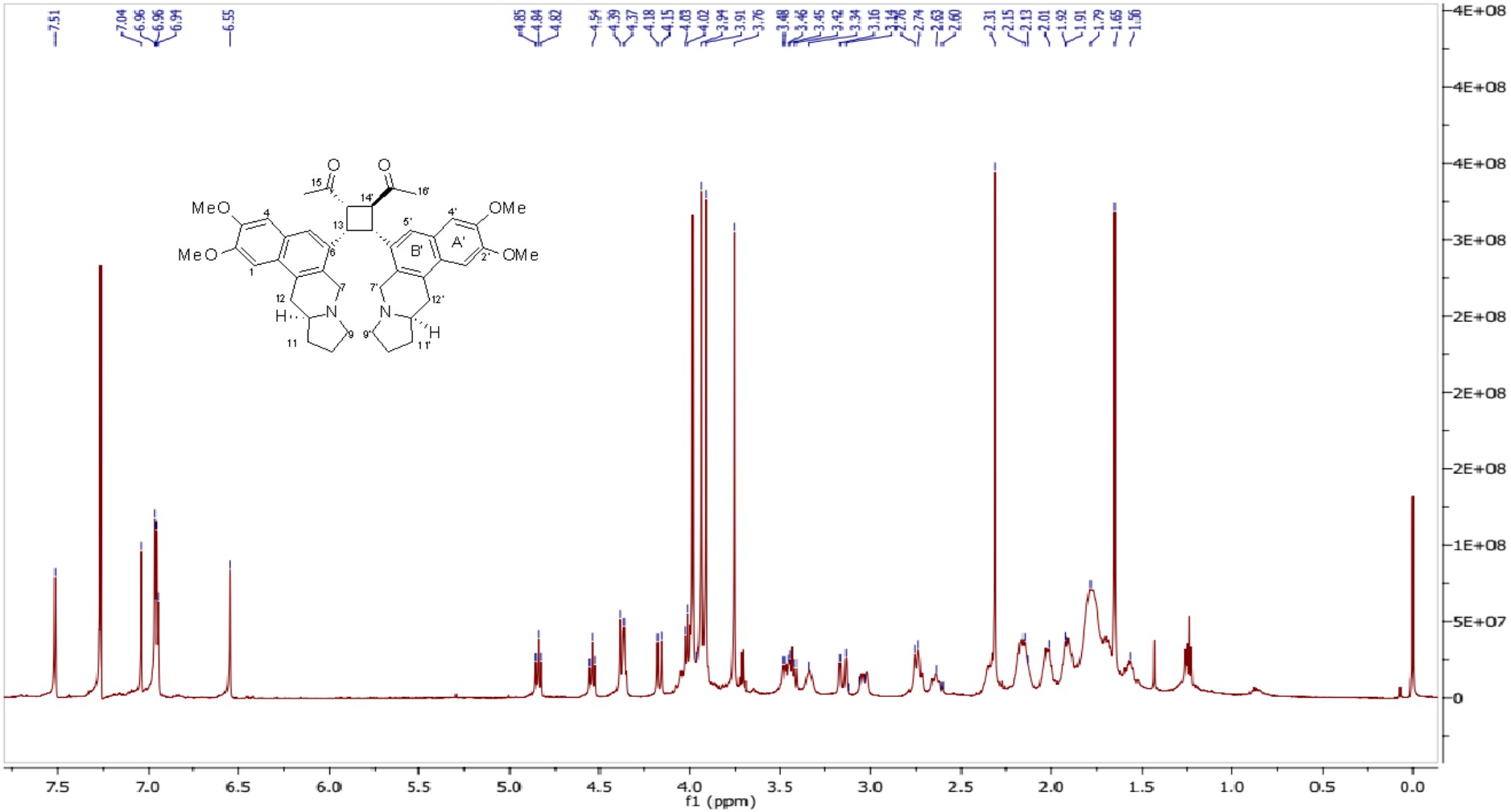

Figure 2.3 – Structure and ^{1}H NMR spectrum of **1**

The structure of **1** as well as its relative configuration were determined by 1D and 2D NMR data analysis. The relatively large molecular mass compared to known phenanthroindolizidines and benzopyrroloisoquinoline, as well as the presence of two sets of signals in both ^{13}C and ^{1}H NMR spectra further indicated **1** to be a dimeric molecule. The tetra-substituted cyclobutane ring (C-13 – C-14–C-14'–C-13'), which was alluded to above, was the starting point to connect other partial structures together by using correlations in the HMBC spectrum. The first connections to the cyclobutane ring (at C-14 and C-14') were by the two acetyl groups, i.e., the C-15–C-16 and C-15'–C-16' fragments, based on HMBC correlation from H-16 to C-14, and from H-16' to C-14'. Based on the HMBC data, the four *O*-methyl singlets at δ_H 3.76, 3.91, 3.94 and 3.98 were assigned to their place by the correlations observed from 2-OMe to C-2; 3-OMe to C-3; 2'-OMe to C-2'; and 3'-OMe to C-3'. Thus the naphthalene rings A, B, A', and B' were partially characterized and their connections to the cyclobutane ring were established by the long-range correlations from H-13 to C-5 and C-6a (for the B ring) and correlations from H-13' to C-5' and C-6a' (for B' ring). Due to severe overlapping of ^{1}H NMR resonances, establishment of the indolizidine moieties of tengerensine (**1**) was not possible by using COSY data alone. However, the presence of ^{13}C resonances due to two aminomethine carbons at δ_C 60.05 (x 2C) as well as four aminomethylene carbons at δ_C 55.51 (x 2C), 53.70 and 55.16, indicated the presence of the two indolizidine moieties fused to both of the naphthalene rings. This was further confirmed by comparison of the NMR data of **1** with those of fislutosine, a benzopyrroloisoquinone alkaloid recently obtained from another *Ficus* species (Table 2.3).[43] The structure proposed is consistent with the molecular formula established by the HRESIMS measurements as well as the full HMBC data. The gross structure of tengerensine (**1**) is shown in Figure 2.2, while Figure 2.4 shows the key HMBC correlations.

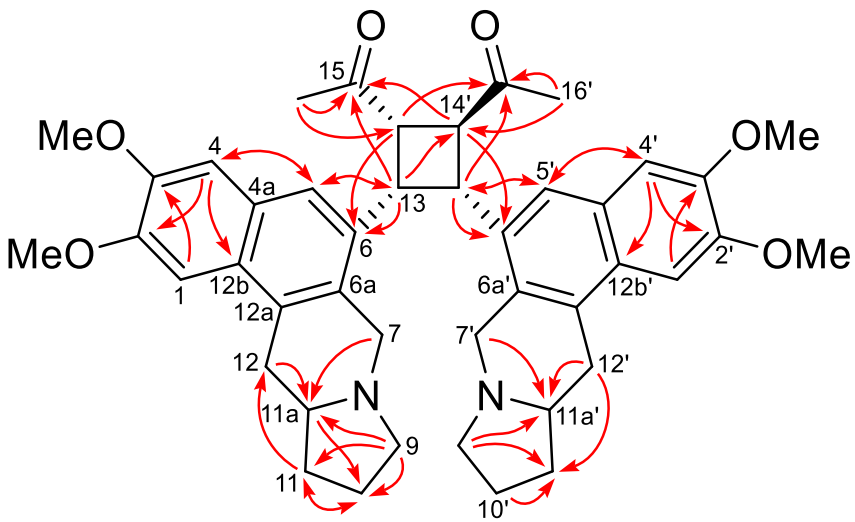

Figure 2.4 – Selected HMBC's of **1**

Table 2.3 - Comparison of NMR data between **1** and fistulosine.[43]

Tengerensine (**1**)						Fistulosine		
Position	^{1}H	^{13}C	Position	^{1}H	^{13}C	Position	^{1}H	^{13}C
1	6.96 *s*	101.51	1’	6.96 *s*	101.85	1	7.15, *s*	103.2
2	-	149.36	2’	-	149.19	2		150.5
3	-	148.59	3’	-	148.79	3		150.0
4	6.55 *s*	106.98	4’	7.04 *s*	106.73	4	7.11, *s*	108.0
4a	-	128.98[c]	4a’	-	129.67[c]	4a		128.6
5	6.94 *s*	124.84	5’	7.51 *s*	123.02	5	7.56, *s*	124.7
6	-	129.26	6’	-	130.87	6		134.9
6a	-	126.94[c]	6a’	-	127.38[c]	6a		129.9
7	3.47 *m*	55.51[a]	7’	2.75 *d* (14.5)	53.70	7	3.43 d (14.9)	53.8
	4.37 *d* (13.7)			4.16 *d* (14.5)			4.28 d (14.9)	
9	2.33 *m*	55.51[a]	9’	2.16 *m*	55.16[a]	9	2.35 q	55.7
	3.43 *m*			3.34 *m*			3.37 s	
10	1.82 *m*[d]	21.55	10’	1.*95 m*[d]	21.55	10	1.91 m	22.5
	1.92 *m*[d]			2.04 *m*[d]			2.01 m	
11	1.70 *m*	31.14[a]	11’	1.58 *m*	31.14[a]	11	1.72 m	32.2
	2.19 *m*			2.05 *m*			2.23, m	
11a	2.16 *m*	60.05[b]	11a’	1.83 *m*	60.05[b]	11a	2.43, m	61.2
12	2.74 *m*	33.51	12’	2.64 *m*	33.14	12	2.87, m	34.0
	3.16 *dd* (15, 2)			3.04 *d* (15)			3.37, m	
12a	-	128.67[c]	12a’	-	128.87[c]	12a	-	129.9
12b	-	126.53	12b’	-	126.63	12b	-	128.2
13	4.54 *t* (10)	39.42	13’	4.39 *m*	40.88	13	4.70 s	64.1
14	4.02 *t* (10)	50.60	14’	4.84 *t* (10)	47.78	-	-	
15	-	206.27	15’	-	207.82	-	-	-
16	1.65 *s*	28.43	16’	2.31 *s*	29.05	-	-	-
2-OMe	3.94 *s*	55.69[b]	2’-OMe	3.91 *s*	55.75[b]	2-OMe	4.02 s	56.8
3-OMe	3.76 *s*	55.75[b]	3’-OMe	3.98 *s*	55.81[b]	3-OMe	4.00 s	56.8

[a-d] signals are interchangeable

The relative configuration of tengerensine (**1**) was determined using the key NOESY correlations observed for hydrogens attached to the stereogenic centres C-13, C-14, C-14' and C-13'. NOESY correlations from H-5 and H-5' to H-14' as well as from H-7 to H-7' suggests that the two indolizidine partial structures of the benzopyrroloisoquinoline moieties were pointing toward one another, while the naphthalenyl part of the benzopyrroloisoquinoline moieties were pointing away from each other. NOESY correlations from H-5 and H-5' to H-14' also indicates that both the benzopyrroloisoquinoline moieties are on the same face of the cyclobutane ring, i.e., both H-13 and H-13' are cis to each other. NOESY correlations from H-7' to H-13 and H-13' further confirmed the previous statement. On the other hand, the absence of NOESY correlation between H-5/H-5' and H-14 suggested that H-14 have opposite orientation to the benzopyrroloisoquinoline moieties and that H-14 and H-14' are *trans* to each other. Furthermore, the presence of NOESY correlations from H-7 to H-13; H-5 to H-14'; H-7' to H-13'; and H-5' to H-14' dictated that both H-13' and H-14' were *trans* to each other. Taken together, it can be concluded that the cyclobutane ring in **1** was *cis*,*trans*,*trans*-configured, i.e., H-13, H-14, and H-13' were on the same face, while H-14' on the opposite face of the cyclobutane ring (Figure 2.5).

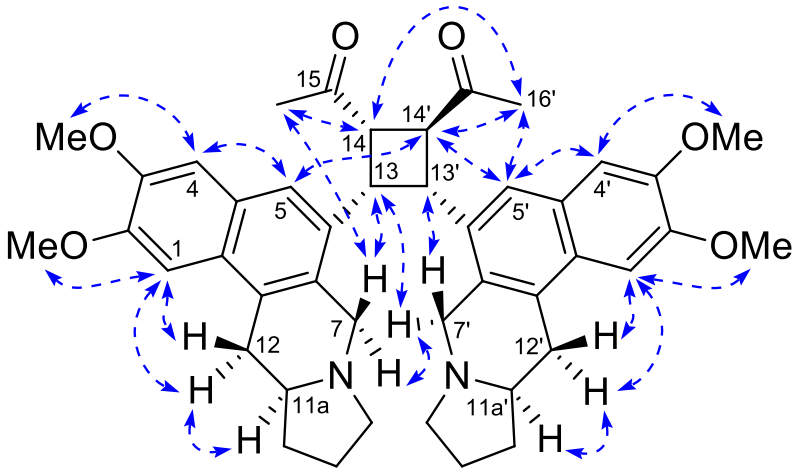

Figure 2.5 – Selected NOESY correlations of tengerensine (**1**)

Since tengerensine (**1**) affords suitable crystals from CH_2Cl_2/CH_3OH, an X-ray diffraction analysis was carried out. The X-ray structure (Figure 2.6) is in agreement with the proposed structure so far disclosed, including the relative configuration determined by the NOESY correlations. Additionally, the X-ray analysis showed an interesting feature in **1** where the configuration of the two stereocentres at C-11a and C-11a' are opposite to each other. This means that if the buten-2-one side chains were to be disregarded, both monomeric benzopyrroloisoquinoline halves are in fact enantiomers.

The X-ray crystal structure (Figure 2.6) also revealed that the acetyl group at C-14 is in the vicinity of an aromatic shielding zone, thus providing an explanation for the notably shielded acetyl signal (δ_H 1.65, Me-16) observed in the ^{1}H NMR spectrum.

The crystals of **1** were triclinic (crystal system having three unequal oblique axes) with a space group of P–1 (a centrosymmetric space group), indicating a racemic mixture of two enantiomers. This is consistent with the fact that **1** was virtually optically inactive. Chiral HPLC separation of the two enantiomers was performed and afforded (+)-**1** and (–)-**1** in a ratio of approximately 1:1 (Figure 2.7).

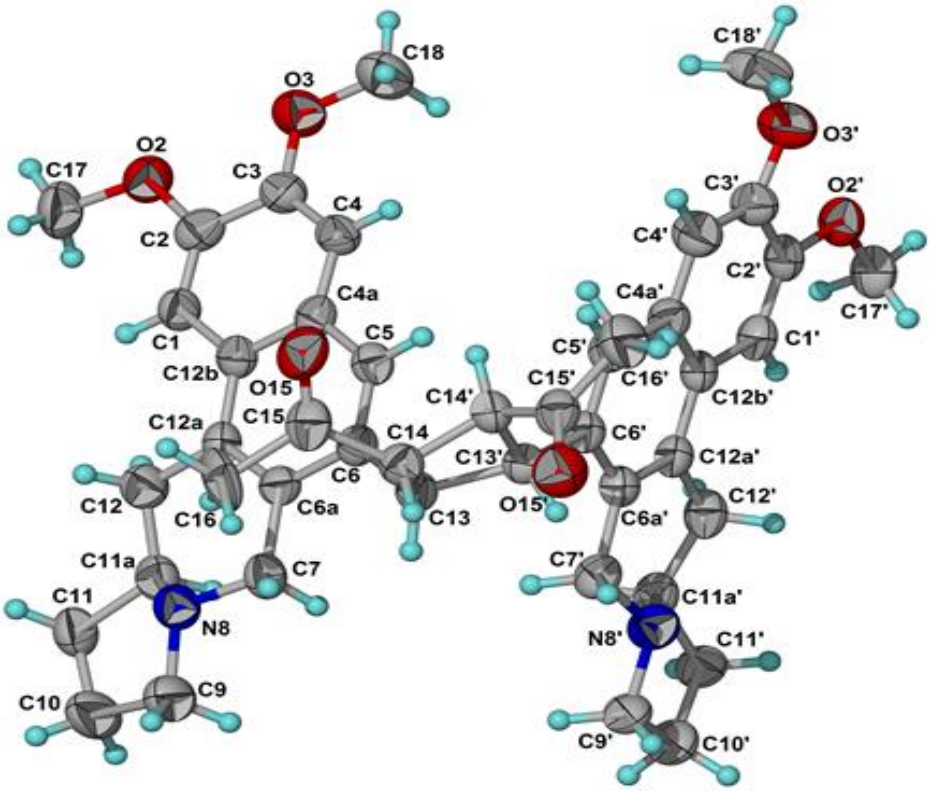

Figure 2.6 – X-Ray crystal structure of (±)-tengerensine (**1**) obtained by single-crystal X-ray diffraction analysis using Cu K α radiation

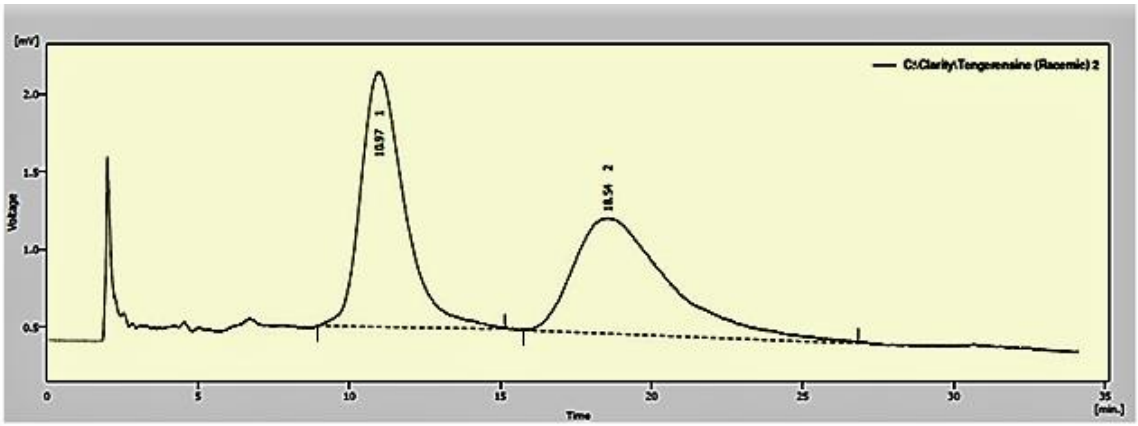

Result Table (Uncal - C:\Clarity\Tengerensine (Racemic) 2)

	Reten. Time [min]	Start Time [min]	End Time [min]	Start Value [mV]	End Value [mV]	Area [mV.s]	Height [mV]	Area [%]	Height [%]	W05 [min]
1	10.970	8.942	15.170	0.508	0.486	164.072	1.842	50.1	68.6	1.46
2	18.543	15.770	26.843	0.479	0.393	163.517	0.750	49.9	31.4	3.12
	Total	Total	Total	Total	Total	327.590	2.392	100.0	100.0	

Figure 2.7 – Chiral HPLC chromatogram for the separation of (±)-tengerensine (**1**) with 1:1 enantiomeric ratio

The two separated enantiomers of (±)-tengerensine (**1**) were then subjected to electronic circular dichroism (ECD) analysis which as expected showed opposite Cotton effects (Figure 2.8). Finally, comparison of the experimental and calculated ECD spectra (Figure 2.7) of the enantiomers allowed the absolute configurations of (+)-**1** and (–)-**1** to be established as 11a*S*,13*S*,14*S*,11a'*R*,13'*R*,14'*S* and 11a*R*,13*R*,14*R*,11a'*S*,13'*S*,14'*R*, respectively.

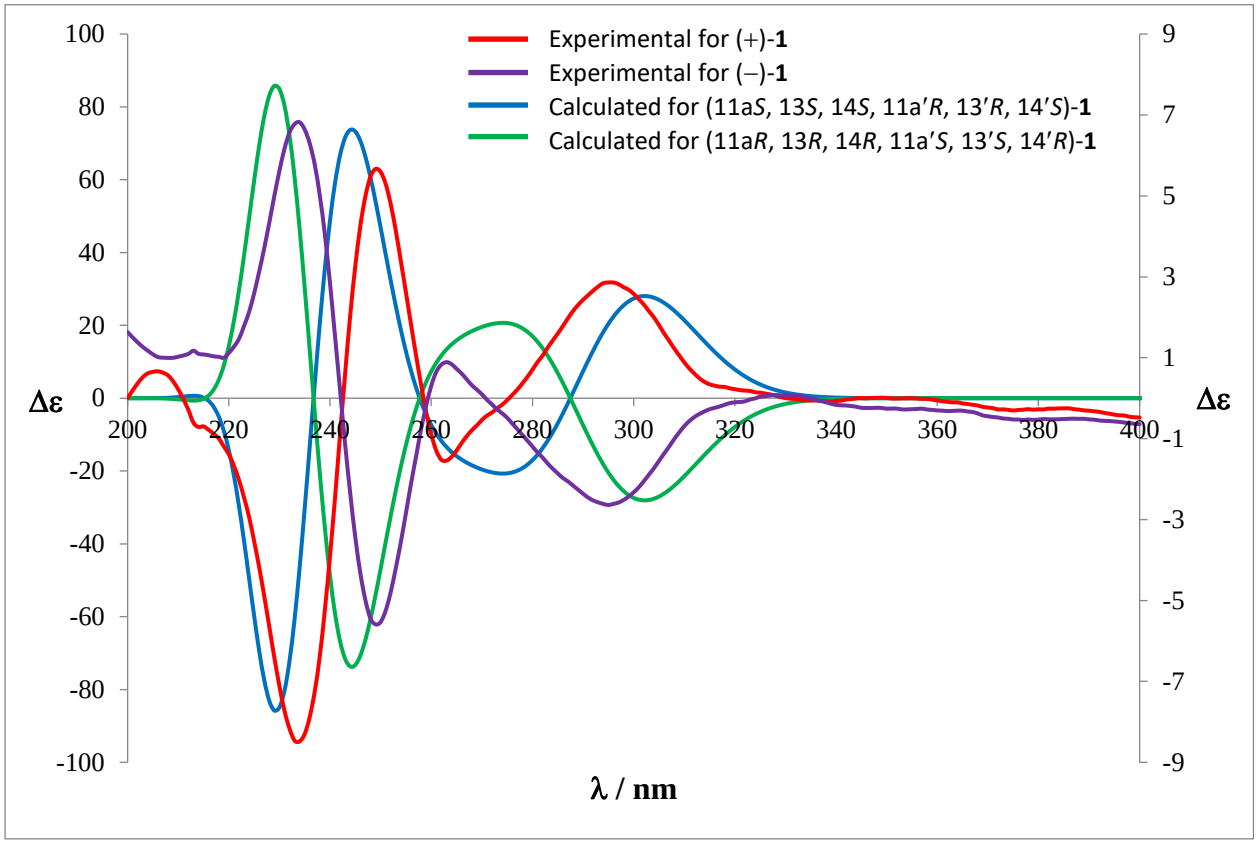

Figure 2.8 Experimental and calculated ECD spectra of (+)-**1** and (–)-**1**.

Cyclobutane-containing secondary metabolites occur widely in bacteria, fungi, plants and marine invertebrates. These compounds have an exclusive non-enzymatic biosynthetic pathway. They are formed by photochemical [2+2] cycloaddition reaction, a mechanism involving the reaction of two alkenes where the π electrons of two alkene groups form two C–C bonds with each other (Scheme 2.1).[76]

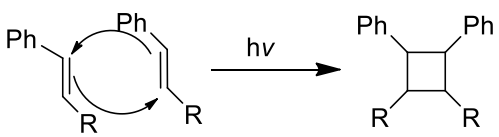

Scheme 2.1 – General mechanism of cyclobutane formation via 2+2 cycloaddition.

The stereochemistry of this non-enzymatic reaction depends on the configuration around the double bound of the alkene precursors (Scheme 2.2). The stereochemistry is usually symmetrical at the cyclobutane ring because the starting alkenes in most cases have the same configuration, i.e., either 'cis + cis' or '*trans* + *trans*'.[76]

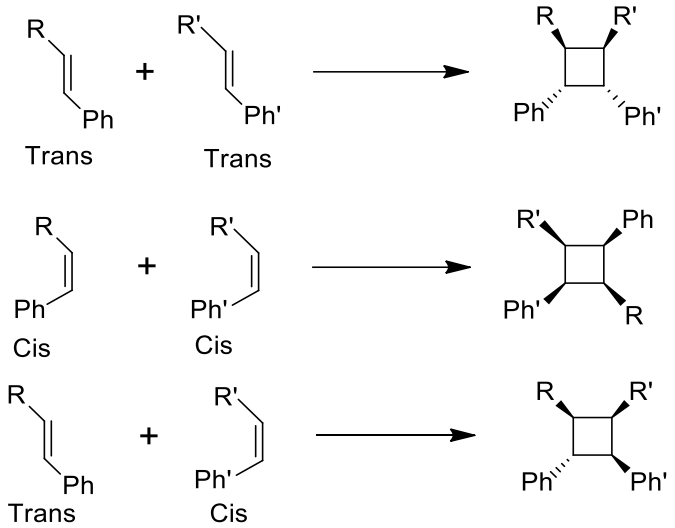

Scheme 2.2 – Possible stereochemical outcomes of [2+2] cycloadditions

In the case of tengerensine **1** the two stereoisomeric benzopyrroloisoquinoline alkene monomers reacting to form **1** have an opposite configuration at the C-11a stereogenic centre according to the X-ray data. Another key observation from the X-ray 3D structure of **1** is that the cyclobutane is unsymmetrical which in turn means that the two benzopyrroloisoquinoline alkene monomers are each incorporating either a Z- or E-double bond in the bute-2-one side chain.

The structure of tengerensine (**1**) therefore represents a rare instance of an unsymmetrical cyclobutane dimeric adduct and the first example of a dimeric benzopyrroloisoquinoline alkaloid. A possible partial biosynthetic pathway is shown in Scheme 2.3.

Scheme 2.3 – Partial biosynthetic pathway to (±)-**1**.

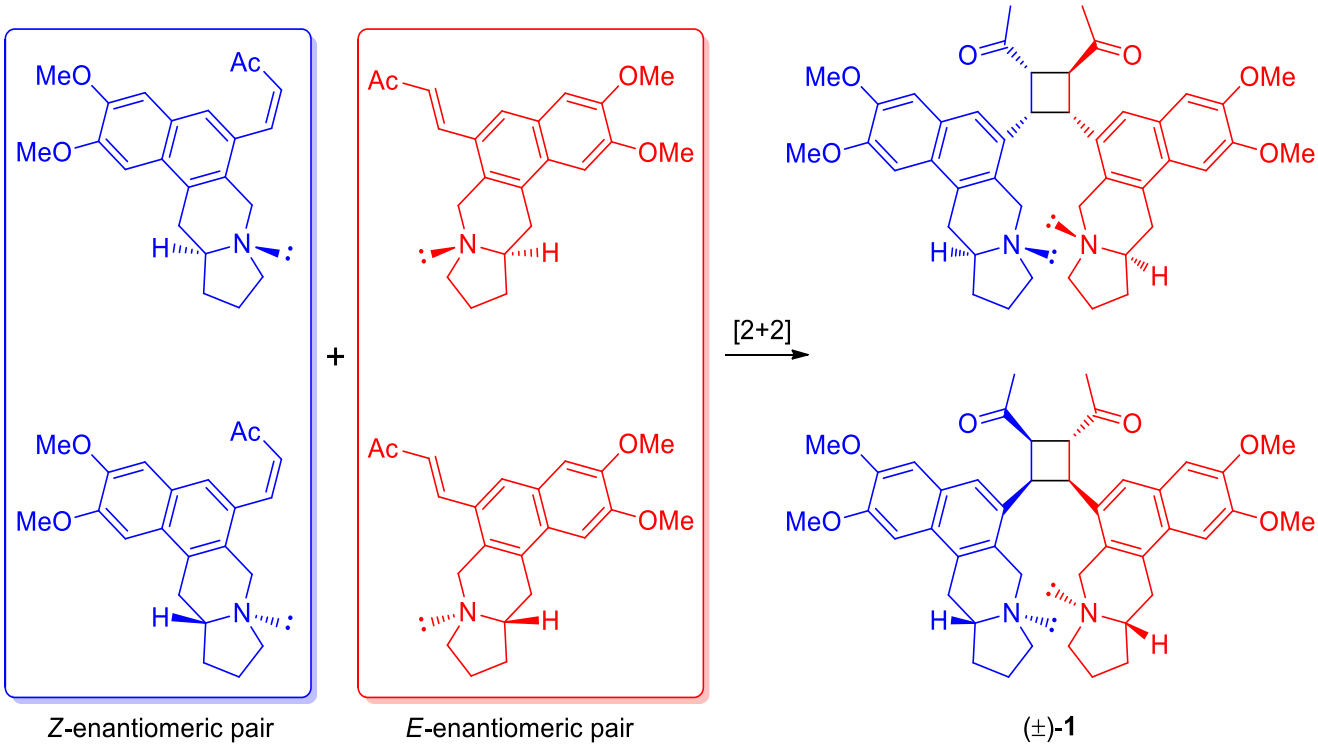

2.2.2 Tengechlorenine (**2**)

Alkaloid **2** was isolated as colourless crystals (mp 192 – 195 °C), with $[\alpha]_D$ + 11.4 (*c* 0.08, $CHCl_3$). The UV spectrum showed characteristic phenanthrene absorption maxima at 232, 269, 347.40 and 366 nm. HRESIMS gave a protonated molecular ion peak at m/z 398.15115, which was unintelligible at first (Appendix B).

The ^{1}H NMR spectrum (Table 2.4) revealed the presence of one 1,2,4,5-tetrasubstituted benzene ring [δ 9.39 (1H, s), 7.32 (1H, s)] and one 1,2,3,4-tetrasubstituted benzene ring [δ 7.79 (1H, d, *J*=9), 7.27 (1H, d, *J*=9)]. The signal at δ 9.39 indicates that the affected hydrogen is in the proximity of a lone-pair electrons bearing atom, where the lone-pair electrons of that atom are causing a paramagnetic anisotropic deshielding on that hydrogen. This phenomenon is termed paramagnetic anisotropic effect and it is affected by non-bonding electrons, as opposed to diamagnetic anisotropy which is caused by the bonding σ and π electrons. Such significantly deshielded aromatic protons are associated with phenanthroindolizidines having a lone-pair bearing atom at C-5 when a hydrogen is present at C-4 and *vice versa* (Figure 2.9).[53]

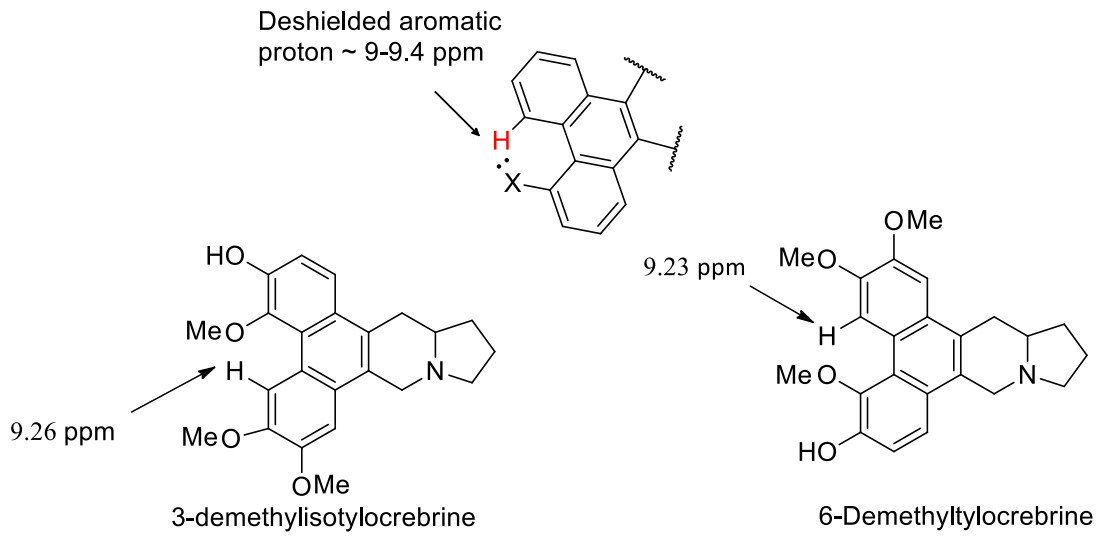

Figure 2.9 – Significantly deshielded aromatic protons due to paramagnetic anisotropic deshielding in 3-demethylisotylocrebrine and 6-demethyltylocrebrine

Additionally, the ^{1}H NMR spectrum showed two characteristic AX doublets at δ 4.62 (1H, d, *J*=14.8) and 3.66 (1H, d, *J*=14.8) corresponding to a pair of isolated benzylic methylene hydrogens bound to an electron-withdrawing heteroatom, i.e., H_2C-9–N (Figure 2.10). The noticeably different chemical shifts of the two geminal hydrogens can be explained by their spatial orientation in the ring. The

proton that is closer in space to the lone pair electrons of nitrogen is significantly deshielded (paramagnetic deshielding).

Table 2.4 – ^{1}H, ^{13}C and HMBC NMR data of **2**

Position	**^{1}H**	**^{13}C**	**HMBC**
1	7.32 *s*	103.45	C-2,C-3, C-14a, C-4a
2	-	148.96	
3	-	146.68	
4	9.39 *s*	109.83	C-3, C-2, C-4b
4a	-	123.16[b]	
4b	-	128.34	
5	-	118.34	
6	-	153.88	
7	7.27 *d* (9)	111.29	C-5, C-6, C-8a
8	7.79 *d* (9)	122.01	C-5, C-6, C-8b
8a		126.31	
8b		127.79	
9	4.62 *d* (14.8)	54.21	C-8a, C-13a
	3.66 *d* (14.8)		
11	3.45 *td* (8.5, 1.7)	55.08	C-12, C-13, C-13a
	2.44 *m*		
12	1.92 *m*	21.70	C-11, C-13
	2.02 *m*		
13	2.23 *m*	31.27	C-12
	1.77 *m*		
13a	2.47 *m*	60.04	C-12, C-9
14	3.29 *dd* (15.7, 2.4)	33.96	C-13a, C-8b
	2.90 *m*		
14a	-	127.12	
14b	-	126.38[b]	
2-OMe	4.06 s	55.80[a]	C-2
3-OMe	4.08 s	56.03[a]	C-3
6-OMe	4.05 s	57.00	C-6

[a,b] Overlapping signals, $CDCl_3$, 600 MHz (^{1}H), 150 MHz (^{13}C)

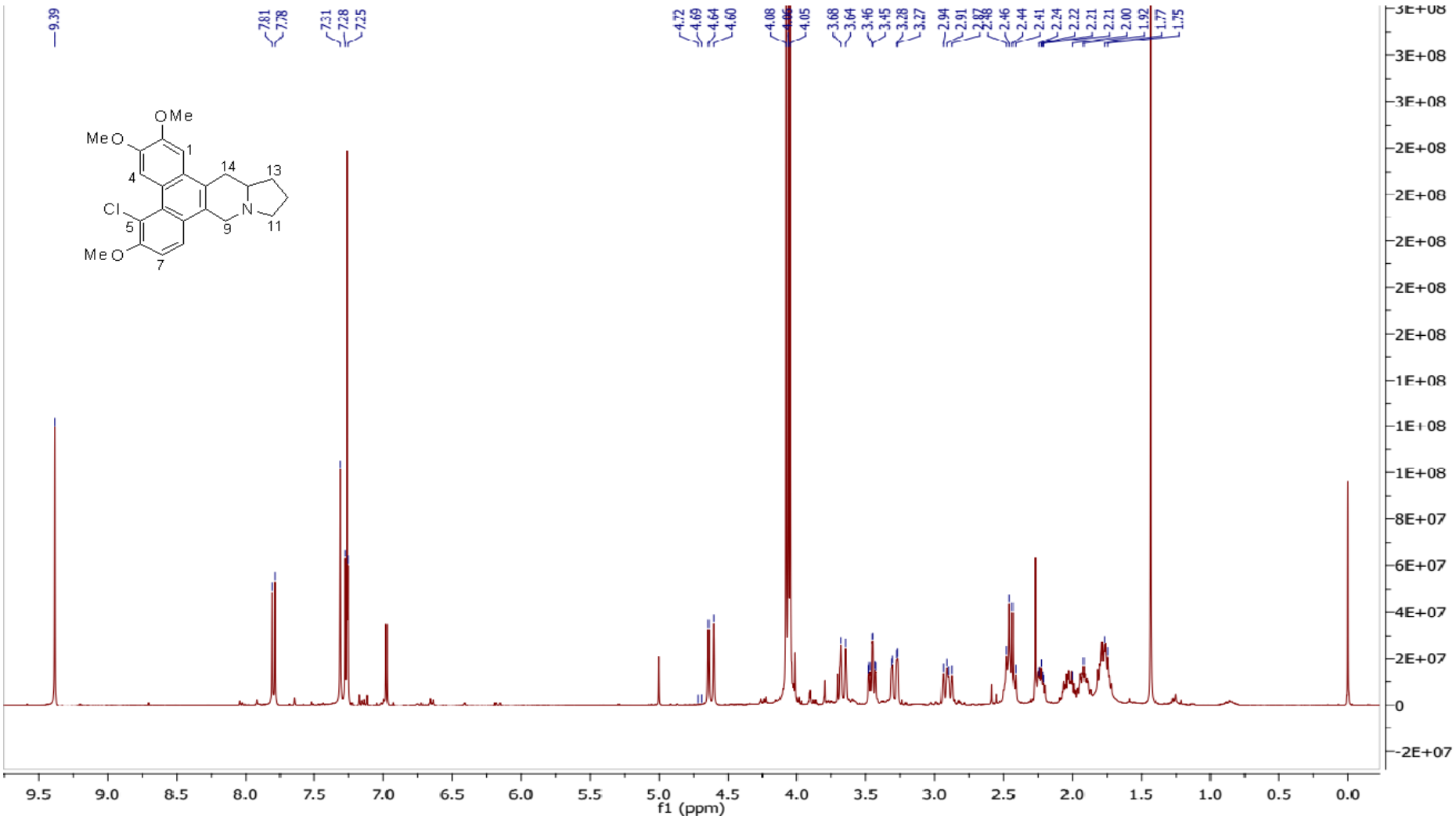

Figure 2.10 – Structure and ^{1}H NMR spectrum of **2**

The ^{1}H NMR also showed three aromatic methoxy singlets at δ 4.05, 4.06 and 4.08. The signals appearing in the region between 1.0 and 4.7 ppm bear a general resemblance to those of phenanthroindolizidine alkaloids with an unsubstituted indolizidine moiety.[41 51]

A search through the literature for phenanthroindolizidines that possess an unsubstituted indolizidine moiety, three aromatic methoxy groups and a paramagnetic deshielded aromatic proton (δ > 9 ppm), which are present in the ^{1}H NMR spectrum of **2**, yielded only two alkaloids, *viz.*, 6-demethyltylocrebrine and 3-demethylisotylocrebrine (Figure 2.9). Although both alkaloids possess almost identical ^{1}H NMR spectra to that of alkaloid **2**, the HRESIMS data of **2** suggested otherwise. Thus, more extensive study of the 2D NMR was needed to establish the structure of **2.**

The ^{13}C NMR spectrum (Table 2.4) showed a total of 23 carbon signals. With the aid of the HSQC spectrum, the 23 carbon signals were determined to be due to fourteen aromatic carbons (including three oxygenated quaternary carbons), three methoxy carbons, five methylene (including two aminomethylene) carbons and one aminomethine carbon.

The presence of the unsubstituted indolizidine moiety was further confirmed by the COSY spectrum that showed the partial structure $NCH_2CH_2CH_2CHCH_2$ which corresponds to the N–C-11–C-12–C-13–C-13a–C14 fragment (Figure 2.11). NOESY correlations observed between H-8/H-9, H-1/H-14, 2-OMe/H-1, 6-OMe/H-7, together with HMBC correlations from H-1 to C-3, H-4 to C-2, H-7 to C-5 and H-8 to C-6, unambiguously established the substitution pattern on the phenanthrene ring with the three methoxy groups being placed at C-2, C-3 and C-6 (Figure 2.11). To explain the noticeably deshielded H-4 (δ 9.39) the aromatic C-5 must be substituted with a lone pair electrons bearing atom. However, the carbon chemical shift of C-5 was too low to be an oxygenated aromatic carbon, i.e., 118.34 ppm, suggesting that the substituent is a halogen atom instead. This was in agreement with the HRESIMS data that showed a protonated ion peaks at m/z 398.15115 and 400.15070, both corresponding to $[C_{23}H_{24}{}^{35}ClNO_3+H]^+$ and $[C_{23}H_{24}{}^{37}ClNO_3+H]^+$, with an intensity ratio of 3:1 (confirming that **2** must contain a chlorine atom).

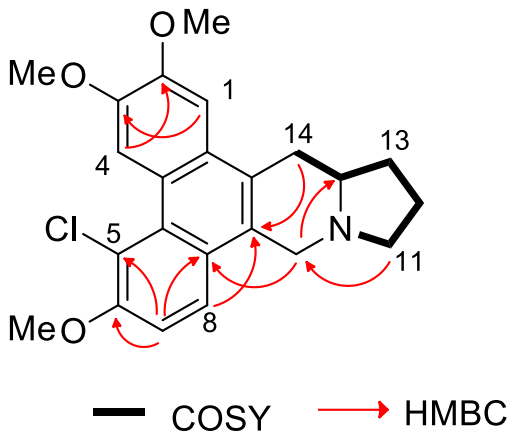

Figure 2.11 – COSY and selected HMBC's of tengechlorenine **2**

The structure of **2**, which was established via detailed examination of the spectroscopic data were further confirmed by X-ray crystallographic analysis since suitable crystals were obtained (Figure 2.12). The crystals of **2** were triclinic with a space group of P–1 (a centrosymmetric space group), indicating a racemic mixture of two enantiomers. However, the optical activity observed for the sample solution of **2**, suggested that **2** existed as a mixture of enantiomers with enantiomeric excess of one component.

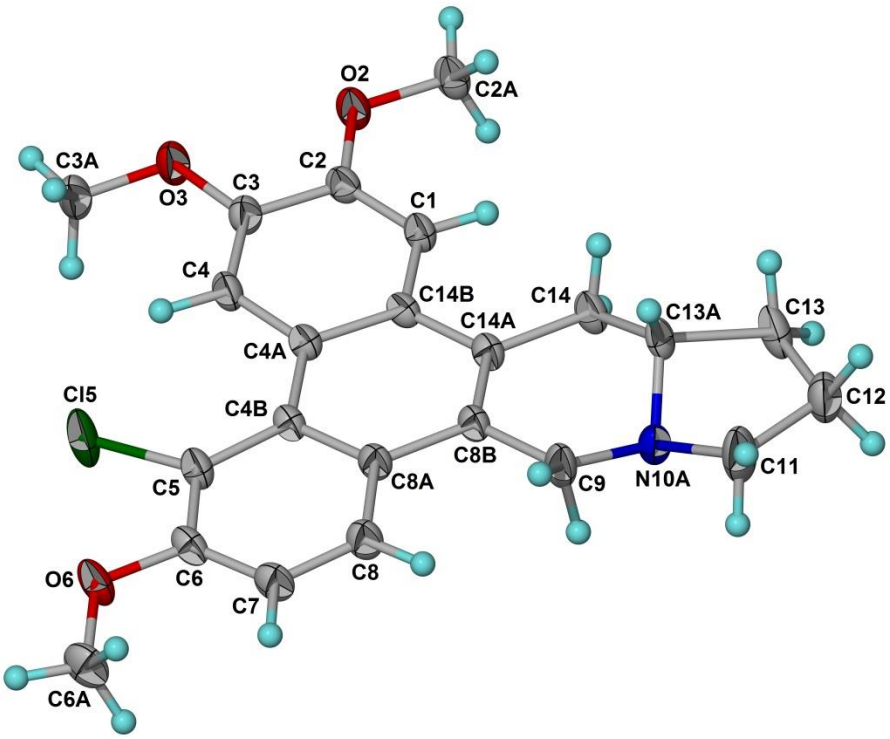

Figure 2.12 – X-ray diffraction analysis of **2**

The isolation of some phenanthroindolizidine alkaloids as a mixture of both enantiomers is a well-documented phenomenon. According to literature, some naturally occurring phenanthroindolizidines were isolated as pairs of enantiomeric mixtures with one enantiomer being in slight excess, which may explain the significantly lower optical activity of those naturally isolated compounds compared to their pure enantiomeric synthetic counterparts. It also appeared that modification of the isolation process had no effect on the phenomenon, e.g., increased heating during extraction or isolation of the alkaloids.[75]

(±)-Tengechlorenine (**2**) represents the first naturally occurring halogenated phenanthroindolizidine alkaloid to be discovered, which reopens the door for the diversity of this class of alkaloids and the possibilities of new and possibly more biologically active phenanthroindolizidines.

Halogenated natural products were once considered as rare and sometimes termed as "biological mistakes" with only dozen known examples in the 1950s. However, by 2015 more than 5000 halogenated natural products have been isolated and fully characterized. Multiple theories and evidences have been gathered and discussed to explain the biosynthesis of these compounds, such as, the involvement of halogenating enzymes that are either highly specific (targeting one substrate usually an amino acid) or less specific enzymes known as haloperoxidases (HPO).[77]

As mentioned in section 1.3.2, a biosynthetic study using radiolabeled carbon was carried out and determined phenanthroindolizidines are derived from tyrosine, orthinine and phenylalanine. Since tyrosine is the primary targeted molecule of multiple $FADH_2$-dependent plant halogenases, the halogenation of tyrosine probably took place in an early integrated step of this multi-enzymatic biosynthesis.[77] Scheme 2.4 shows a possible pathway for the biosynthesis of **2**.

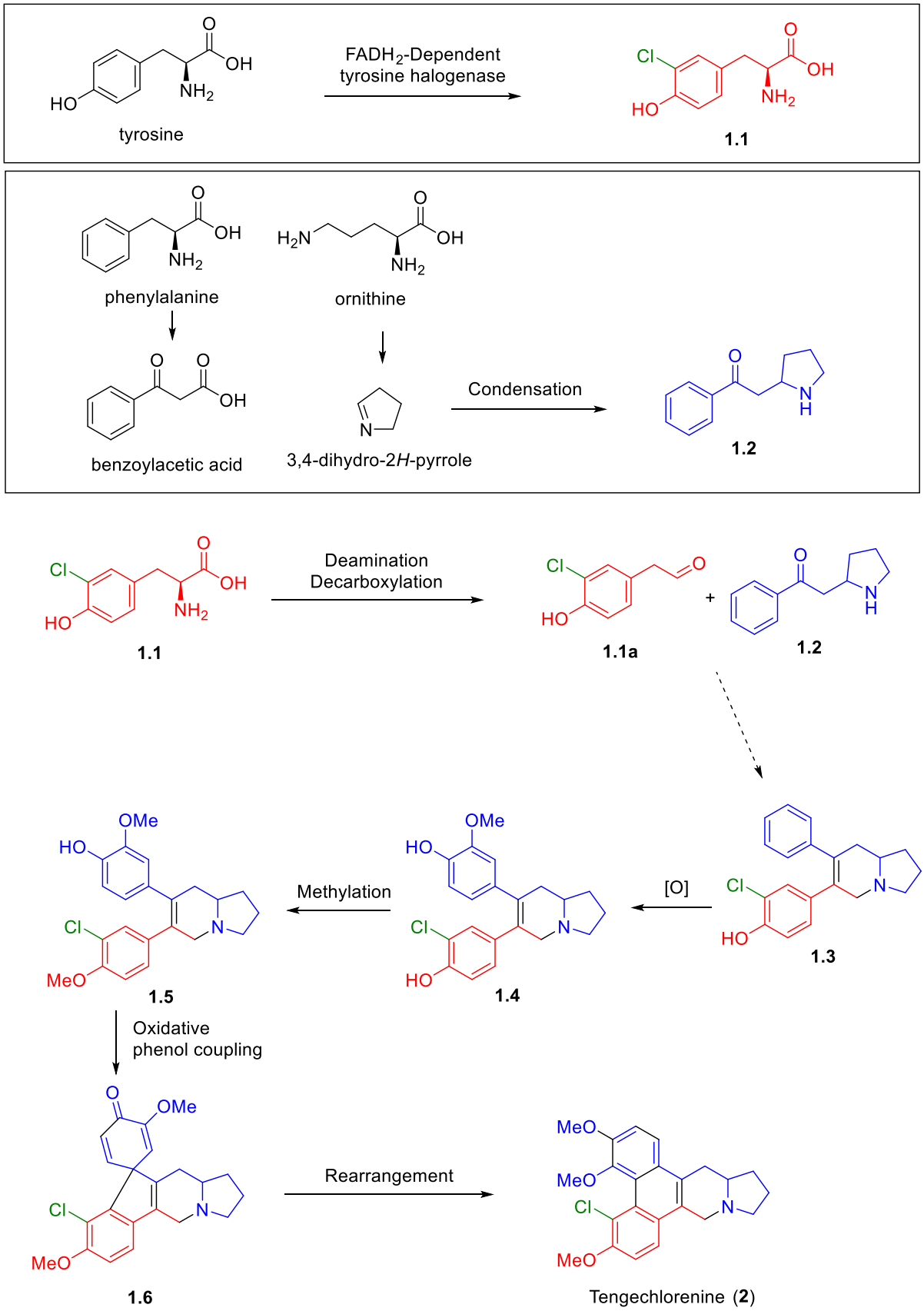

Scheme 2.4 – A possible biosynthetic pathway of tengechlorenine (**2**)

2.2.3 (±)-Fistulosine (**3**)

Alkaloid **3** was isolated as light yellowish amorphous powder, with $[\alpha]_D$ 0 (*c* 0.06, MeOH). The UV spectrum showed characteristic naphthalene absorption maxima at 239, 282, 314 and 328 nm. The IR spectrum showed a band at 3360 cm^{-1} due to the presence of OH group. HRESIMS measurements yielded the molecular formula $C_{19}H_{23}NO_3$, with a protonated ion peak detected at m/z 314.1754, corresponding to $C_{19}H_{23}NO_3+H^+$ (see appendix C). The ^1H, ^{13}C NMR and HMBC data of (±)-**3** are shown in Table 2.5.

Table 2.5 – ^1H, ^{13}C and HMBC NMR data of (±)-fistulosine (**3**) [a]

Position	**^1H**	**^{13}C**	**HMBC**
1	7.13 *s*	101.99	C-2,C-12b, C-4a
2	-	149.54	
3	-	149.00	
4	7.10 *s*	106.98	C-3, C-5, C-4a, C-12b
4a	-	127.63	
5	7.56 *s*	123.74	C-4, C-6a, C-13
6	-	133.85	
6a	-	128.99	
7	3.43 *d* (15)	52.70	C-6, C-6a, C-9, C-11a
	4.28 *d* (15)		
9	2.36 *m*	54.72	C-7, C-10
	3.35 *m*		
10	1.89 *m*	21.56	C-9, C-11
	2.01 *m*		
11	1.70 *m*	31.26	C-9, C-10, C-11a
	2.23 *m*		
11a	2.47 *m*	60.23	
12	2.88 *m*	33.02	C-6a, C-11, C-11a
	3.33 *m*		
12a	-	127.30	
12b	-	128.23	
13	4.64 *s*	63.31	C-5, C-6
2-OMe	4.00 *s*	55.81	C-2
3-OMe	4.01 *s*	55.81	C-3

[a]$CDCl_3$, 600 MHz (^1H), 150 MHz (^{12}C)

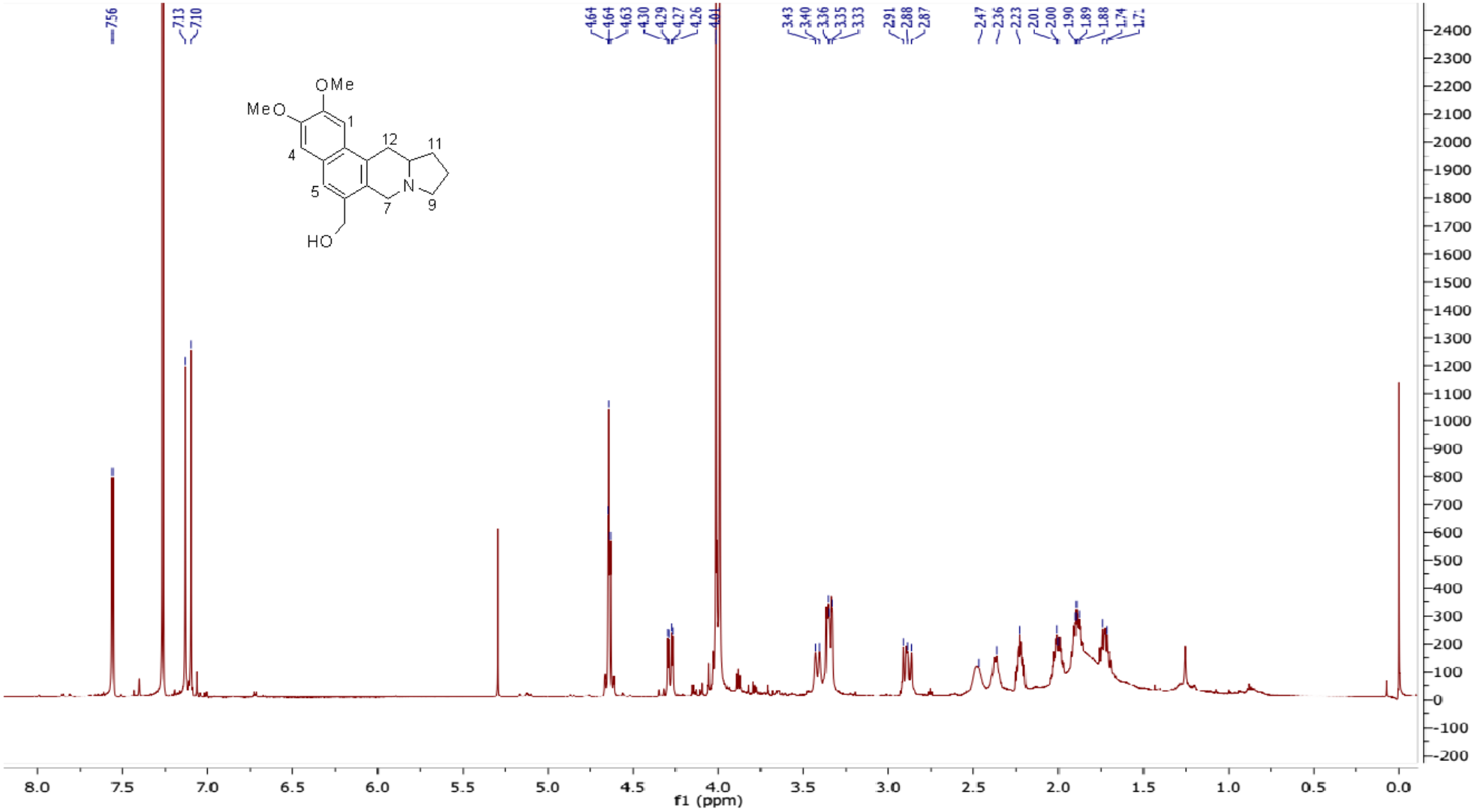

Figure 2.13 – Structure and ^{1}H NMR spectrum of (±)-**3**

The ^{13}C NMR spectrum (Table 2.5) showed 19 carbon signals corresponding to ten aromatic carbons (two oxygenated), two methoxy carbons, six methylene carbons (two aminomethylene and one hydroxymethylene) and one aminomethine carbon. The ^{13}C resonances were therefore in agreement with the molecular formula established by HRESIMS.

The ^{1}H NMR spectrum (Figure 2.13) showed three aromatic singlets at δ 7.10, 7.13 and 7.56, which together with the 10 aromatic carbon signals observed in the ^{13}C NMR, as well as the UV data, suggested that **3** has a naphthalene moiety. Two aromatic methoxy resonances at δ 4.00 and 4.01, were also observed, with each showing HMBC three-bond correlations to the aromatic C-2 and C-3 at δ_C 149.54 and 149.0, respectively. This readily established the placement of these methoxy groups at C-2 and C-3. In addition to an isolated methylene group due to C-7, the COSY data showed a $CH_2CHCH_2CH_2CH_2$ partial structure corresponding to the C-12–C-11a–C-11–C-10–C-9 fragment in alkaloid **3**, thus confirming the presence of an indolizidine structure. The NMR data disclosed so far suggested that alkaloid **3** is fistulosine, a benzopyrroloisoquinoline alkaloid previously obtained from *F. fistulosa*. Finally, the structure of alkaloid **3** was confirmed by comparing its ^{1}H and ^{13}C NMR data with those previously reported for fistulosine.[43] The structure proposed for alkaloid **3** was also in complete agreement with the HMBC data (Figure 2.14).

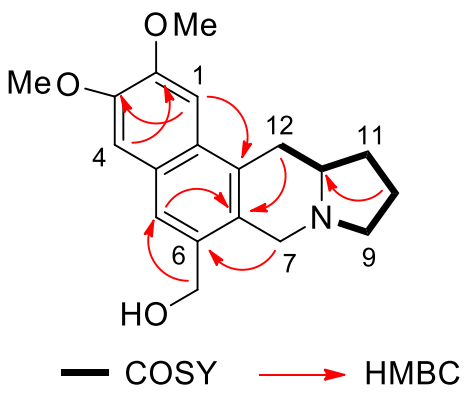

Figure 2.14 – COSY and selected HMBC's of **3**

Determination of the relative configuration at C-11a was not possible by using NMR data. Fistulosine was previously isolated from *F. fistulosa* and showing a negative optical rotation with $[\alpha]_D$ -11 (*c* 0.08, MeOH). The three other phenanthroindolizidine alkaloids isolated in that study all showed a negative optical rotation and their configuration at C-11a was assigned as *R.* It was only by analogy

that (-)-fistulosine was assigned as *R*.[43] However, alkaloid **3** obtained in the present study as a racemic mixture.

2.2.4 Antofine (**4**)

Alkaloid **4** was isolated in minute amount as a light yellowish residue, with $[\alpha]_D$ +17.5 (*c* 0.03, $CHCl_3$). HRESIMS measurements yielded the molecular formula $C_{23}H_{25}NO_3$, with a protonated ion peak detected at m/z 364.19150, corresponding to $C_{23}H_{25}NO_3+H^+$. The UV spectrum showed characteristic phenanthrene absorption maxima at 258, 282 and 285 nm. The ^{1}H NMR data are shown in Table 2.6.

Table 2.6 – ^{1}H NMR data of alkaloid **4** compared to those of (+)-antofine and (+)-deoxytylophorinine retrieved from literature.[78 79]

Position	Alkaloid **4**[a]	(+)-Antofine	(+)-Desoxytylophorinine
1	7.32 *s*	7.32 *s*	7.92 *d* (9)
2	-	-	7.20 *dd* (9, 2.5)
4	7.92 *s*	7.92 *s*	7.87 *d* (2.5)
5	7.91 *d* (2.4)	7.91 *d* (2.5)	7.89 *s*
7	7.21 *dd* (8.9, 2.4)	7.82 *dd* (9.2, 2.5)	-
8	7.83 *d* (8.9)	7.83 *d* (9.2)	7.12 *s*
9	4.70 *d* (14.8)	4.71 *d* (14.8)	4.57 d (15)
	3.70 *d* (14.8)	3.71 *d* (14.7)	3.61 d (15)
11	3.46 *m*	3.47 *m*	3.46 *m*
	3.37 *m*	3.35 *m*	2.48 *m*
12	1.92 *m*	1.90 *m*	2.01 *m*
	1.87 *m*	1.85 *m*	1.91 *m*
13	2.20 *m*	2.24 *m*	2.21 *m*
	2.02 *m*	2.01 *m*	1.71 *m*
13a	3.47 *m*	3.45 *m*	3.46 *m*
14	3.40 *m*	3.40 *m*	3.38 *dd* (16, 14)
	3.37 *m*	3.35 *m*	2.91 *dd* (16, 2.5)
2-OMe	4.11 *s*	4.11 *s*	4.09 *s*
3-OMe	4.06 *s*	4.07 *s*	4.04 *s*
6-OMe	4.02 *s*	4.02 *s*	4.00 *s*

[a]$CDCl_3$, 600 MHz

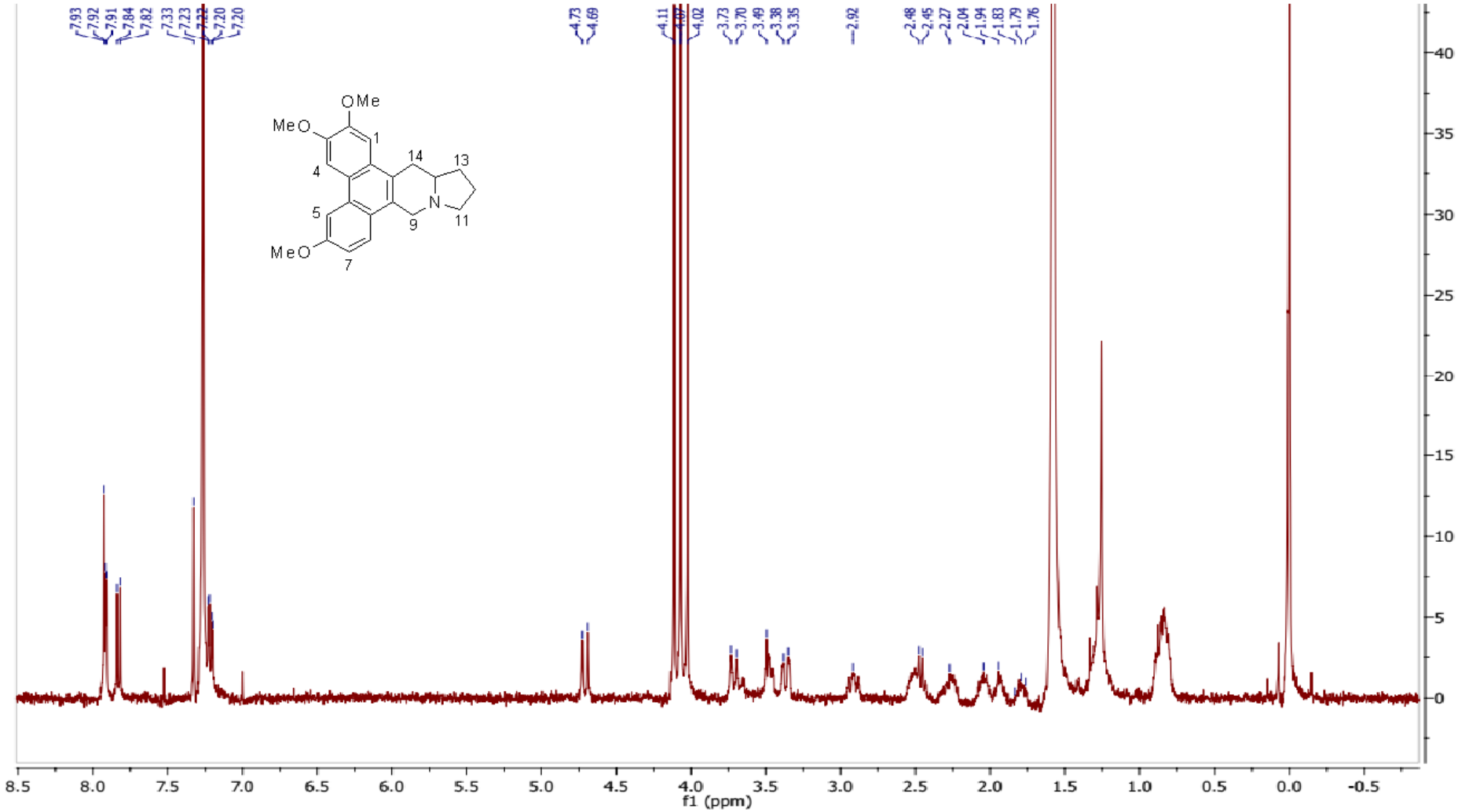

Figure 2.15 – Structure and ^{1}H NMR spectrum of **4**

Detailed inspection of the ^{1}H NMR data (Table 2.6) of alkaloid **4** revealed it to be a phenanthroindolizidine alkaloid with an unsubstituted indolizidine moiety. The presence of three aromatic methoxy singlets at δ 4.02, 4.06 and 4.11 indicated that the phenanthrene portion is substituted with three methoxy groups. A search through the literature based on the splitting patterns of the remaining five unsubstituted aromatic hydrogens in **4** suggested that it is either antofine[78] or deoxytylophorinine[79] (Figure 2.16). This inference was also supported by the molecular formula established for alkaloid **4**. Finally, direct comparison of the ^{1}H NMR data of **4** with those of antofine and deoxytylophorinine (Table 2.6) revealed alkaloid **4** to be antofine. Figure 2.15 shows the ^{1}H NMR spectrum and gross structure of antofine (**4**).

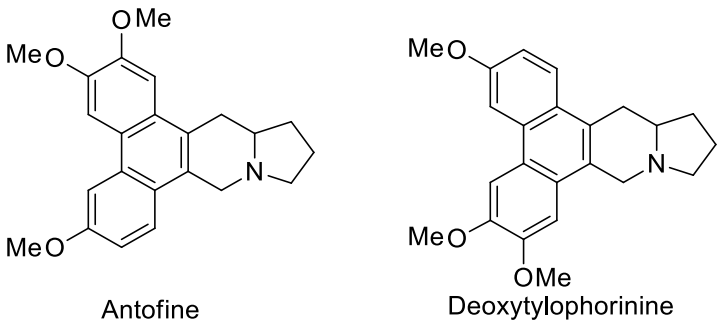

Figure 2.16 – Structures of antofine and deoxytylophorinine

The stereocenter at C-13a in the structure of **4** was assigned as *S* due to the fact that it showed a positive optical rotation ($[\alpha]_D$ +8.2), which according to literature, phenanthroindolizidines with a positive optical rotation have *S* configuration at C-13a, while those with a negative rotation have *R* configuration.[41]

2.2.5 *Seco*antofine (**5**)

*Seco*antofine (**5**) was isolated as a colorless oil with $[\alpha]_D$ -7.3 (*c* 0.15, $CHCl_3$). HRESIMS showed the molecular formula to be $C_{23}H_{27}NO_3$ with a protonated ion peak detected at m/z 366.2063 corresponding to $C_{23}H_{27}NO_3+H^+$. The UV spectrum showed absorption maxima at 230.4 and 282.2 nm. The ^{1}H NMR data of **5** are shown in Table 2.7 with comparison to that of *seco*antofine from literature.[80]

Table 2.7 – ^{1}H NMR data of alkaloid 5 compared to those of *seco*antofine retrieved from literature.[80]

Position	Alkaloid **5**	*Seco*antofine
1	6.47 *d* (1.2)	6.47 d (1.1)
4	6.66 *m*[a]	6.66 m[a]
4a	6.66 *m*[a]	6.66 m[a]
4b	6.69 *d* (AA'XX')	6.69 *d* (AA'XX')
5	6.69 *d* (AA'XX')	6.69 *d* (AA'XX')
7	6.97 *d* (AA'XX')	6.97 *d* (AA'XX')
8	6.97 *d* (AA'XX')	6.97 *d* (AA'XX')
9	3.87 *d* (15)	3.87 *d* (15)
	3.08 *d* (16)	3.07 *d* (16)
11	2.10 *m*	2.11 *m*
	3.31 *m*	3.29 *m*
12	1.53 *m*	1.53 *m*
	2.06 *m*	2.06 *m*
13	1.78 *m*	1.78 *m*
	2.01 *m*	2.01 *m*
13a	2.38 *m*	2.36 *m*
14	2.77 *m*	2.68 *m*
	2.25 *m*	2.25 *dd* (9, 9)
MeO-2	3.81 *s*	3.81 *s*
MeO-3	3. 73 *s*	3.72 *s*
MeO-6	3. 55 *s*	3.54 *s*

[a] Signals are overlapping. $CDCl_3$, 600 MHz

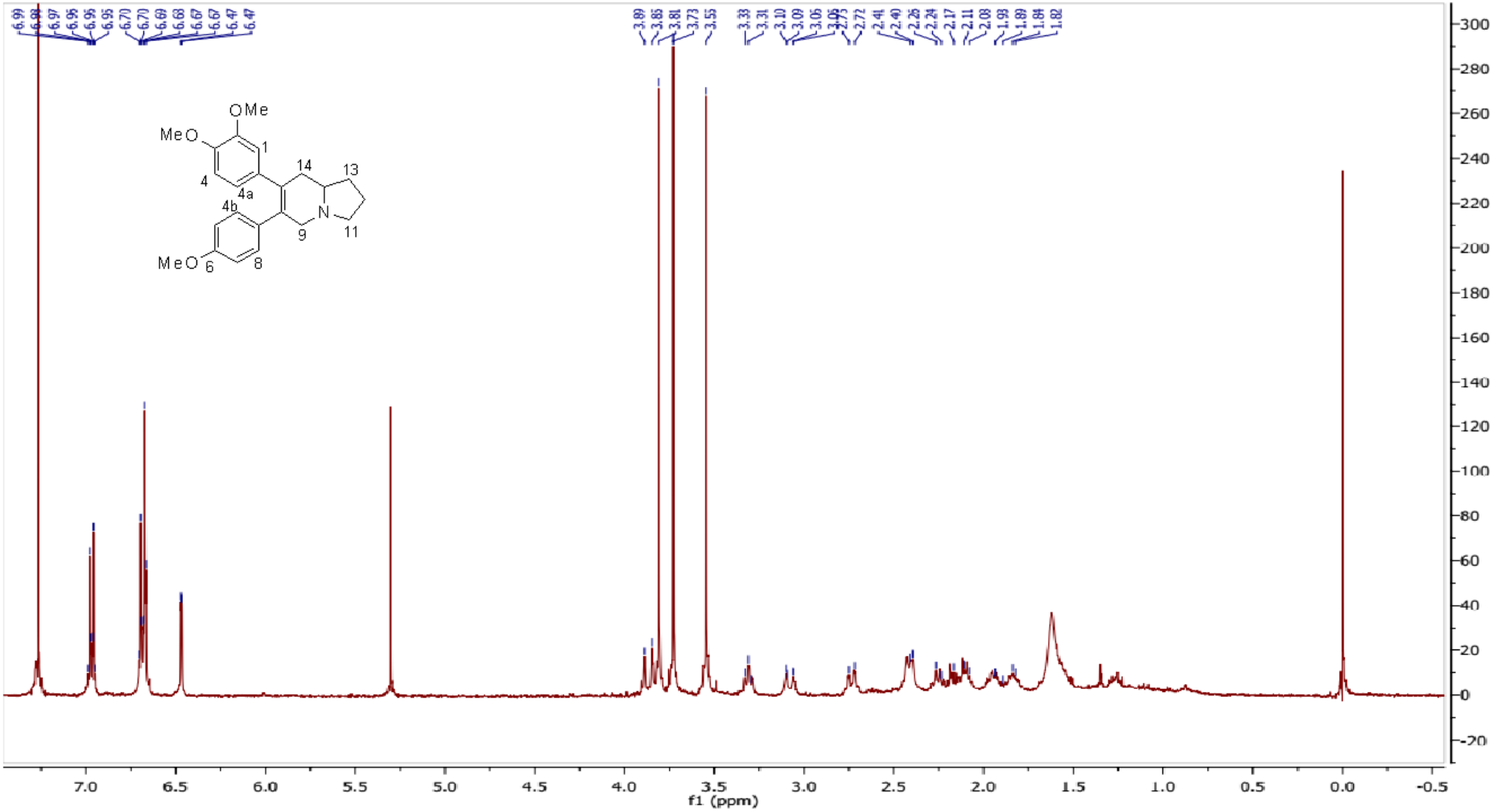

Figure 2.17 - Structure and ^{1}H NMR spectrum of **5**

The ^{1}H NMR spectrum of **5** (Table 2.7) showed seven aromatic signals, four of which correspond to a typical AA'XX' spin system resonating at δ 6.97 and 6.69, suggested the presence of a 1,4-di-substituted benzene ring, which in turn suggested that **5** is a *seco*-phenanthroindolizidine-type alkaloid. In addition, three aromatic methoxy singlets were observed at δ 3.81, 3.73 and 3.55, as in the case with antofine (**4**). The presence of an unsubstituted indolizidine moiety in **5**, was evident from the remaining ^{1}H NMR signals as well as the corresponding splitting patterns.

A search through the literature for *seco*-phenanthroindolizidine alkaloids possessing an unsubstituted indolizidine moiety and three aromatic methoxy substituents, yielded only the structure of *seco*antofine (Figure 2.17). Finally, the structure of **5** was unambiguously determined to be *seco*antofine by direct comparison of the ^{1}H NMR data of **5** with those reported in the literature for *seco*antofine (Table 2.7).[41 80]

Since alkaloid **5** showed a negative optical rotation, $[\alpha]_D$ -7.3 (c 0.15, $CHCl_3$), the configuration at C-13a can be assigned as *R*.[41]

2.3 Biological Activity

Alkaloids have been known to possess various pharmacological effects. In addition to the phytochemical investigation, (±)-tengerensine (**1**) and its enantiopure components, (±)-tengechlorenine (**2**) and (±)-fistulosine (**3**) were assayed for cytotoxic activity. This part of the research was carried out by School of Pharmacy, International Medical University, Malaysia.

(±)-Tengechlorenine **2** showed to be the most potent compound against all cell lines, while having little selectivity (moderately cytotoxic against non-tumorigenic breast epithelial cells). The racemic bisbenzopyrroloisoquinoline (±)-**1** and the enantiopure component (–)-**1** showed weak activity with IC_{50} range between 18-46 μM. However, the other enantiopure component (+)-**1** showed appreciable cytotoxicity with IC_{50} 7.4 μM while maintaining selectivity and showing no cytotoxicity against the non-tumorigenic cell line. Lastly, (±)-fistulosine (**3**) showed no apparent cytotoxicity against all the tested cell lines, which is in consistence with literature that reported this group compounds as non-cytotoxic.[67]

Table 2.8 – Cytotoxic effects of the isolated compounds and 5-fluorouracil (positive control)

Alkaloid	IC_{50} ± SD (μM)			
	MDA-MB-468[a]	MDA-MB-231[a]	MCF7[a]	MCF-10A[b]
(±)-**1**	17.9 ± 3.3	37.9 ± 5.9	46.5 ± 9.6	>100
(+)-**1**	7.4 ± 2.1	36.0 ± 5.6	19.0 ± 4.6	>100
(–)-**1**	23.7 ± 3.1	37.5 ± 3.2	37.7 ± 4.3	>100
(±)-**2**	0.038 ± 0.01	0.48 ± 0.05	0.91 ± 0.06	10.7 ± 3.7
(±)-**3**	>100	50.3 ± 4.3	>100	>100
5-Fluorouracil	43.3 ± 1.3	20.1 ± 1.1	24.1 ± 1.2	34.6 ± 1.2

[a]MDA-MB-468, MDA-MB-231 and MCF-7 are human breast adenocarcinoma; MCF-10A is non-tumorigenic human breast epithelial cells.

To sum up, phenanthroindolizidines are extremely potent cytotoxic agents even at very low concentrations *in vitro*, while having no clinical value due to their non-selectivity and extreme side effects.[56] On the other hand, although monomeric benzopyrroloisoquinolines are non-cytotoxic, the same cannot be said of the dimeric form as selective and moderate cytotoxic activity was observed for (+)-**1**, suggesting that enantiomerism played a role in how alkaloid **1** exert its cytotoxic effect in the breast cancer cell lines tested. This opens the door for future research in synthesizing analogues of dimeric benzopyrroloisoquinolines with the correct stereochemistry to enhance cytotoxic activity towards cancer cells while maintaining selectivity.

Chapter Three

Experimental

3.1 Plant Source and Authentication

The plant material of *Ficus fistulosa* var. *tengerensis* was collected in Hutan Simpan Berembun, Negeri Sembilan, Malaysia, and was identified by Dr. K. T. Yong (Institute of Biological Science, University of Malaya). Voucher specimens (KLU49073, KLU49074, KLU49075 and KLU49076) are deposited at the Herbarium, University of Malaya. The plant material was subjected to preliminary screening to determine the presence of alkaloids before any large scale collection took place. The weight of dried leaves used was approximately 15 Kg.

3.2 General

Melting points were determined on Electrothermal IA9100 digital melting point apparatus and are uncorrected. Optical rotations were determined on a JASCO P-1020 automatic digital polarimeter. IR spectra were recorded on a PerkinElmer Spectrum 400 FT-IR/FT-FIR spectrophotometer. UV spectra were obtained on a Shimadzu UV-3101PC spectrophotometer using absolute ethanol. ^{1}H and ^{13}C NMR spectra were recorded in $CDCl_3$ using TMS as internal standard on Bruker 600 MHz and 150 MHz spectrometer. HRESIMS were obtained on a JEOL Accu TOF-DART mass spectrometer. Chiral HPLC was performed on a Waters liquid chromatograph with a Waters 600 controller and a Waters 2489 tunable absorbance detector. A Chiralpak AS-H column (4.6 × 150 mm, Daicel, Japan) packed with amylose tris[(S)-α methylbenzylcarbamate] coated on 5 µm silica gel was used, at ambient temperature, and fractions were collected manually. ECD spectra were obtained on a J-815 Circular Dichroism Spectrometer. X-ray diffraction analysis was carried out on a Rigaku Oxford (formerly Agilent Technologies) SuperNova Dual diffractometer with Cu Kα (λ = 1.54184 Å) radiation at rt. The structures were solved by direct methods (SHELXS-2014) and refined with fullmatrix least-squares on F2 (SHELXL-2014). All non-hydrogen atoms were refined anisotropically, and all hydrogen atoms were placed in idealized positions and refined as riding atoms with the relative isotropic parameters. All solvents used throughout this research were analytical grade and during bulk extraction distilled ethanol was used. HPLC grade solvents were used when the chiral HPLC analysis was carried out.

3.3 Extraction of Alkaloids

The collected leaves of *F. fistulosa* var. *tengerensis (*15 kg) were left to dry indoors. The dried leaves were then coarsely ground and extracted by adding 95% ethanol and soaking the leaf material for two days at room temperature. The ethanol extract was then decanted and subjected to rotary evaporation to concentrate the extract. The plant material was then re-extracted with another batch of distilled 95% ethanol and this process was repeated four times. The concentrated combined bulk ethanolic extract was subjected to acid-base treatment to selectively extract alkaloids from the bulk crude extract. Firstly, the crude extract was added to 1 L of 2% tartaric acid solution with vigorous stirring in a 5 L conical flask. The acidic solution was then filtered through Kieselghur to get rid of any insoluble material that was regarded as non-alkaloidal substances. The pH of the filtered acidic solution was then adjusted to about 10 by the addition of concentrated ammonia solution. The basified solution was extracted with ethyl acetate (1:1 volume ratio, three times). The combined ethyl acetate extract was partially concentrated and treated with sodium sulphate anhydrous. Finally, the ethyl acetate solution was dried using rotary evaporator to yield the crude alkaloidal extract of 10.45 g.

3.4 Chromatographic Techniques

Various chromatographic methods were employed on the crude alkaloidal extract until pure alkaloids were obtained. Methods including column chromatography, thin layer chromatography, centrifugal thin layer chromatography and HPLC.

3.4.1 Column Chromatography

i. Vacuum Column Chromatography (VCC):

VCC was used to fractionate the alkaloid crude extract (10.045 g) using Merck silica gel 60 (0.040 – 0.063 mm) at approximately 20:1 silica to sample ratio. The silica was made into slurry and packed into the column under vacuum with repeated solvent refills until sufficient packing was achieved and the column was equilibrated. The sample was dissolved in minimum amount of solvent and with the least possible polarity. The sample solution was then pipetted gently onto the silica bed. The sample was then eluted using $CHCl_3$/Hex at 4:1 ratio while gradually increasing polarity using methanol. The collected eluents were monitored using TLC.

ii. Flash Column Chromatography (FCC):

FCC was used on sub-fractions obtained from VLC which were too much to be separated using centrifugal thin layer chromatography i.e. sample weight >800 mg. Merck silica gel 60 (0.04 – 0.06

mm) or Scharlab Silica Gel 60 (0.04-0.06 mm) were used at approximately 80:1 silica to sample ratio. Slurry packing was performed while gently tapping the column with a thick rubber to ensure tight packing. After the sample was applied the column was filled with solvent and air pump was used by placing it on the top of the column. Gradient elution was used and the collected eluents were monitored using TLC.

3.4.2 Thin Layer Chromatography

Thin Layer Chromatography was the most used procedure for qualitative analysis during isolation steps. It was used for a number of purposes, namely, to monitor and detect the presence of alkaloids within samples; to find the most optimum starting solvent for both column chromatography and preparative centrifugal thin layer chromatography; and to check for the purity of collected fractions. By using this technique, the collected fractions that showed similar profiles were combined together. Samples were spotted onto 2.5 cm x 10 cm aluminium sheets which had been pre-coated with silica gel 60 F_{254} of 0.25 mm thickness (Merck). Samples were spotted using a glass pipette. Once the samples had been loaded onto the plates, the plates were then placed in saturated chromatographic tanks which contained different solvent systems. The plates were then removed from the tanks when the solvent front was 1 cm away from the end of the plate. The plate was then examined using a UV lamp with UV light (254nm). This caused the visualisation of molecules as dark spots. These spots were then drawn around using a pencil and the plate then sprayed with Dragendorff's reagent. The spots which reacted with the reagent turned orange and indicated the presence of alkaloids. The addition of 1% ammonia was necessary in most cases to overcome the 'tailing' of the spots which appeared in majority of the fractions. The 'tailing' of the compounds on TLC is caused by the protonation of the nitrogen in the alkaloids, by the acidic silica stationary phase. Some of the solvents that were used as a mobile phase in TLC:

a) Chloroform
b) Diethyl Ether
c) Ethyl Acetate

3.4.3 Centrifugal Thin Layer Chromatography (CTLC)

Preparative Centrifugal Thin Layer was carried out using a circular chromatographic plate measuring 24 cm in diameter with the action of a centrifugal force to speed up mobile phase flow across the circular plate. To prepare the chromatographic plate, the edge of the plate was secured with cellophane tape to form a mould. Silica gel (Kieselgel 60 PF256, Merck, 40 g) was added to about 90

mL of cold distilled water in case of preparing 1 mm thick plate. The 2 mm plate was prepared by mixing 60 g of silica powder with 110 mL cold water. This slurry was shaken vigorously and was then quickly poured onto the circular glass plate before setting commences. The circular glass plate was then manually rotated while the gel was being poured to obtain an even setting. The plate was then left to air-dry for about an hour before being dried in an oven at about 55˚C overnight. Before the plate was used it was activated at 100 ˚C for one hour. After the activation is completed the plate is left outside to cool down for few minutes then using the proper blade it was shaved to the required size 1 mm or 2 mm. The chromatotron was then cleaned using solvents like acetone before placing the plate. The sample was dissolved in a minimum volume of a suitable solvent and loaded at the centre of the plate while the plate was spinning to form a thin band. Elution was then carried out with the appropriate solvent system. Fractions were collected, concentrated by rotary evaporator, examined by TLC and combining of similar fractions was then done when needed.

Some of the solvent systems used as eluents were:

1. Chloroform: Hexane with 1% ammonia
2. Chloroform: Methanol
3. Diethyl ether: Methanol with 1% ammonia
4. THF: Hex with 1% ammonia
5. THF: Methanol

All CTLC runs were made using an increased methanol gradient to up to 35%.

3.5 Spray Reagent

Dragendorff's reagent was used to detect the presence of alkaloids within a sample and it composed of the following:

Solution A: 850 mg of bismuth subnitrate was mixed with 40 mL of water and 10 mL of glacial acetic acid.

Solution B: 20 g of potassium iodide was dissolved in 50 mL of water.

In order to make the reagent, equal proportions of solutions A and B were mixed together. This produced a stock solution which can be stored for several months in a dark bottle. Then 10 mL of the stock solution was mixed with 20 mL of glacial acetic acid and diluted with water up to 100 mL. This solution was poured into the spray bottle.

3.6 Isolation of Alkaloids

The basic crude alkaloidal mixture of 10.45 g obtained from the extraction procedure described above was initially fractionated by vacuum column chromatography over silica gel. The column was eluted with chloroform, followed by a stepwise increase of methanol gradient. TLC was used to monitor the progress of the fractionation. Based on TLC, the many fractions collected were pooled into several major fractions, i.e., 11 fractions altogether, namely, FT1 – FT11. The combined fractions were then subjected to further purification by flash column chromatography or preparative centrifugal TLC. A flow diagram of the isolation procedure of the pure alkaloids is shown in figure 3.1.

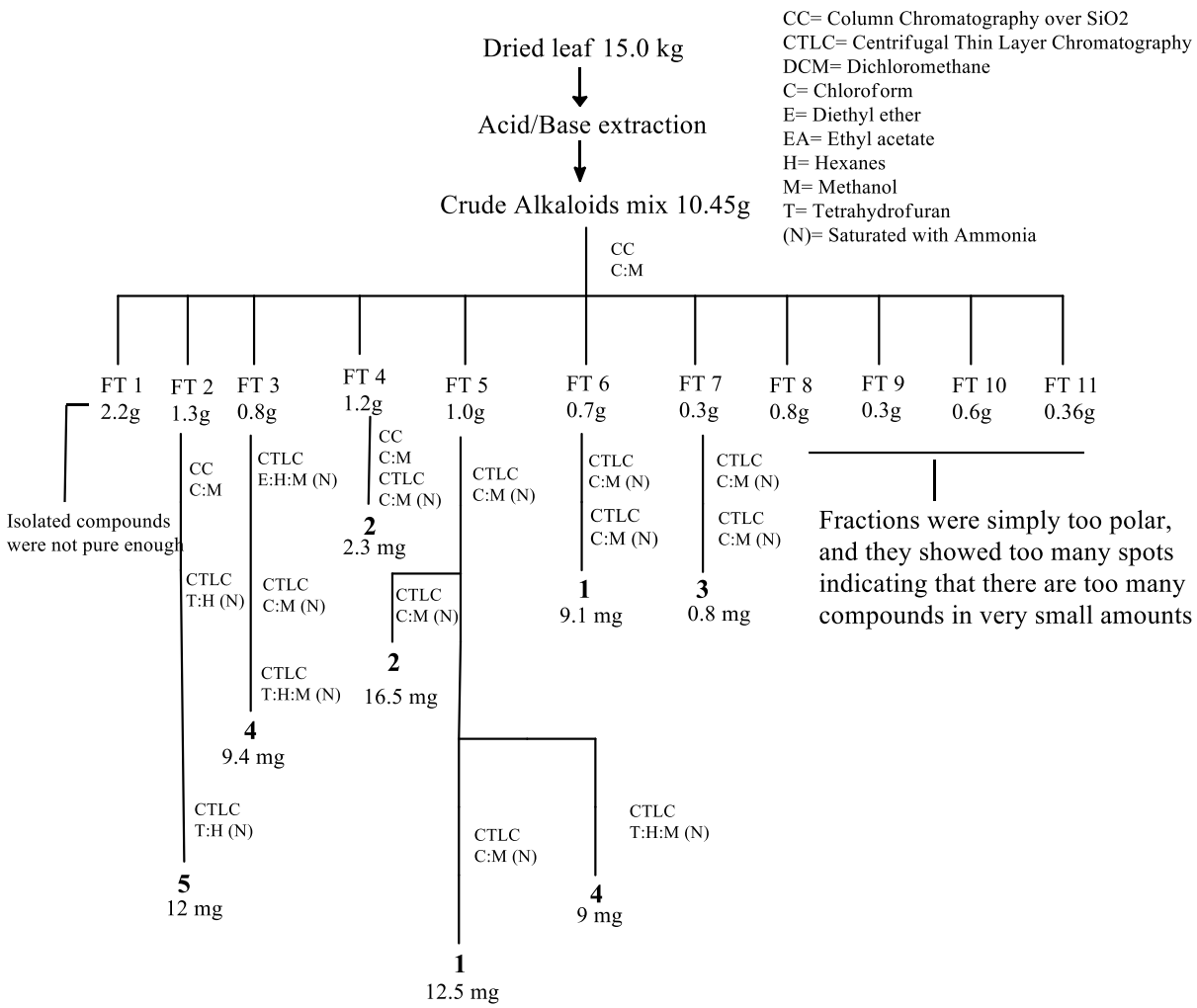

Figure 3.1 – Isolation of alkaloids from the leaves of *F. fistulosa* var. *tengerensis*

Separation of Enantiomers (+)-1 and (–)-1 by Chiral-Phase HPLC

(±)-Tengerensine (**1**) (2.3 mg) was dissolved in EtOH (0.75 mL) and resolved using a chiral column (eluting solvent: *n*-hexane/EtOH/Et_2NH, 85:15:0.1; flow rate 1.0 mL/min; 150 injections, 5.0 µL each) to yield two fractions. Fraction 1: retention time 10 min 58 s, 0.9 mg. Fraction 2: retention time 18 min 32 s, 1.2 mg.

3.7 Compound Data

(±)-Tengerensine (1): light yellowish block crystals; mp > 190 ºC (dec); $[\alpha]^{25}_{D}$ –0.7 (*c* 0.30, $CHCl_3$); UV (EtOH), λ_{max} (log ε) 239 (4.62), 280 (4.13), 332 (3.89) nm; IR (dry film) ν_{max} 1705 cm^{-1}; HRESIMS m/z: 703.3752 $[M+H]^+$ (calcd. for $C_{44}H_{50}N_2O_6$ + H, 703.3747); ^1H ,^{13}C and HMBC NMR data, Table 2.2. (+)-Tengerensine (**1**) (Fraction 1): $[\alpha]^{25}_{D}$ +62 (*c* 0.02, $CHCl_3$); (–)-Tengerensine (**1**) (Fraction 2): $[\alpha]^{25}_{D}$ –58 (*c* 0.06, $CHCl_3$).

Crystallographic data of (±)-**1:** light yellowish blocks, $C_{44}H_{50}N_2O_6$, *M*r = 702.86, triclinic, space group *P−1*, *a* = 12.709(2) Å, *b* = 12.8666(12) Å, *c* = 14.9876(16) Å, *α* = 112.962(10) °, *β* = 111.821(16) °, *γ* = 90.977(11) °, *V* = 2057.0(5) $Å^3$, *Z* = 2, D_{calcd} = 1.135 gcm^{-3}, crystal size 0.40 x 0.15 x 0.02 mm^3, *F*(000) = 752, Cu Kα radiation (*λ* = 1.54178 Å), *T* = 293 K. The final R_1 value is 0.0856 (wR_2 = 0.2399) for 7852 reflections [*I>2σ(I)*].

(±)-Tengechlorenine (2): colorless crystals; mp 192 – 195 °C; $[\alpha]^{25}_{D}$ +11.4 (*c* 0.08, $CHCl_3$); UV (EtOH), λ_{max} (log ε) 231.4 (3.47), 269 (3.68), 347.40 (2.76), 366 (2.58) nm; HRESIMS m/z: 398.15115 $[M+H]^+$ (calcd. for $C_{23}H_{24}ClNO_3$ + H, 398.15230); ^1H, ^{13}C and HMBC NMR data, Table 2.4.

Crystallographic data of (±)-**2**: light yellowish plates, $C_{23}H_{24}NO_3Cl$, *M*r = 397.88, triclinic, space group *P−1*, *a* = 8.7014(6) Å, *b* = 10.2583(7) Å, *c* = 11.1747(8) Å, *α* = 99.612(6)°, *β* = 106.611(6)°, *γ* = 93.943(6)°, *V* = 935.23(12) $Å^3$, *Z* = 2, D_{calcd} = 1.413 gcm^{-3}, crystal size 0.1 x 0.1 x 0.01 mm^3, *F*(000) = 420, Cu Kα radiation (*λ* = 1.54178 Å), *T* = 165 K. The final R_1 value is 0.0761 (wR_2 = 1841) for 3723 reflections [*I>2σ(I)*].

(±)-Fistulosine (3): light yellowish amorphous powder; $[\alpha]^{25}_{D}$ 0 (*c* 0.06, MeOH); UV (EtOH), λ_{max} (log ε) 239 (3.78), 281.8 (3.43), 313.8 (2.85), 328.4 (2.60) nm; IR (dry film) ν_{max} 3360 cm^{-1}; HRESIMS m/z: 314.1754 $[M+H]^+$ (calcd. for $C_{19}H_{23}N_1O_3$+H, 314.1756); ^1H, ^{13}C, HMBC NMR data, Table 2.5.

Antofine (4): light yellowish oil $[\alpha]^{25}_{D}$ +17.5 (*c* 0.025, $CHCl_3$); UV (EtOH), λ_{max} (log ε) 258 (4.41), 282.2 (4.29), 285 (4.27) nm; HRESIMS m/z: 364.19150 $[M+H]^+$ (calcd. For $C_{23}H_{25}NO_3$+H, 364.19127); ^{1}H NMR data, Table 2.6.

***Seco*antofine (5):** colourless oil $[\alpha]^{25}_{D}$ –7.3 (*c* 0.15, $CHCl_3$); UV (EtOH), λ_{max} (log ε) 230.4 (3.66) and 282.2 (3.41) nm; HRESIMS m/z: 366.20633 $[M+H]^+$ (calcd for $C_{23}H_{27}NO_3$+H, 366.20692); ^{1}H NMR data, Table 2.6.

3.8 Cytotoxicity Assay

Cell lines and cell culture

A panel of human breast cancer cell lines (MCF7, MDA-MB-231, MDA-MB-468) and human non-tumorigenic breast epithelial cells (MCF10A) were purchased from the American Type Culture Collection. All cancer cells were maintained in RPMI 1640 medium with 10% fetal bovine serum (FBS), 100 IU/mL penicillin, and 100 µg/mL streptomycin (Sigma-Aldrich, St. Louis, MO, USA) while MCF10A cells were cultured with 5% horse serum, 20 ng/mL epidermal growth factor, 0.5 µg/mL hydrocortisone, 10 µg/mL insulin, 100 IU/mL penicillin, and 100 µg/mL streptomycin. All cells were maintained in an incubator at 37°C and 5% carbon dioxide.

Luminescent cell viability assay

Cell viability of cells after treatment with (±)-**1**, (+)-**1**, (–)-**1**, (±)-**3** and 5-fluorouracil (positive control) were determined using the CellTitre-Glo® Luminescent Cell Viability Assay kit (Promega, USA). All compounds were prepared in 100mM DMSO as stock solution and diluted to various concentrations (1.5 to 100 µM) using sterile phosphate buffer solution. All cancer or noncancer cells were seeded in 384-well opaque plates for 24 h at a density of 1000 cells/well and followed by treatment with (±)-**1**, (+)-**1**, (–)-**1**, (±)-**3** and 5-fluorouracil (positive control) for 72 hours. Cells treated with 0.1% DMSO were the negative controls. Luminescence reading was measured using SpectraMax M3 Multi-Mode Microplate Reader (Radnor, USA). The inhibitory concentration of 50% cell viability (IC_{50}) was determined based on the luminescent reading of treated cells and cells treated with negative control.

References

1. Petrovska, B. Historical review of medicinal plants' usage. *Pharmacogn. Rev.* **2012** 6**,** 1–5.
2. Duffin, J. *History of medicine: a scandalously short introduction*; University of Toronto Press; Toronto, 2010.
3. Bottcher H. *Medicine in China: A history of Pharmaceutics*; University of California Press; California, 1986.
4. Wirat, C. *Etnopharmacology of medicinal plants;* Humana Press; New Jersy, 2006.
5. Hallmann-Mikołajczak, A. Ebers Papyrus. The book of medical knowledge of the 16th century B.C. Egyptians. *Arch. Hist. Filoz. Med.* ***2004,*** 67**,** 5–14.
6. Dias, D. A.; Urban, S.; Roessner, U. A Historical Overview of Natural Products in Drug Discovery. *Metabolites.* **2012,** 2, 303–336 2012.
7. Newman, D. J.; Cragg, G. M.; Snader, K. M. The influence of natural products upon drug discovery. *Nat. Prod. Rep.* **2000***,* 17**,** 215–234.
8. Hosztafi, S. The discovery of alkaloids. *Pharmazie.* **1997**, 52**,** 546–550.
9. Firn, R. D.; Jones, C. G. Natural products - a simple model to explain chemical diversity. *Nat. Prod. Rep.* **2003**, 20**,** 382–391.
10. Meger, S. Discovery of Penicillin. *Am. Biol. Teach.* **2011**, 2, 1–9.
11. Baker, D. D.; Chu, M., Oza, U.; Rajgarhia, V. The value of natural products to future pharmaceutical discovery. *Nat. Prod. Rep.* **2007***,* 24, 1225–1244.
12. Takenaka, T. Classical vs reverse pharmacology in drug discovery. *BJU International*. **2001**, 88, 7–10.
13. Lee, J. Uhlik, M. Modern Phenotypic Drug Discovery Is a Viable, Neoclassic Pharma Strategy. *J. Med. Chem.* **2012**, 55**,** 4527–4538.
14. Swinney, D. C.; Anthony, J. How were new medicines discovered? *Nat. Rev. Drug. Discov.* **2011**, 10, 507–519.
15. Newman, D. J.; Cragg, G. M. Natural Products as Sources of New Drugs from 1981 to 2014. *J. Nat. Prod.* **2016**, 79, 629–661.
16. Tu, Y. The discovery of artemisinin (qinghaosu) and gifts from Chinese medicine. *Nat. Med.* **2011**, 17, 1217–1220.
17. Campbell, W. C.; Ōmura, S. From bacteria and plants to novel anti-parasite therapies. *Nobel Prize Press Release*. **2015**, 1–5.
18. WHO. Artemisinin Derivatives: Summary of Nonclinical Safety Data Introductory remarks. **2006**, 1–67.
19. Manske, R. H. *The Alkaloids. Chemistry and Physiology*; Academic press; New York, 1965..
20. Saxena, P. B. *Chemistry of Alkaloids*; Discovery Publishing House; London, 2007.

21. Hesse, M. *Alkaloids: Nature's curse or blessing?*; Wiley-VCH Weinheim; Zurich, 2002.

22. Robert, M. F.; Wink, M. *Alkaloids : biochemistry, ecology, and medicinal applications*; Plenum Press; New York, 1998.

23. Pengelly, A. *The Constituents of Medicinal Plants*; Allen & Unwin; Sydney, 2004.

24. Tuyen, N. V.; Kim, L.D.; Xuan L.T. Structure elucidation of two triterpenoids from Ficus fistulosa. *Phytochemistry.* **1998**, 50, 467–469.

25. Mann, J.; Davidson, R.; Hobbs, J. *Natural products: their chemistry and biological significance; John Wiley & sons; New York,* 1994.

26. Albuquerque, E. X.; Daly, J. W.; Witkop, B. Batrachotoxin: chemistry and pharmacology. *Science.* **1971**, 172, 995–1002.

27. Bienz, S.; Bisegger, P.; Guggisberg, A.; Hesse, M. Polyamine alkaloids. *Nat. Prod. Rep.* **2005**, 22, 647–658.

28. Fester, K. Plant Alkaloids. *Encycl. Life Sci.* **2010**, 11, 74–81.

29. Bucheler, W.; Buckley, E.; Deulofeu, V. *Venomous Animals and Their Venoms, Vol II*; Academic Press; New York, 1968.

30. Mann, J.; Mudd, H. Alkaloids and plant metabolism. J. Biol. Chem. **1963,** 283, 381–385.

31. Trease, G.; Evans, W. C. *Trease and Evans Pharmaconogsy*; Elsevier Ltd; London; 2009.

32. Mothes, K. Physiology of alkaloids. *Annu. Rev. Plant Physiol.* **1955***,* 6, 393–432.

33. Waller, G. R. & Nowacki, E. K. *Alkaloid Biology and Metabolism in Plants*; Springer; New Jersy; 1978.

34. Michael, J. P. Indolizidine and quinolizidine alkaloids. *Nat. Prod. Rep.* **2001**, 18, 520–542.

35. Gellert, E. the Indolizidine Alkaloids. *J. Nat. Prod.* **1982**, 45, 50–73.

36. Li, Z.; Jin, Z.; Huang, R. Isolation, Total Synthesis and Biological Activity of Phenanthroindolizidine and Phenanthroquinolizidine Alkaloids. *Synthesis (Stuttg).* **2001**, 16, 2365–2378.

37. Chemler, S. Phenanthroindolizidines and Phenanthroquinolizidines: Promising Alkaloids for Anti-Cancer Therapy. *Curr. Bioact. Compd.* **2009**, 5**,** 2–19.

38. An, T.; Huang, R.; Yang, Z.; Zhang, D.; Li, G. Alkaloids from Cynanchum komarovii with inhibitory activity against the tobacco mosaic virus. **2001**, 58, 1267–1269.

39. Govindachari, R.; Viswanathan, N. Recent progress in the chemistry of Phenanthroindolizidine alkaloids. *Heterocycles* **1978**, 11**,** 588–613.

40. Stærk, D.; Christensen, J.*; Lemmich, E.; Duus, J.* Cytotoxic activity of some phenanthroindolizidine N-oxide alkaloids from Cynanchum vincetoxicum. *J. Nat. Prod.* **2000***,* 63, 1584–1586.

41. Steerk, D.; Lykkeberg, A. K. Christensen, J.; Abe, F.; Budnik, B. In vitro cytotoxic activity of phenanthroindolizidine alkaloids from Cynanchum vincetoxicum and Tylophora tanakae against drug-sensitive and multidrug-resistant cancer cells. *J. Nat. Prod.* **2002***,* 65, 1299–1302.

42. Yap, V. A.; Qazzaz, M. E.; Raja, V. J.; Bradshaw, T. D.; Loh, H. S.; Sim, K. S.; Yong, K. T.; Low, Y. Y.; Lim, K. H. Fistulopsines A and B antiproliferative septicine-type alkaloids from Ficus

fistulosa. *Phytochem. Lett.* **2016,** 15, 136–141.

43. Subramaniam, G.; Ang, K. K. H.; Ng, S.; Buss, A. D.; Butler, M. S. A benzopyrroloisoquinoline alkaloid from Ficus fistulosa. *Phytochem. Lett.* **2009,** 2, 88–90.

44. Peraza-Sanchez, S.; Chai, S.; Shin, Y.; Santisuk, T.; Reutrakul, V. Constituents of the Leaves and Twigs of Ficus hispida. *Planta Med.* **2002**, 68, 186–188.

45. Yap, V. A.; Loong, B. J.; Tng, K. N.; Loh, H. S.; Yong, K. T.; Low, Y. Y.; Kam, T. S.; Lim, K. H. Hispidacine, an unusual 8,4'-oxyneolignan-alkaloid with vasorelaxant activity, and hispiloscine, an antiproliferative phenanthroindolizidine alkaloid, from Ficus hispida Linn. *Phytochemistry.* **2015**, 109, 96–102.

46. Ueda, J. Y.; Takagi, M.; Shin-ya, K. Aminocaprophenone- and pyrrolidine-type alkaloids from the leaves of Ficus septica. *J. Nat. Prod.* **2009**, 72, 2181–2183.

47. Damu, A. G.; Kuo P. C,; Shi L. S.; Li, C. Y.; Kuoh, C. S.; Wu, P. L.; Wu, T. S. Phenanthroindolizidine alkaloids from the stems of Ficus septica. *J. Nat. Prod.* **2005**, 68, 1071–1075.

48. Wu, P. L.; Rao, K. V.; Su, C. H.; Kuoh, C. S; Wu, T. S. Phenanthroindolizidine alkaloids and their cytotoxicity from the leaves of Ficus septica. *Heterocycles.* **2002**, 57, 2401–2408.

49. Damu, A. F.*; Kuo, P. C.; Shi, L. S.; Wu, T. S.* Cytotoxic phenanthroindolizidine alkaloids from the roots of Ficus septica. *Planta Med.* **2009**, 75**,** 1152–1156.

50. Huang, X.; Gao, S.; Fan, L.; Yu, S.; Liang, X. Cytotoxic alkaloids from the roots of Tylophora atrofolliculata. *Planta Med.* **2004**, 70, 441–445.

51. Chen, C. Y.; Zhu, G. Y.; Wang, J. R.; Jiang, Z. H. Phenanthroindolizidine alkaloids from Tylophora atrofolliculata with hypoxia-inducible factor-1 (HIF-1) inhibitory activity. *RSC Adv.* **2016**, 6, 79958–79967.

52. Lee, Y. Z.; Huang, C. W.; Yang, C. W.; Hsu, H. W.; Kang, L. J.; Chao, Y. S. Isolation and biological activities of phenanthroindolizidine and septicine alkaloids from the formosan Tylophora ovata. *Planta Med.* **2011**, 77, 1932–1938.

53. Abe, F.; Iwase, Y.; Yamauchi, T.; Honda, K.; Hayashi, N. Phenanthroindolizidine Alkaloids From Tylophora-Tanakae. *Phytochemistry.* **1995**, 39, 695–699.

54. Herbert, R. B.; Jackson, F. B.; Nicolson, I. T. Biosynthesis of Phenanthroindolizidine Alkaloids: Incorporation of 2-Pyrrolidin- 2-ylacetophenone and Benzoylacetic Acid and Derivatives. *J. Chem. Soc. Perkin. Trans I.* **1984**, 2, 825–831.

55. Govindachari, R.; Viswanathan, N. Recent Progress in the Chemistry of Phenanthroindolizidine Alkaloids. *Heterocycles*. **1978**, 11, 587–613.

56. Niphakis, M. J. *Phenanthropiperidine Alkaloids: Methodology Development, Synthesis and Biological Evaluation*. Ph.D. Thesis, University of Kansas, Kansas, US, 2010.

57. Boyd, M. R. The NCI In Vitro Anticancer Drug Discovery Screen. *Anticancer Drug Dev. Guid. Cancer Drug.* **1997**, 2, 23–42.

58. Donaldson, G. R.; Atkinson, M. R.; Murray, A. W. Inhibition of protein biosynthesis in Ehrlich ascites-tumor cells by the phenanthrene alkaloids tylophorine, tylocrebrine, and cryptopleurine. *Biochem. Biophys. Res. Commun.* **1968**, 31**,** 104–109.

59. Gao, W.; Chen, A. P. C.; Leung, C. H.; Gullen, E. A. Structural analogs of tylophora alkaloids

may not be functional analogs. *Bioorg. Med. Chem. Lett.* **2008** 18**,** 704–709.

60. Wu, C. M.; Yang, C. W.; Lee, Y. Z.; Wu, P. L.; Chao, Y. S. Tylophorine arrests carcinoma cells at G1 phase by downregulating cyclin A2 expression. *Biochem. Biophys. Res. Commun.* **2009***,* 386**,** 140–145.

61. Giaccia, A.; Siim, B. G.; Johnson, R. S. HIF-1 as a target for drug development. *Nat. Rev. Drug Discov.* **2003**, 2, 803–811.

62. Rao, K. N.; Bhattacharya, R. K.; Veankatachalam, S. R. Inhibition of thymidylate synthase by pergularinine, tylophorinidine and deoxytubulosine. *Indian J. Biochem. Biophys.* **1999**, 36, 442–448.

63. Rao, K. N.; Veankatachalam, S. R. Inhibition of dihydrofolate reductase and cell growth activity by the phenanthroindolizidine alkaloids pergularinine and tylophorinidine: In vitro cytotoxicity of these plant alkaloids and their potential as antimicrobial and anticancer agents. *Toxicol. Vitr.* **2000**, 14, 53–59.

64. Gopalakrishnan, C.; Shankaranarayan, D.; Nazimudeen, S. K.; Kameswarn, L. Effect of tylophorine, a major alkaloid of Tylophora indica, on immunopathological and inflammatory reactions. *Indian J. Med. Res.* **1980,** 71, 940–948.

65. Gopalakrishnan, C.; Shankaranarayan, D.; Kameswarn, L.; Natarajan, S. Pharmacological investigations of tylophorine, the major alkaloid of Tylophora indica. *Indian J. Med. Res.* **1979,** 69, 513–520.

66. Budzikiewicz, H.; Faber, L.; Perrolaz F. F.; Wiegrebe, W. Vinceten, ein Benzopyrroloisochinolin-Alkaloid, aus Cynanchum vincetoxicum (L.) Pers. (Asclepiadaceae). *Eur. J. Nat. Chem.* **1979**, 8, 1212–1231.

67. Gaur, S.; Jain, P.; Anand, N. Synthesis of hexahydropyrrolo[1,2-b] isoquinolines - Analogs of phenanthroindolizidine anticancer alkaloids. *Indian J. Chem.* **1982**, - *Sec-B* 21B**,** 46–51.

68. Harrison, R. D; Figs and the Diversity of Tropical Rainforests. *Bioscience.* **2005**, 55, 1053-1064.

69. Berg, C. C.; Corner, E. J. *Moraceae (Ficus)* Flora Malesiana. Nationaal Herbarium; Leiden, 2005.

70. Cruaud, A.; Ronsted, N.; Chou, L. S.; Clement, W.L.; Couloux, A.; Cousins, B.; Genson, G.; Harrison, R.D.; Hanson, P.E.; Hossaert-McKey, M.; Jabbour-Zahab, R.; Jousselin, E.; Kerdelhué, C.; Kjellberg, F.; Lopez-Vaamonde, C.; Peebles, J.; Peng, Y. Q.; Pereira, R. A.; Schramm T.; Ubaidillah, R.; van Noort, S.; Weiblen, G. D.; Yang, D. R,; Yodpinyanee, A.; Libeskind-Hadas, R.; Cook, J.; Rasplus, J.Y.; Savolainen, V. An Extreme case of plant-insect codiversification: Figs and fig-pollinating wasps. *Syst. Biol.* **2012**, 61, 1029–1047.

71. Lansky, E. P.; Paavilainen, H.; Pawlus, A.; Newman, R. A. Ficus spp. (fig): Ethnobotany and potential as anticancer and anti-inflammatory agents. *J. Ethnopharmacol.* **2008**. 119**,** 825–831.

72. Rijksherbarium, M.; Miquel, F. A. W. *Annales Musei botanici lugduno-batavi;* Amsterdam, v.3, p1-315, 1867.

73. Corner, E. J. Checklist of Ficus in Asia and Australasia with keys to identification. *Gard. Bull. Singapore.* **1965**, 21**,** 1–186.

74. Berg, C. C. Corrective notes on the Malesian members of the genus Ficus (Moraceae). *Blumea J. Plant Taxon. Plant Geogr.* **2011**, 56, 161–164.

75. Stoye, A.; Peez, T. E.; Opatz, T. Left, Right, or Both? On the Con fi guration of the Phenanthroindolizidine Alkaloid Tylophorine from Tylophora indica. *J. Nat. Prod.*, **2013**, *76* (2), 275–278.

76. Sergeiko, A.; Poroikov, V. V.;Hanu, L. O.; Dembitsky, V. M. Cyclobutane-Containing Alkaloids : Origin , Synthesis , and Biological Activities. Open Med. Chem. J. **2008**, 2, 26–37.

77. Wagner, C.; Omari, M. El; Ko, G. M. Biohalogenation : Nature ' s Way to Synthesize Halogenated Metabolites. *J. Nat. Prod.*, **2009**, *72*, 540–553.

78. Deng, M.; Su, B.; Zhang, H.; Liu, Y.; Wang, Q. Total synthesis of phenanthroindolizidine alkaloids via asymmetric deprotonation of N-Boc-pyrrolidine. *RSC Adv.* **2014**, 4, 14979-14984 .

79. Lv, H.; Ren, J.; Shuanggang, M.; Xu, S.; Qu, J.; Liu, Z. Synthesis , Biological Evaluation and Mechanism Studies of Deoxytylophorinine and Its Derivatives as Potential Anticancer Agents. *PloS. one.* **2012***,* 7(1), e30342.

80. Niphakis, M. J.; Georg, G. I. & Drive, W. H. Total Syntheses of Arylindolizidine Alkaloids. *J. Org. Chem.*, **2010**, *75*, 6019–6022

APPENDICIES

- **APPENDIX A:**
  NMR, MS and IR spectra of (±)-tengerensine (**1**)

- **APPENDIX B:**
  NMR, MS and IR spectra of (±)-tengechlorenine (**2**)

- **APPENDIX C:**
  NMR, MS and IR spectra of (±)-fistulosine (**3**)

- **APPENDIX D:**
  NMR, MS and IR spectra of (+)-antofine (**4**)

- **APPENDIX E:**
  NMR, MS and IR spectra of (−)-*seco*antofine (**5**)

APPENDIX A

NMR spectra of tengerensine (1)

^{1}H NMR

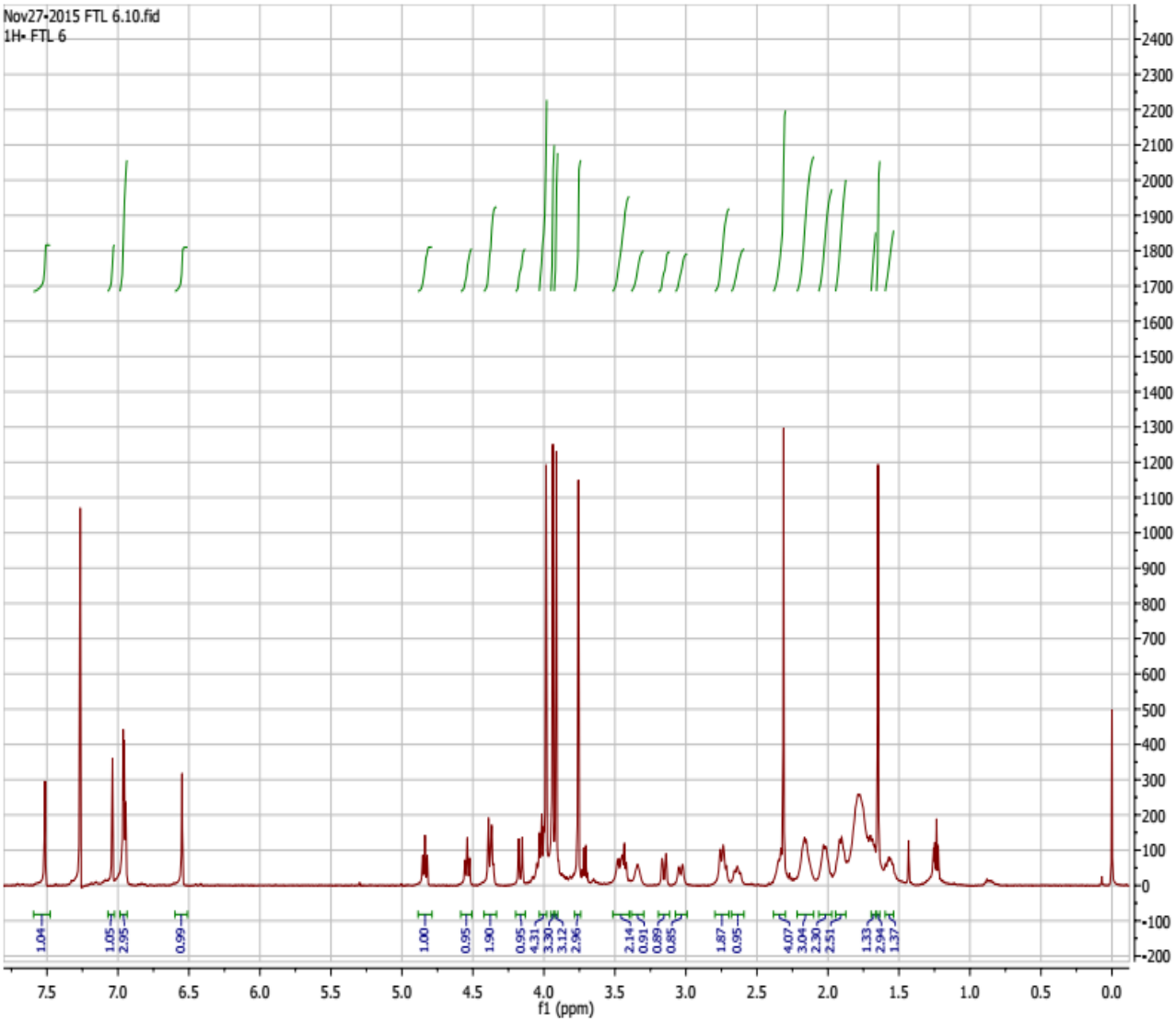

^{13}C NMR

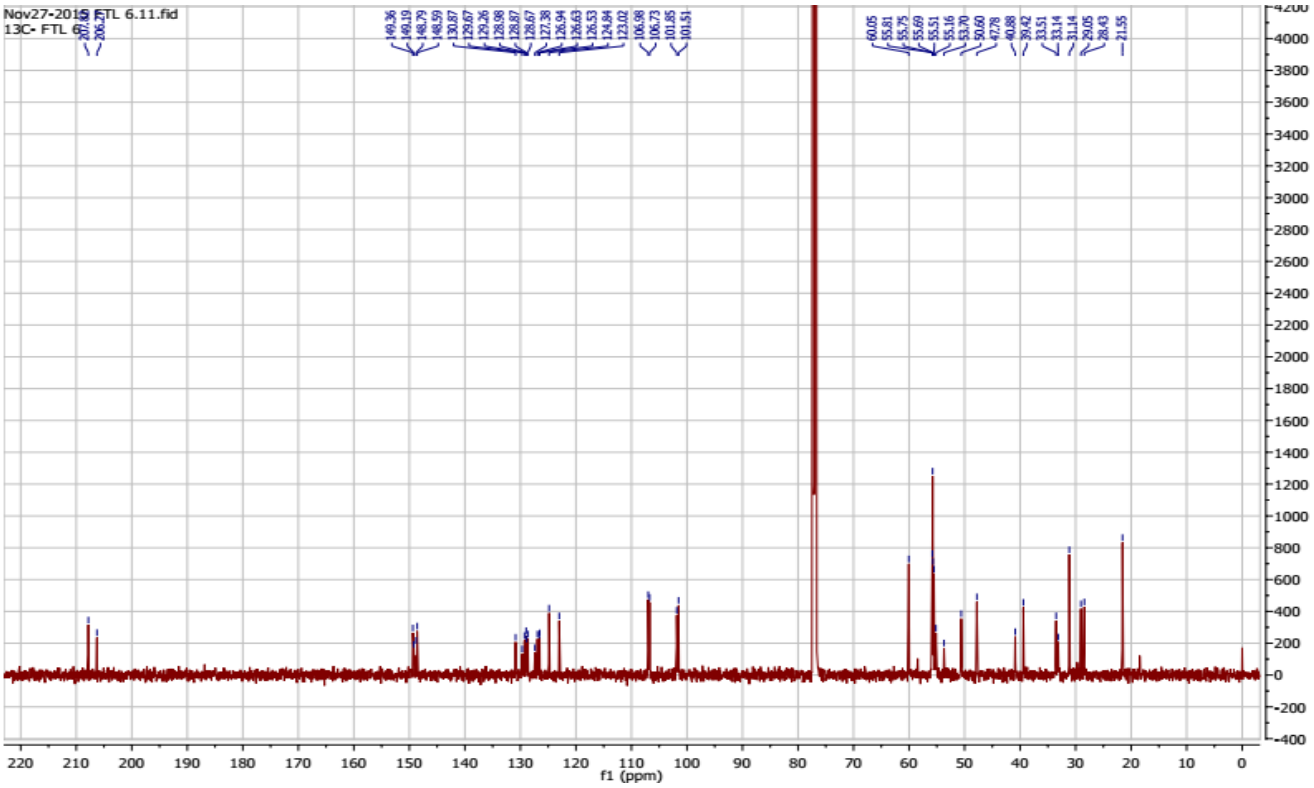
Nov27-2015 FTL 6.11.fid
13C- FTL 6
f1 (ppm)

COSY

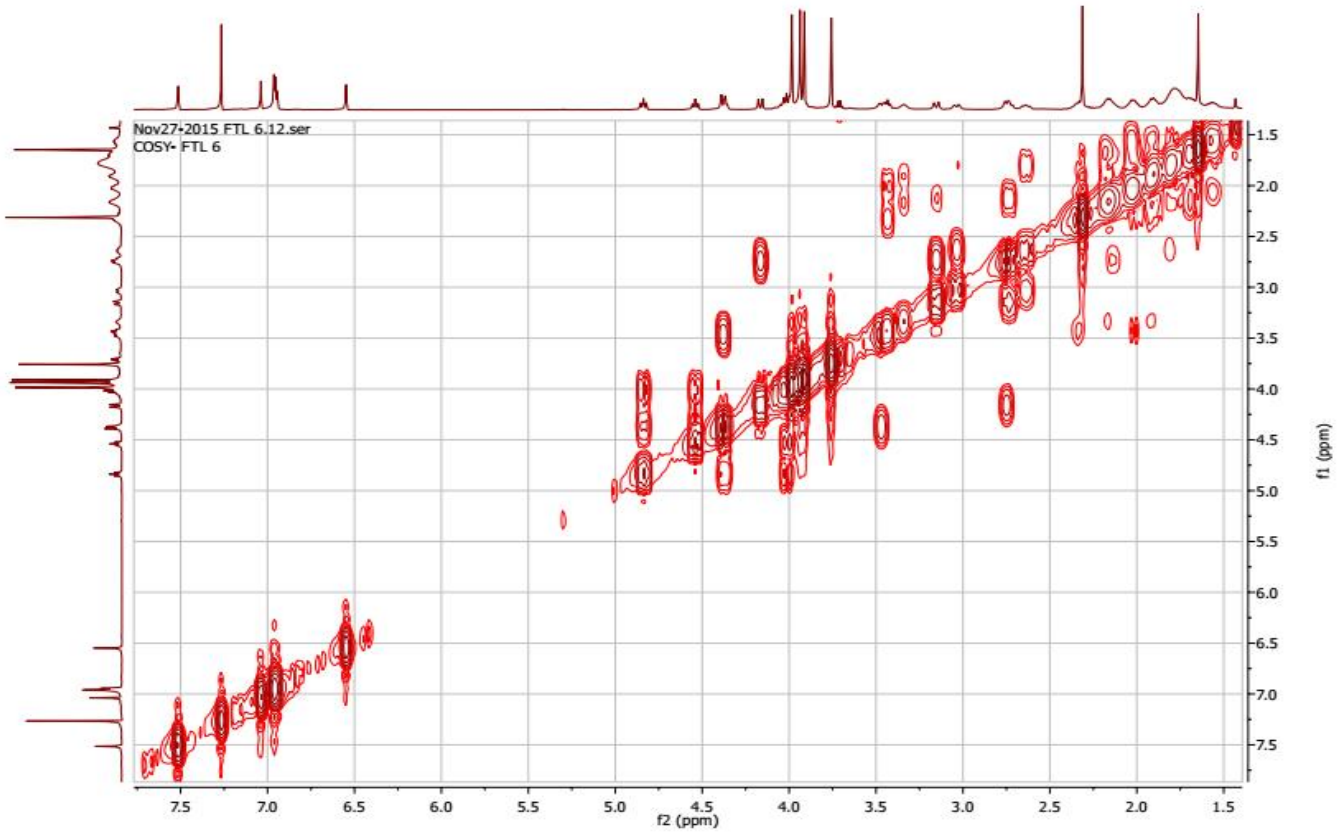
Nov27-2015 FTL 6.12.ser
COSY- FTL 6
f2 (ppm)
f1 (ppm)

HSQC

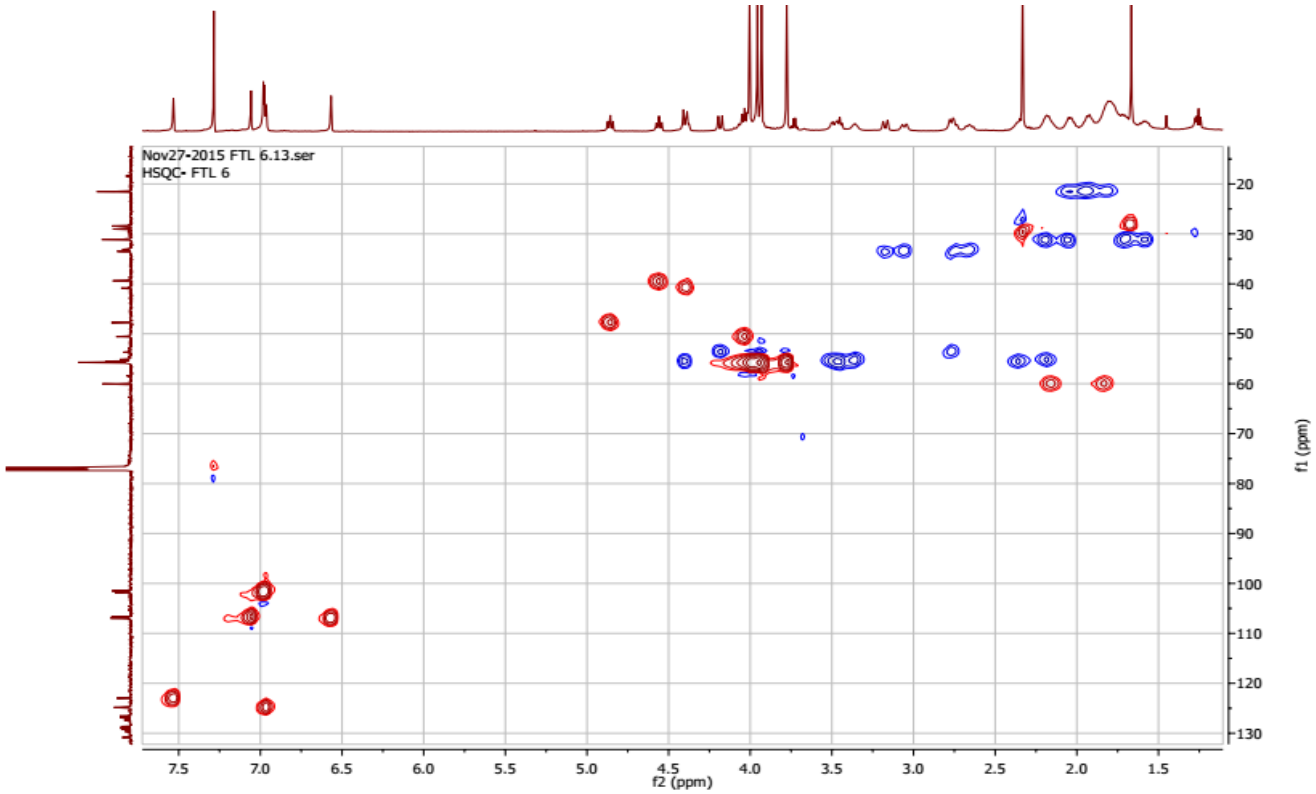
Nov27-2015 FTL 6.13.ser
HSQC- FTL 6
f2 (ppm)
f1 (ppm)

HMBC

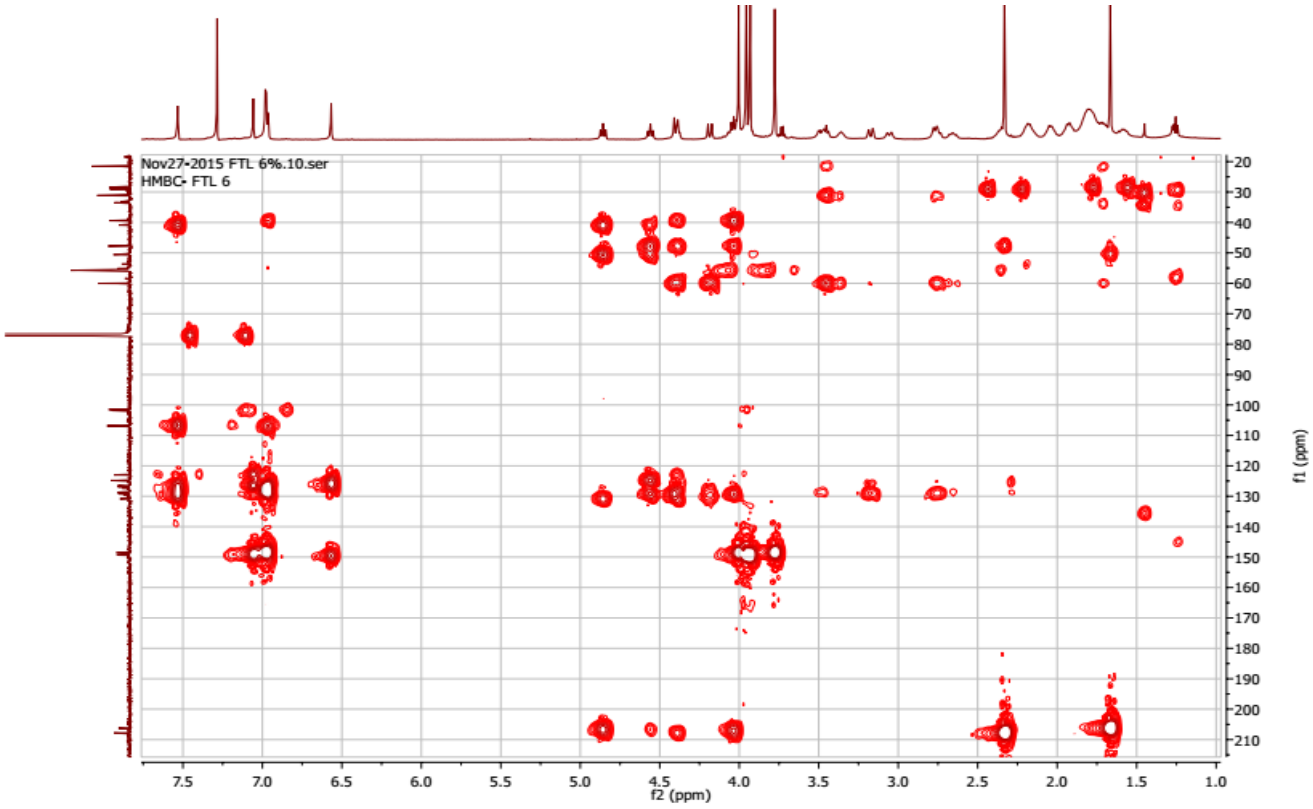
Nov27-2015 FTL 6%.10.ser
HMBC- FTL 6
f2 (ppm)
f1 (ppm)

NOESY

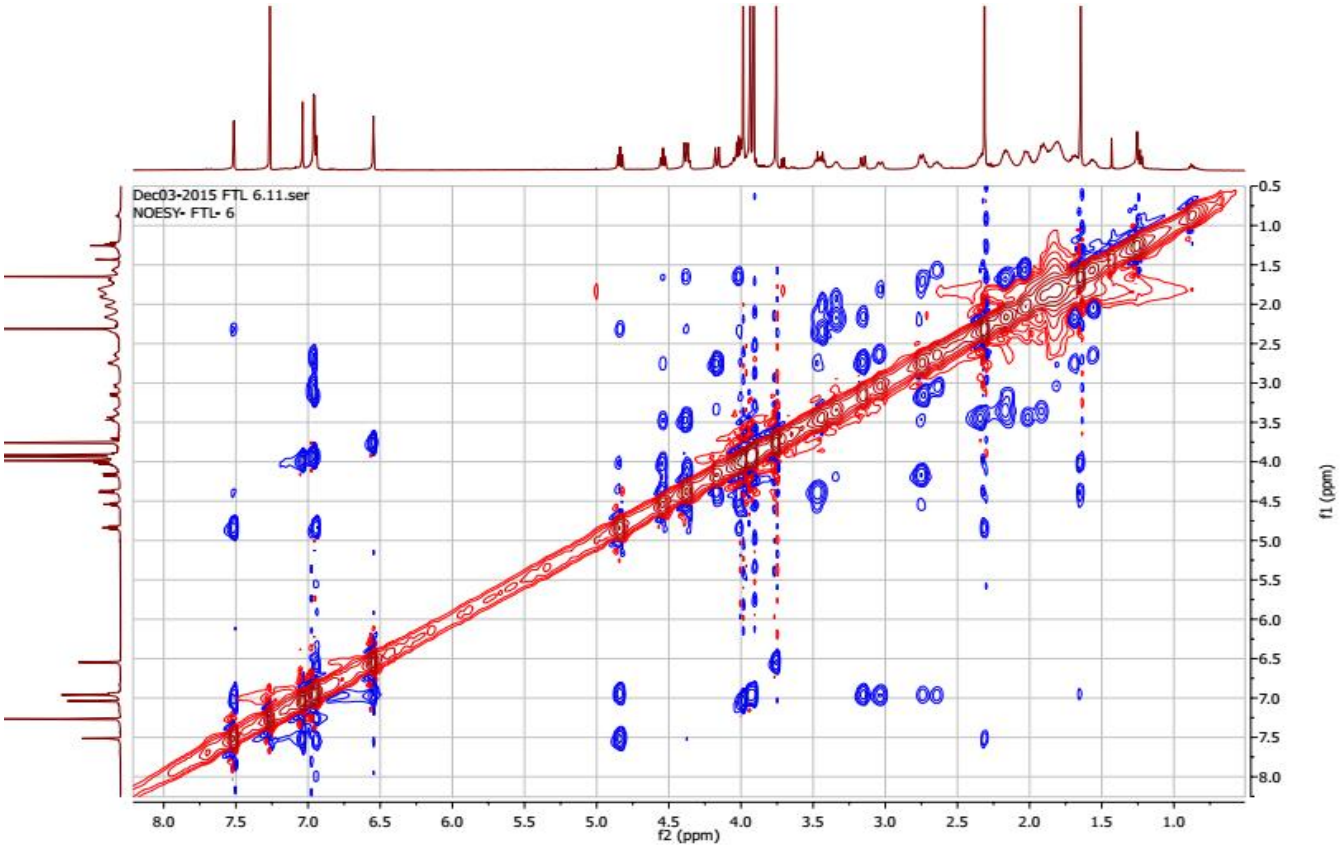

HRESIMS of tengerensine (1)

Data:FTL6x2
Sample Name:
Description:
Ionization Mode:ESI+
History:Determine m/z[Peak Detect[Centroid,30,Area];Correct Base[0.5%]];Correct Ba...

Acquired:12/7/2015 2:55:11 PM
Operator:AccuTOF
Mass Calibration data:iCalibration
Created:12/8/2015 9:07:31 AM
Created by:

Charge number:1 Tolerance:20.00(ppm), 5.00 .. 15.00(mmu) Unsaturation Number:0.0 .. 25.0 (Fractio...
Element:^{12}C:0 .. 50, ^{1}H:0 .. 60, ^{14}N:0 .. 10, ^{16}O:0 .. 10

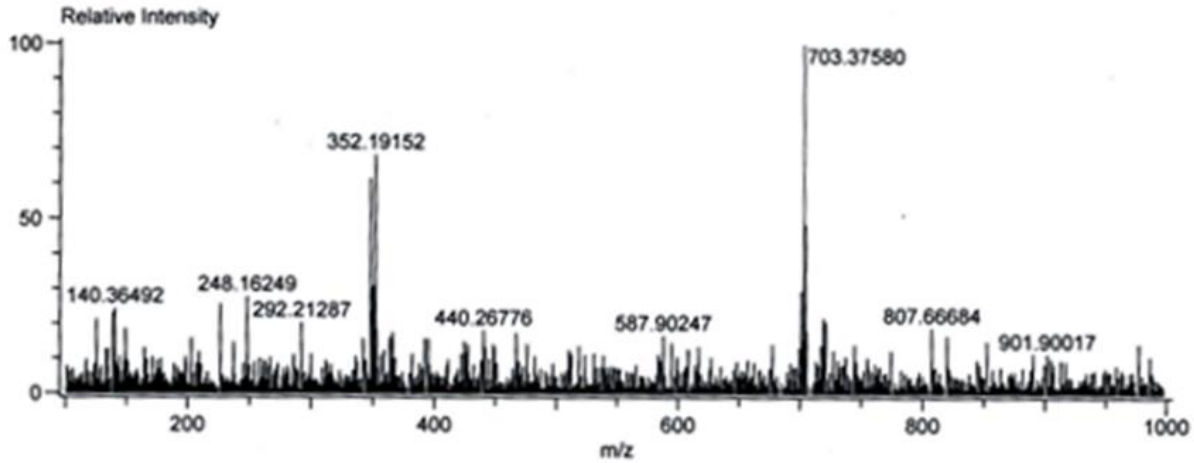

FT-IR spectrum of tengerensine (1)

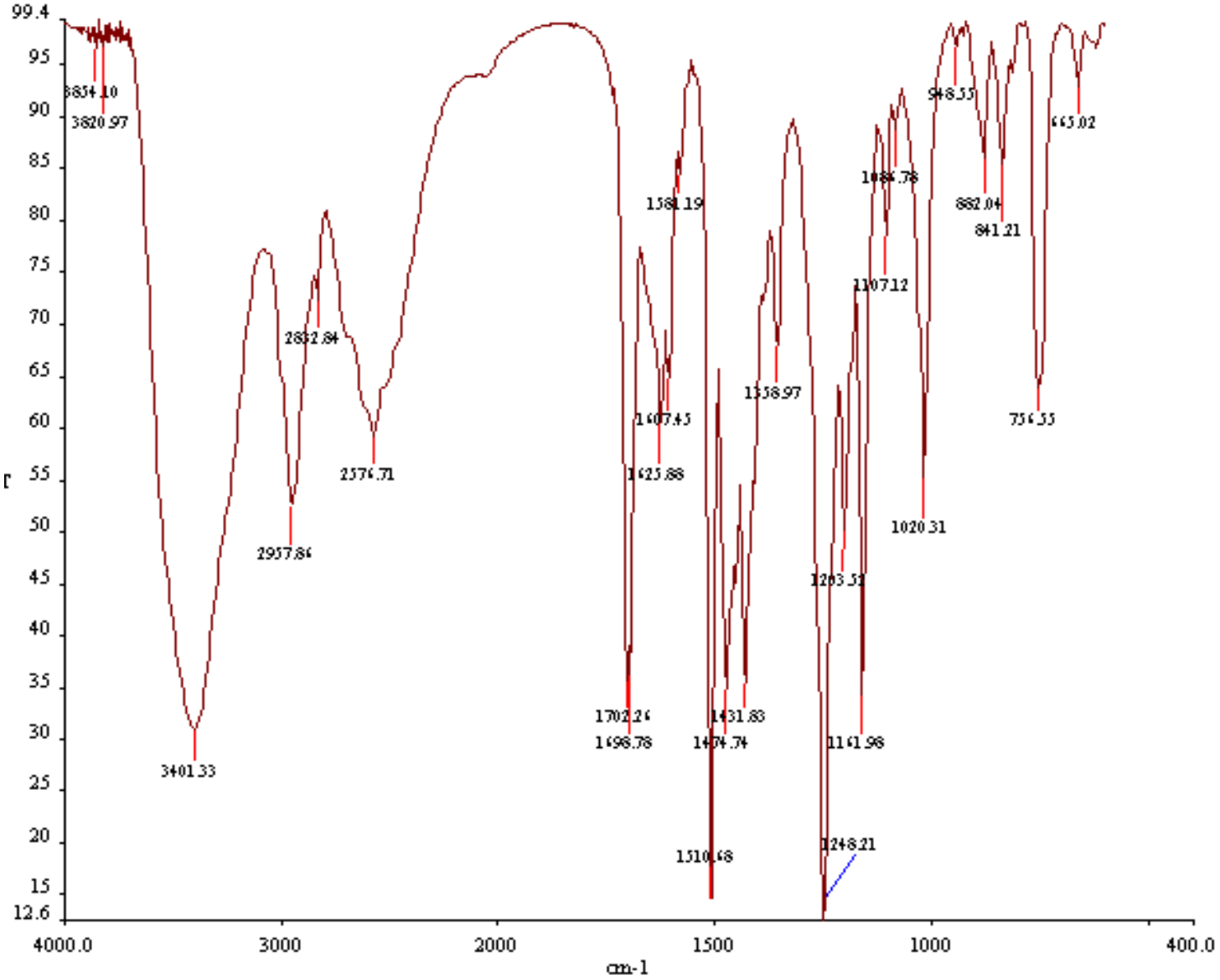

APPENDIX B

NMR spectra of tengechlorenine (2)

^{1}H NMR

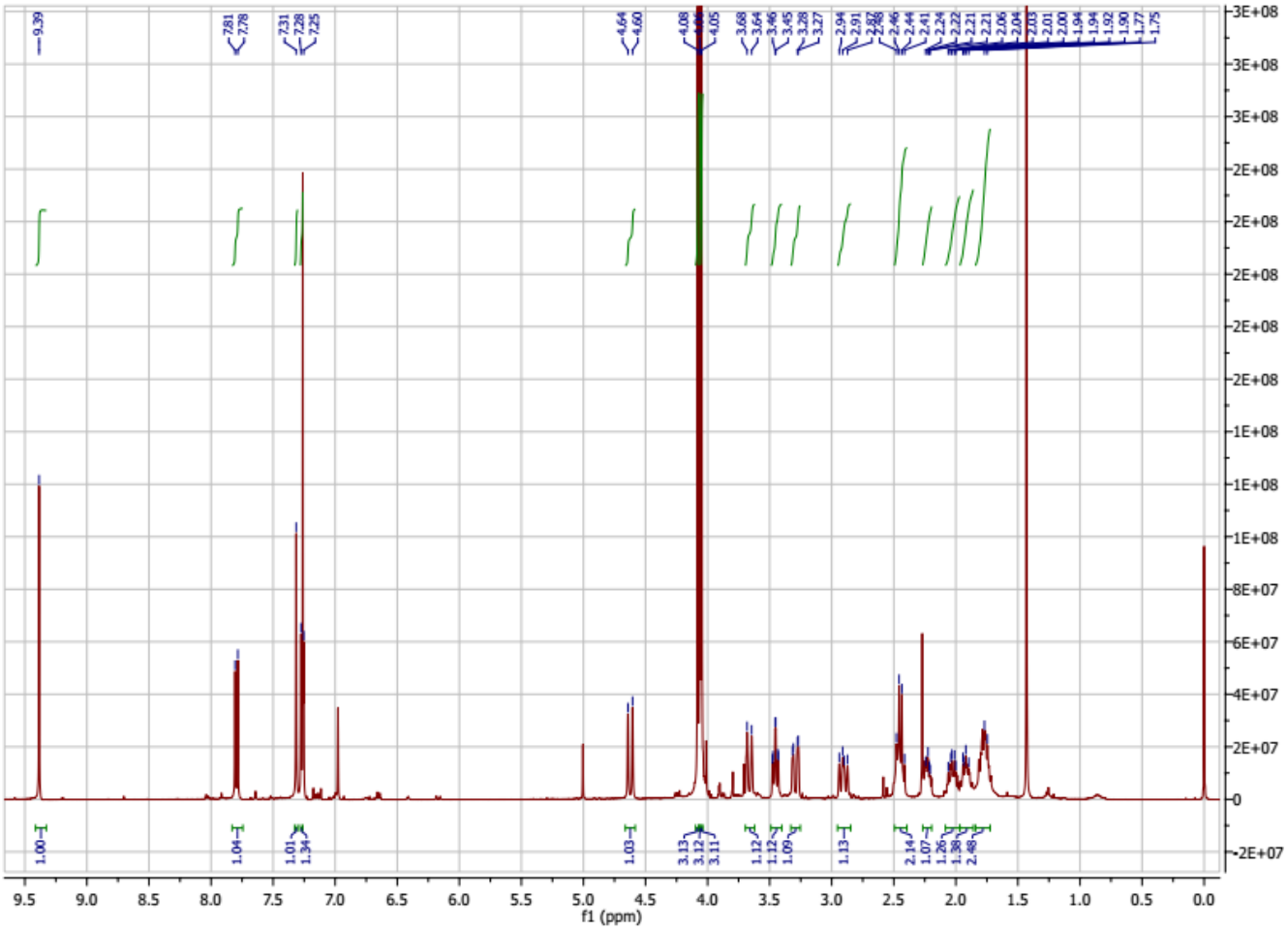

^{13}C NMR

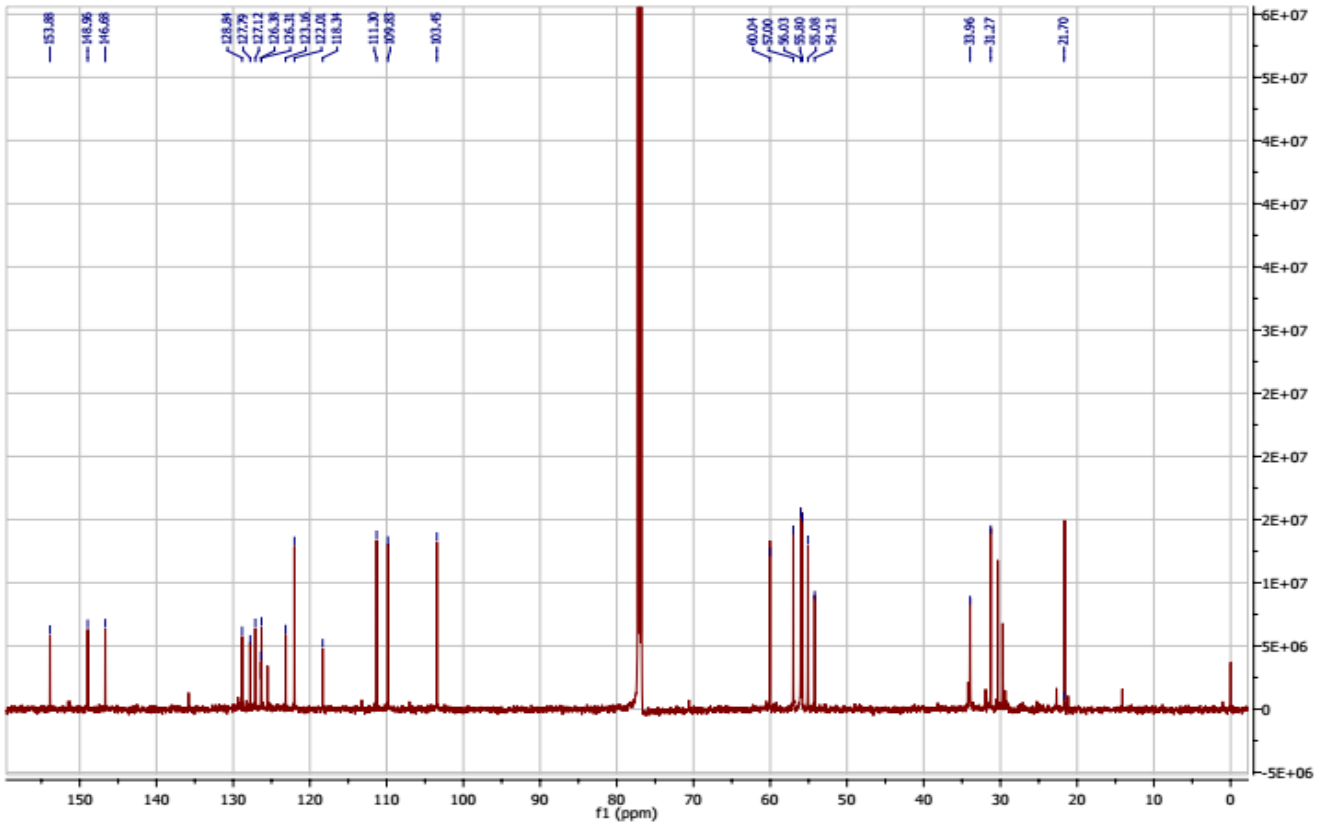
153.88
148.96
146.68
128.84
127.79
127.12
126.38
126.31
123.36
122.01
118.34
111.30
109.83
103.45
60.04
57.00
56.03
55.80
55.08
54.21
33.96
31.27
21.70
f1 (ppm)

COSY

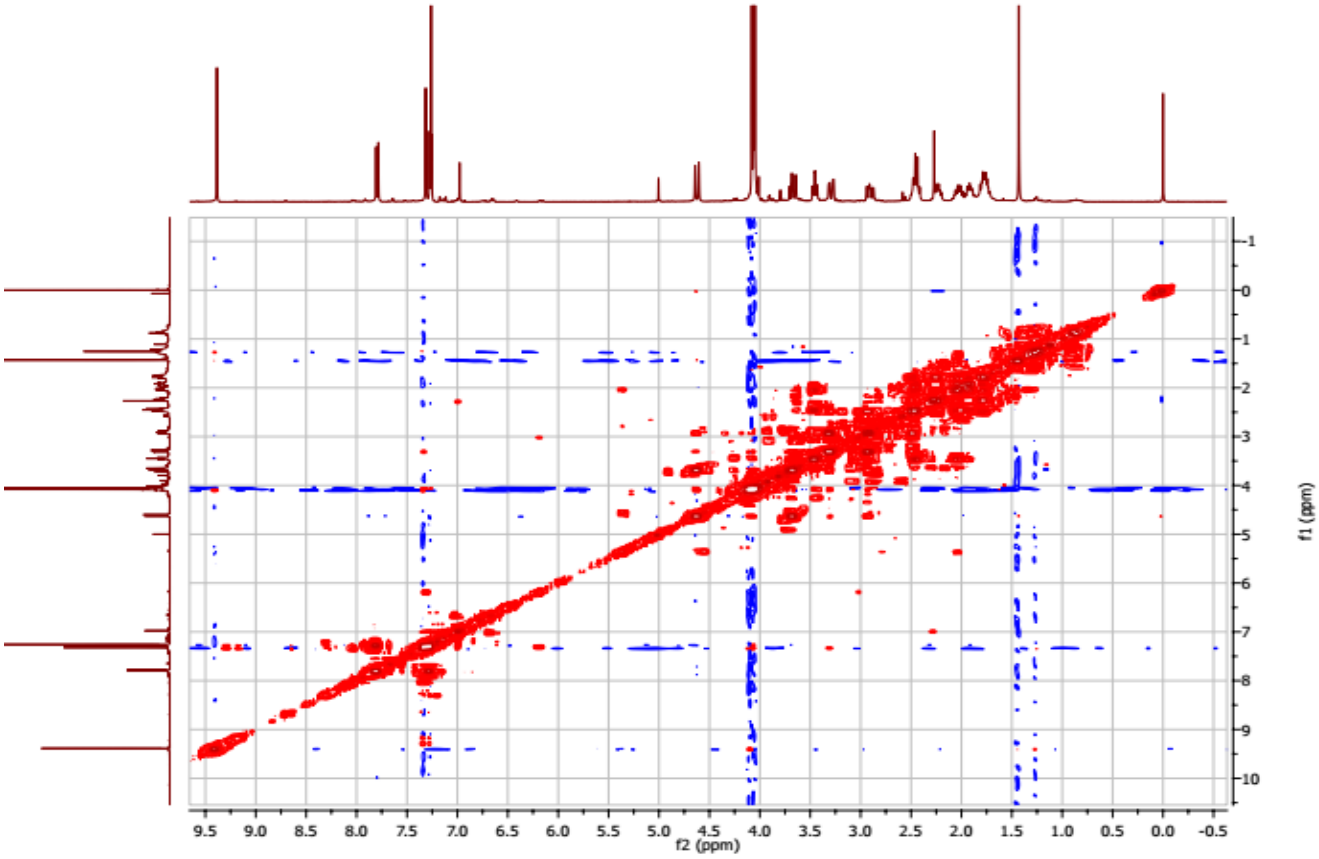
f2 (ppm)
f1 (ppm)

HSQC

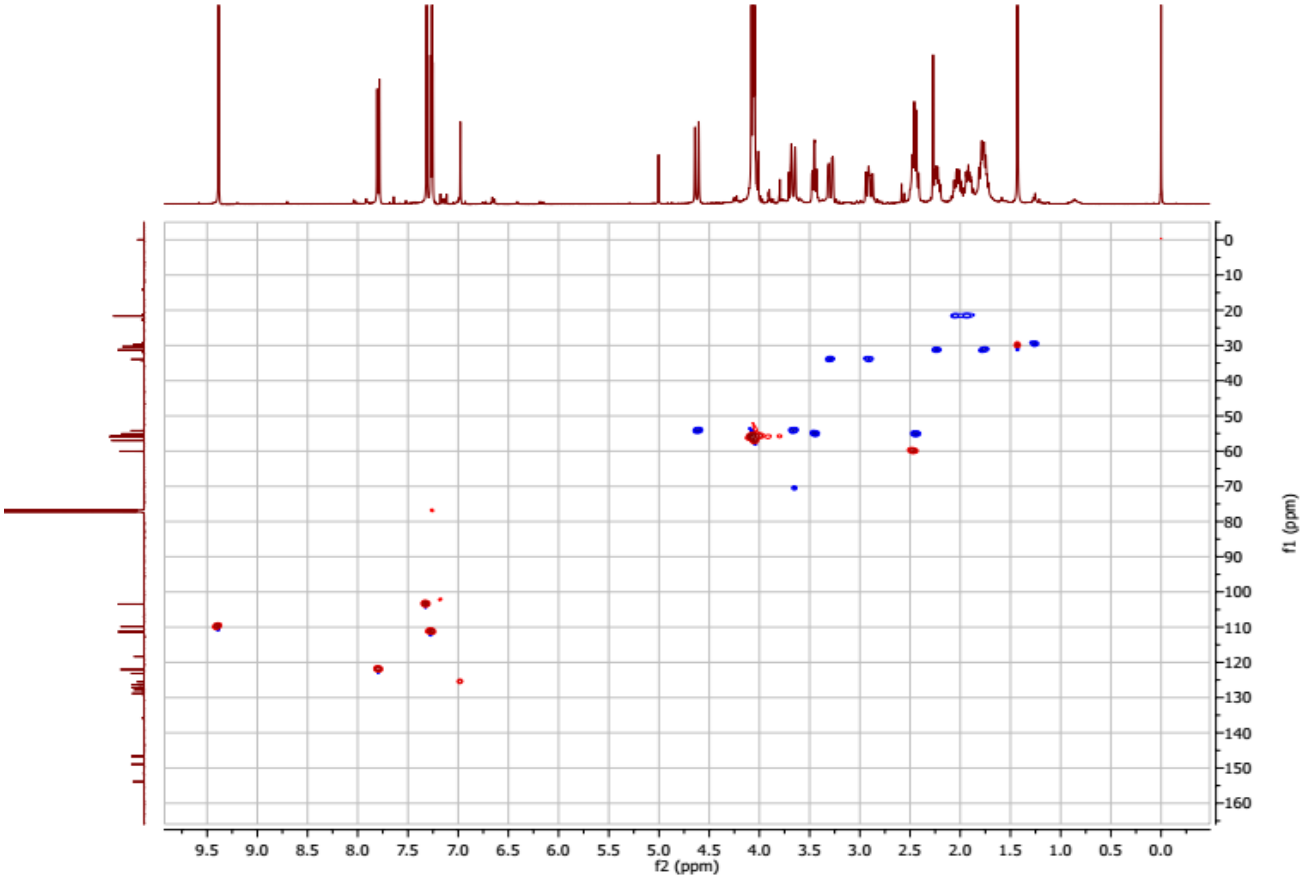

HMBC

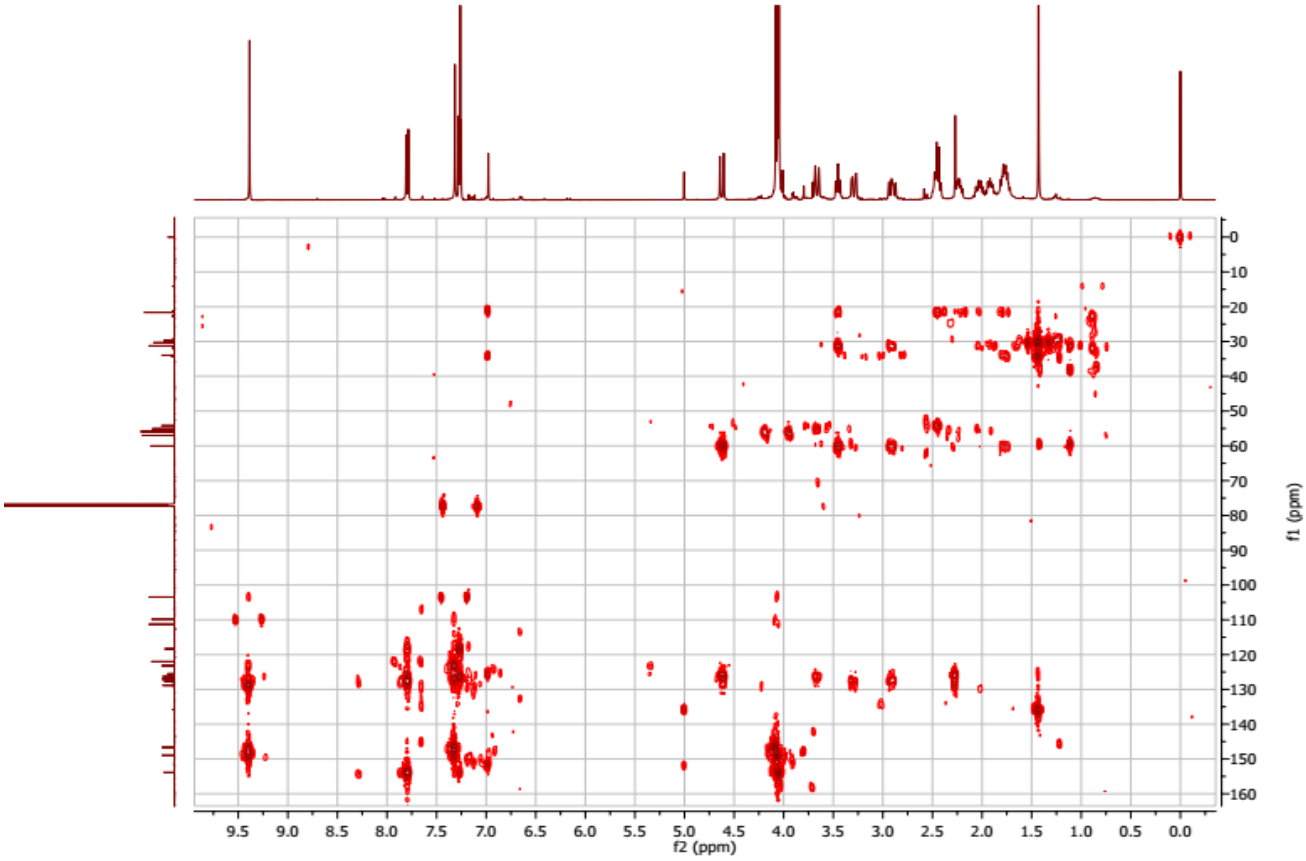

NOESY

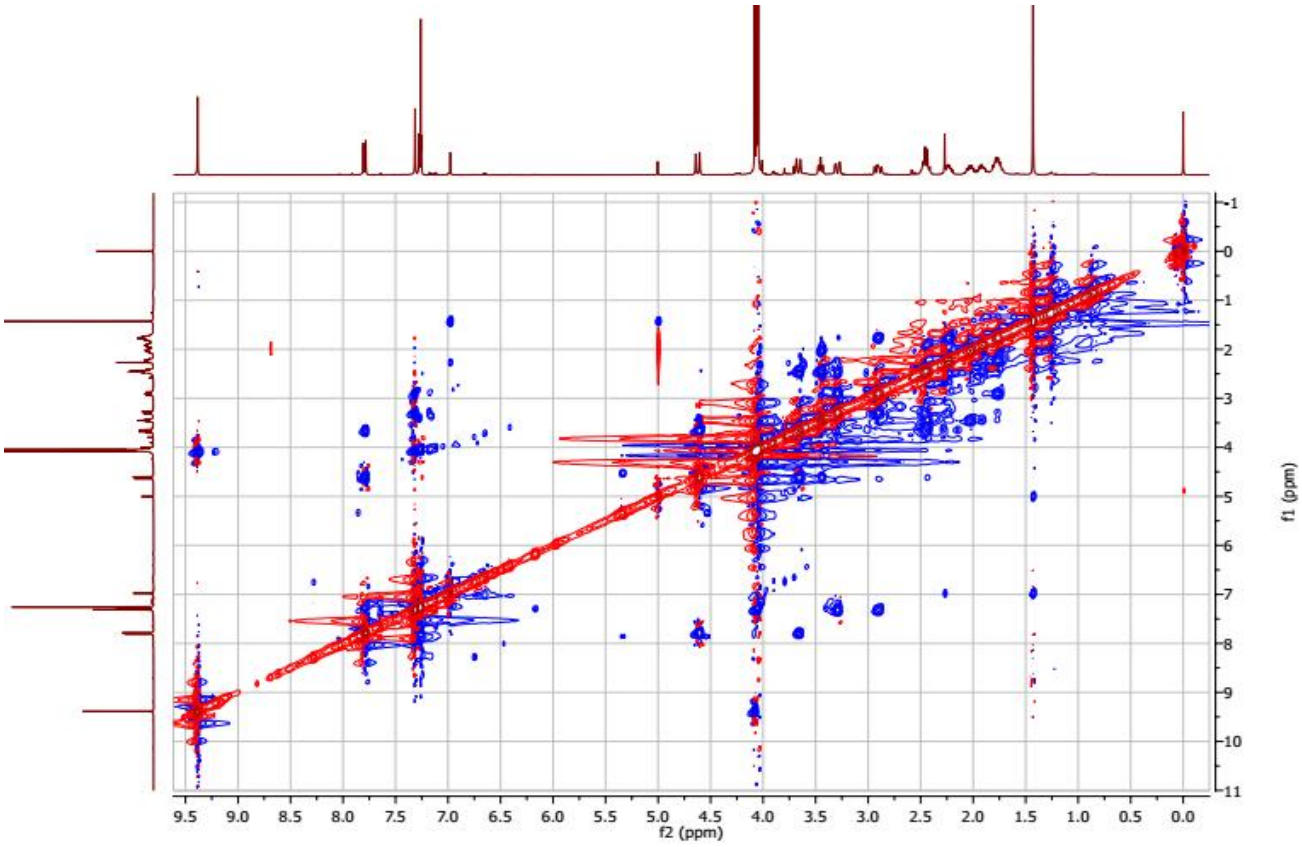

HRESIMS of tengechlorenine (2)

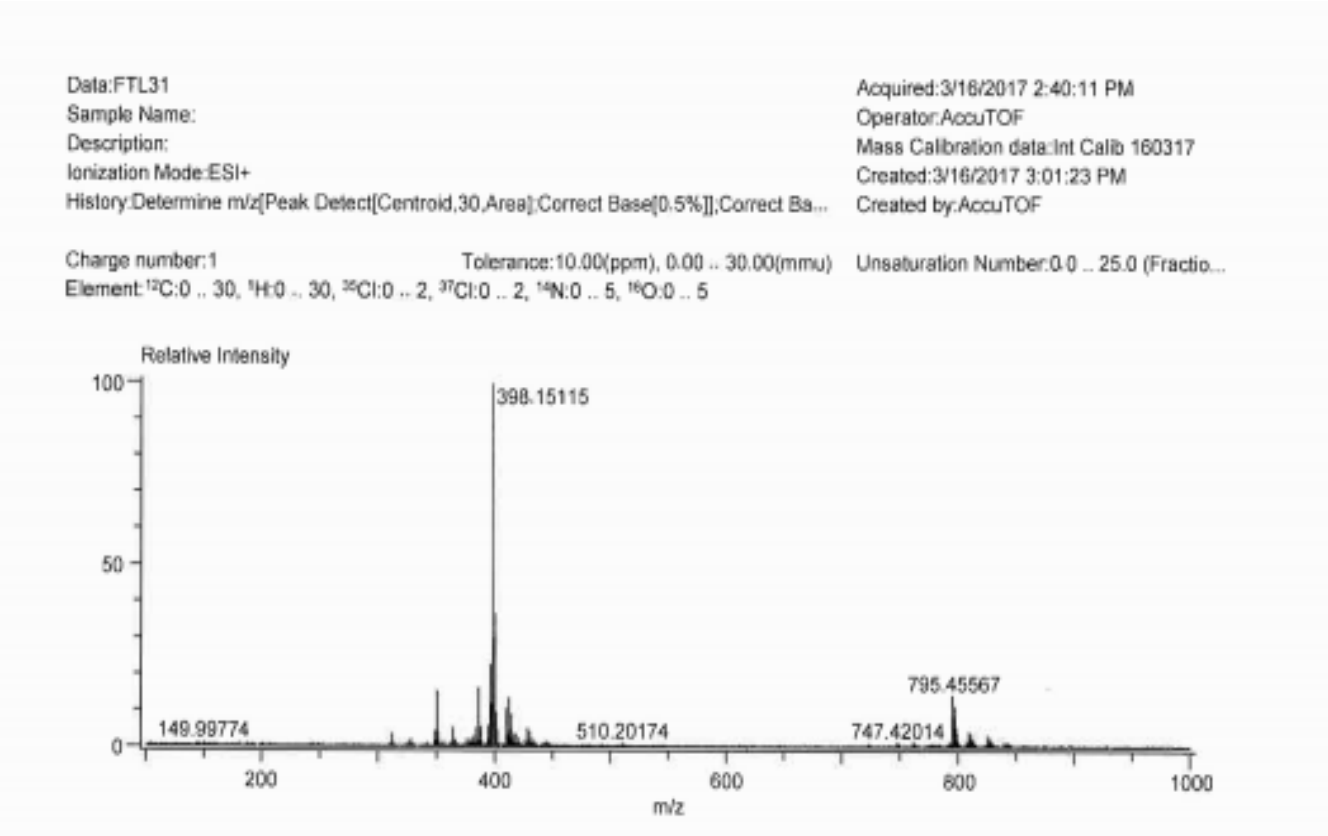

FT-IR spectrum of tengechlorenine (2)

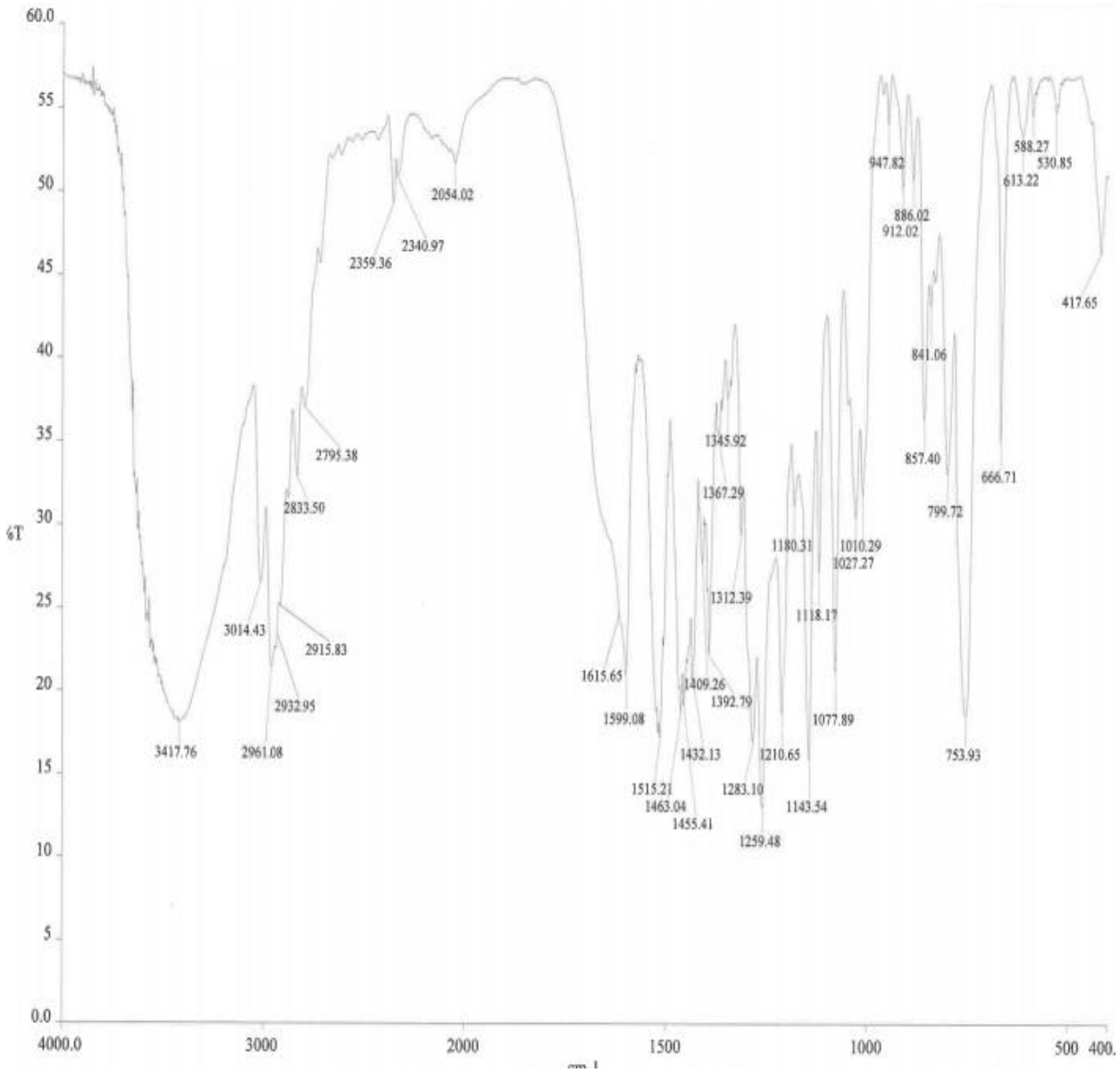

APPENDIX C

NMR spectra of (±)-fistulosine (3)

^{1}H NMR

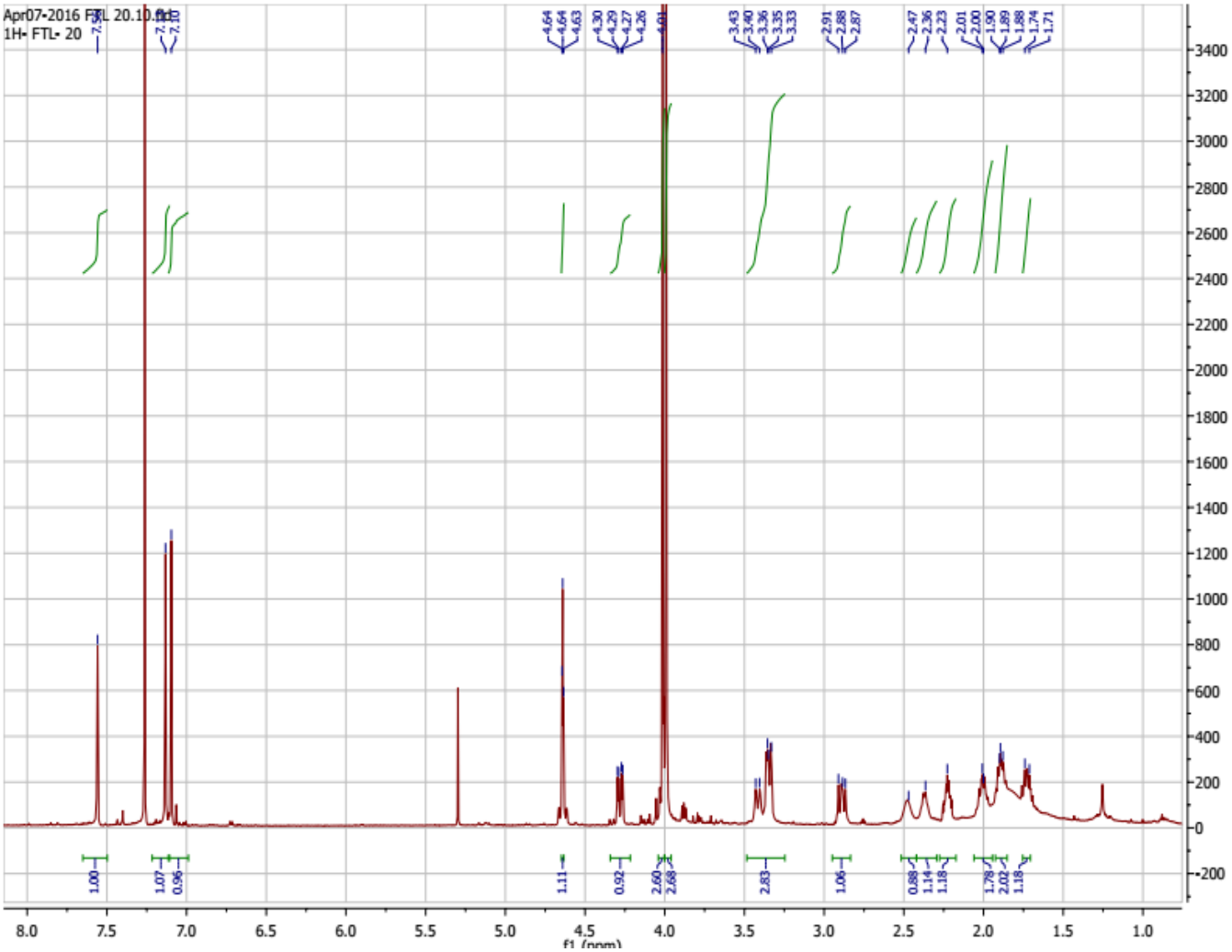

^{13}C NMR

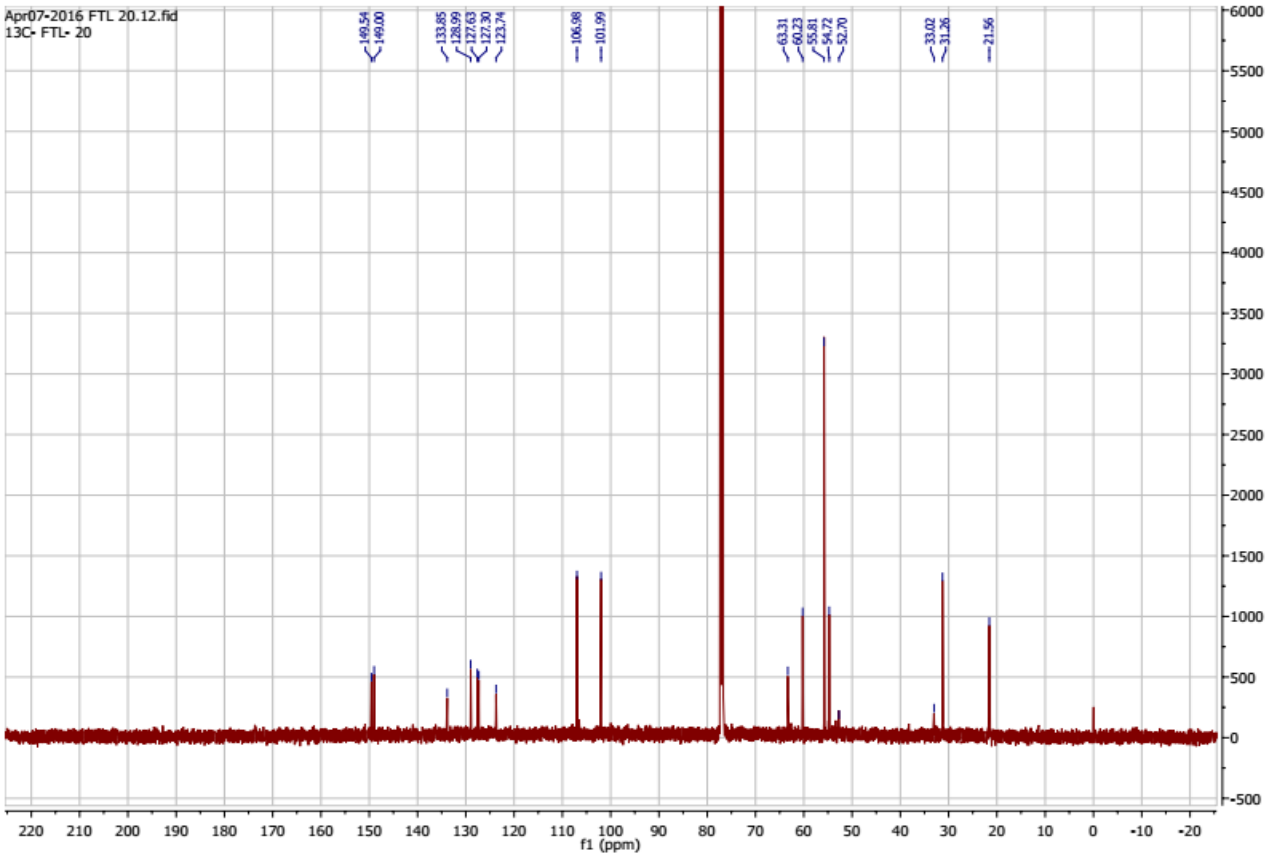
Apr07-2016 FTL 20.12.fid
13C- FTL- 20
149.54
149.00
133.85
128.99
127.63
127.30
123.74
106.98
101.99
63.31
60.23
55.81
54.72
52.70
33.02
31.26
21.56
f1 (ppm)

COSY

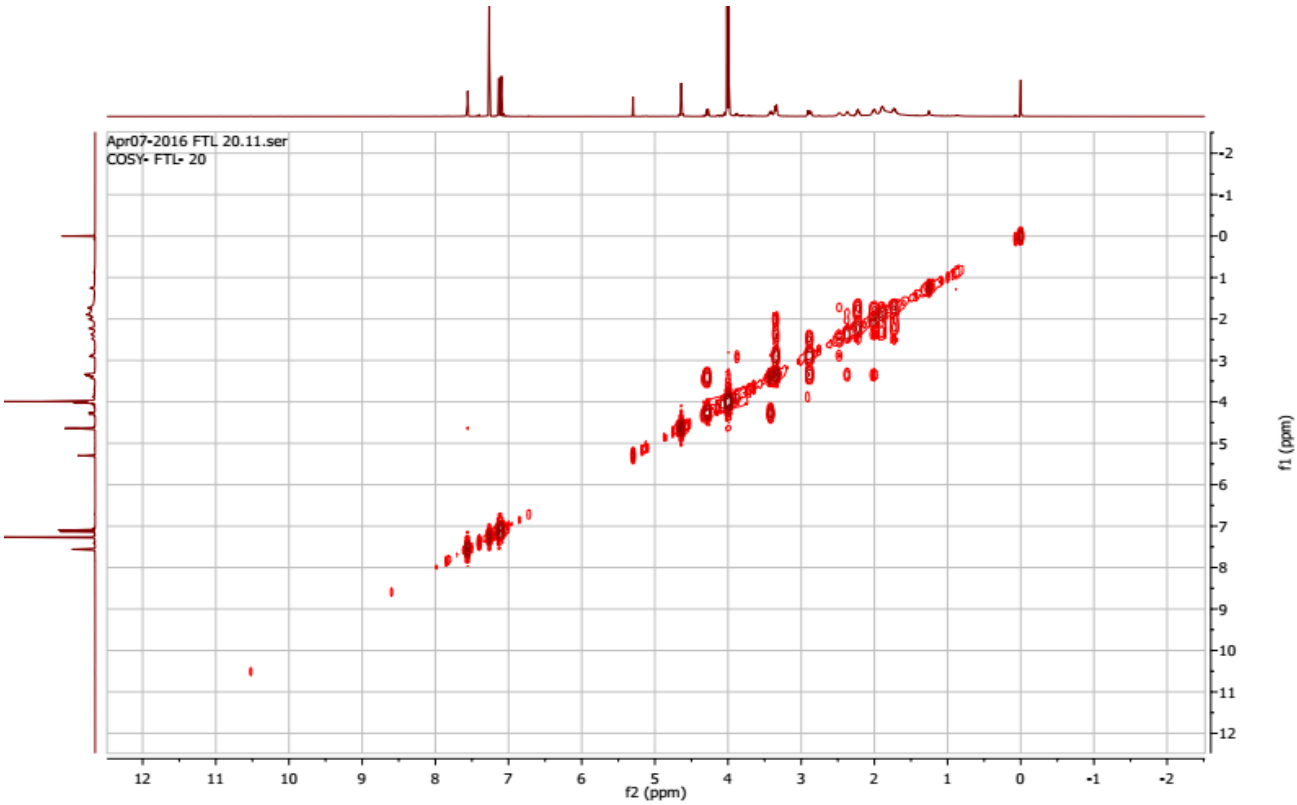
Apr07-2016 FTL 20.11.ser
COSY- FTL- 20
f2 (ppm)
f1 (ppm)

HSQC

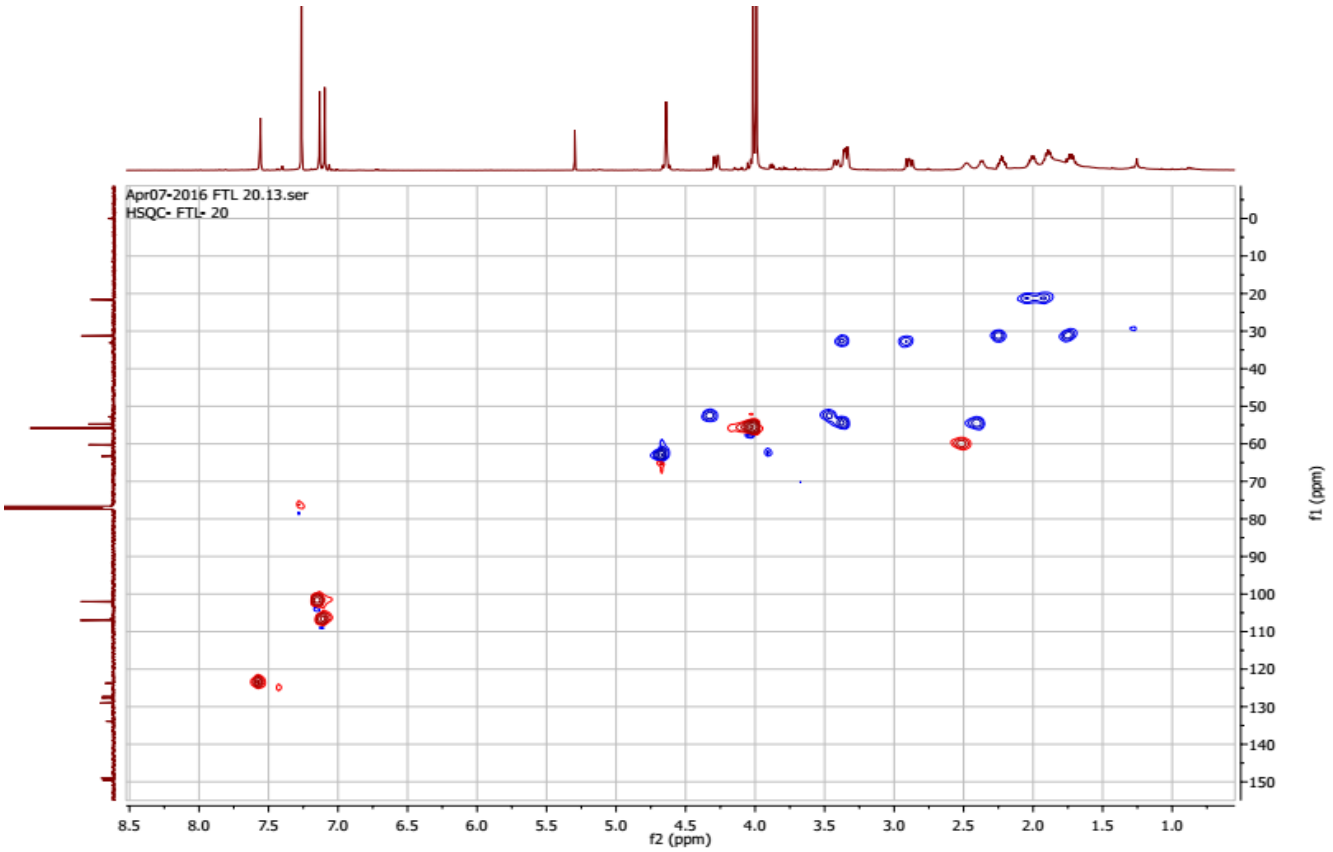
Apr07-2016 FTL 20.13.ser
HSQC- FTL- 20
f2 (ppm)
f1 (ppm)

HMBC

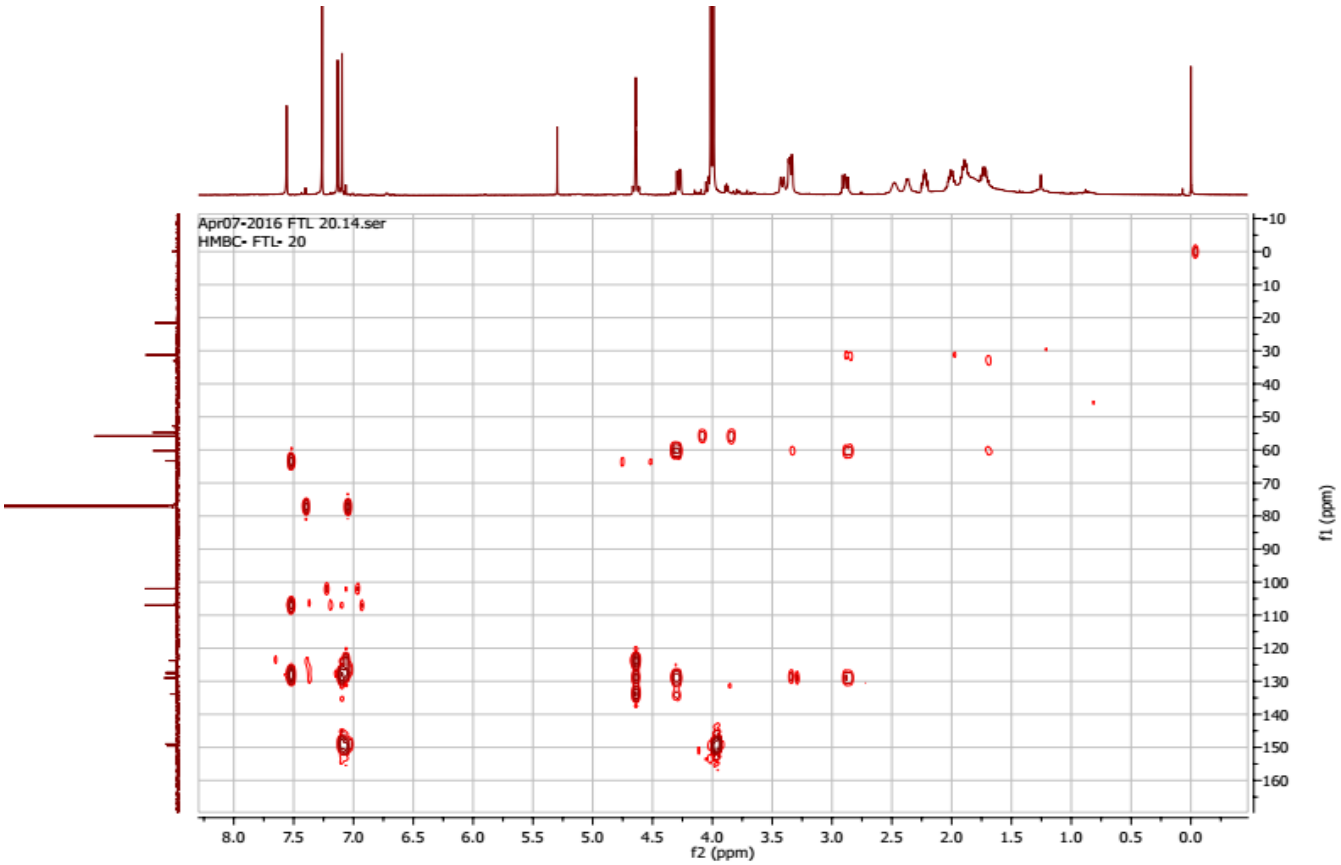
Apr07-2016 FTL 20.14.ser
HMBC- FTL- 20
f2 (ppm)
f1 (ppm)

NOESY

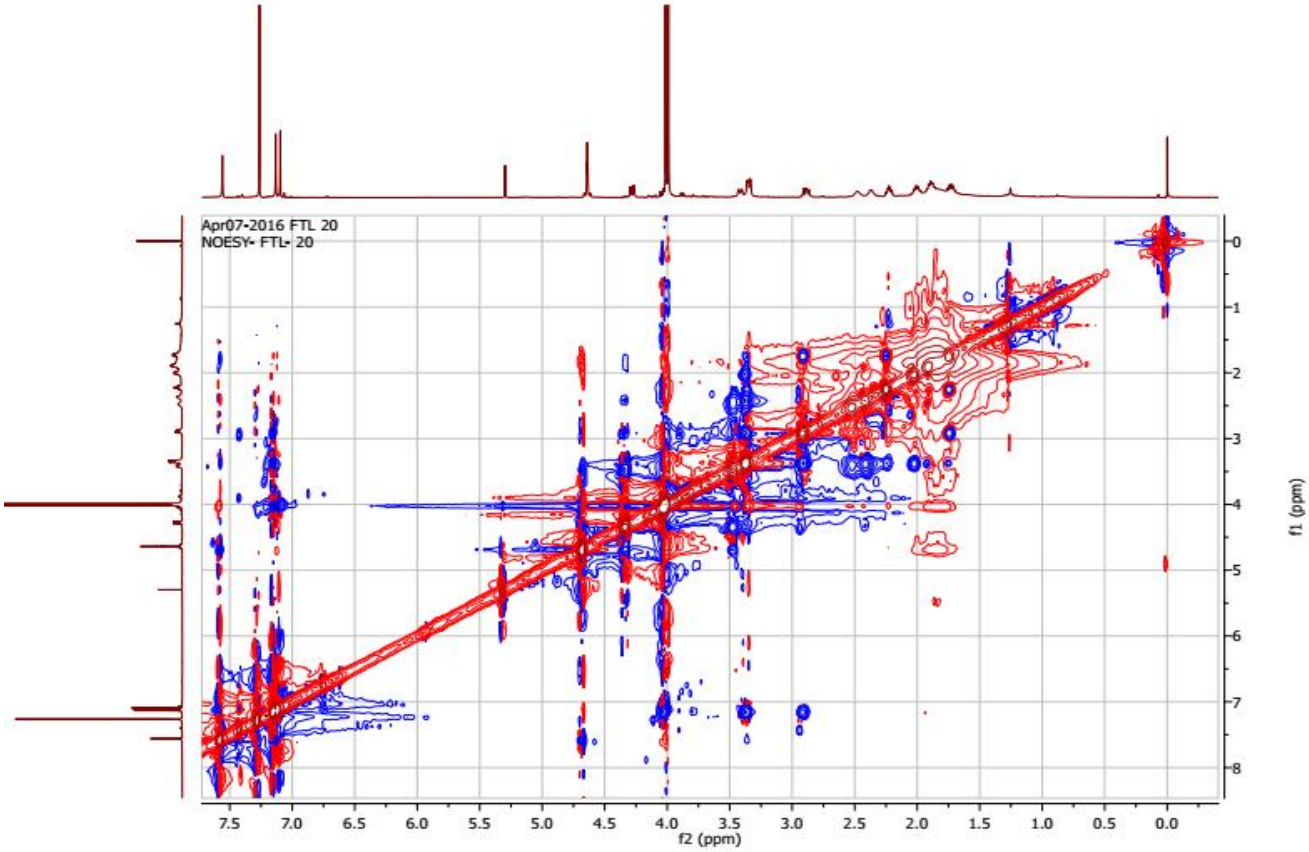

HRESIMS of (±)-fistulosine (3)

Data:FTL20
Sample Name:
Description:
Ionization Mode:ESI+
History:Determine m/z[Peak Detect[Centroid,30,Area];Correct Base[0.5%]];Correct Ba...

Acquired:3/24/2016 5:46:37 PM
Operator:AccuTOF
Mass Calibration data:PEG calib 240316
Created:3/24/2016 6:14:55 PM
Created by:AccuTOF

Charge number:1 Tolerance:30.00(ppm), 5.00 .. 15.00(mmu) Unsaturation Number:0.0 .. 25.0 (Fractio...
Element:^{12}C:0 .. 50, ^{1}H:0 .. 50, ^{14}N:0 .. 10, ^{16}O:0 .. 20

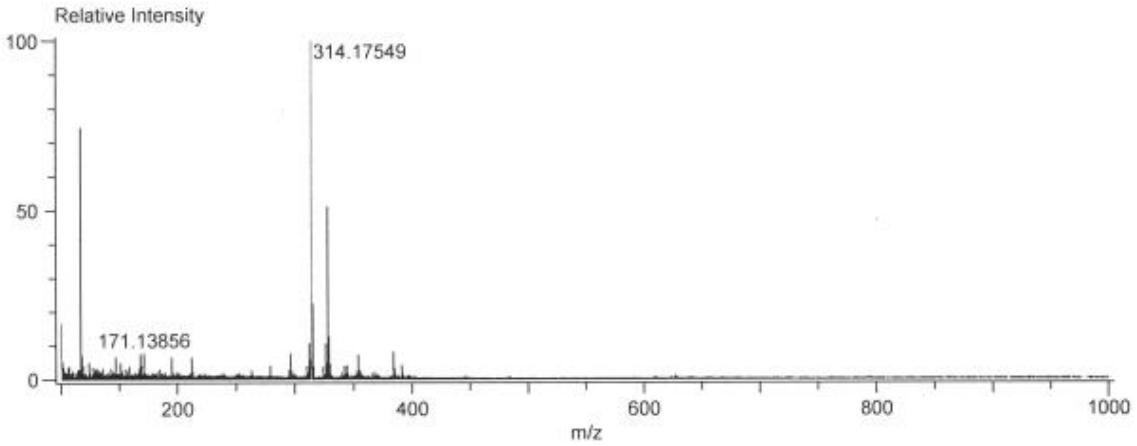

FT-IR spectrum of (±)-fistulosine (3)

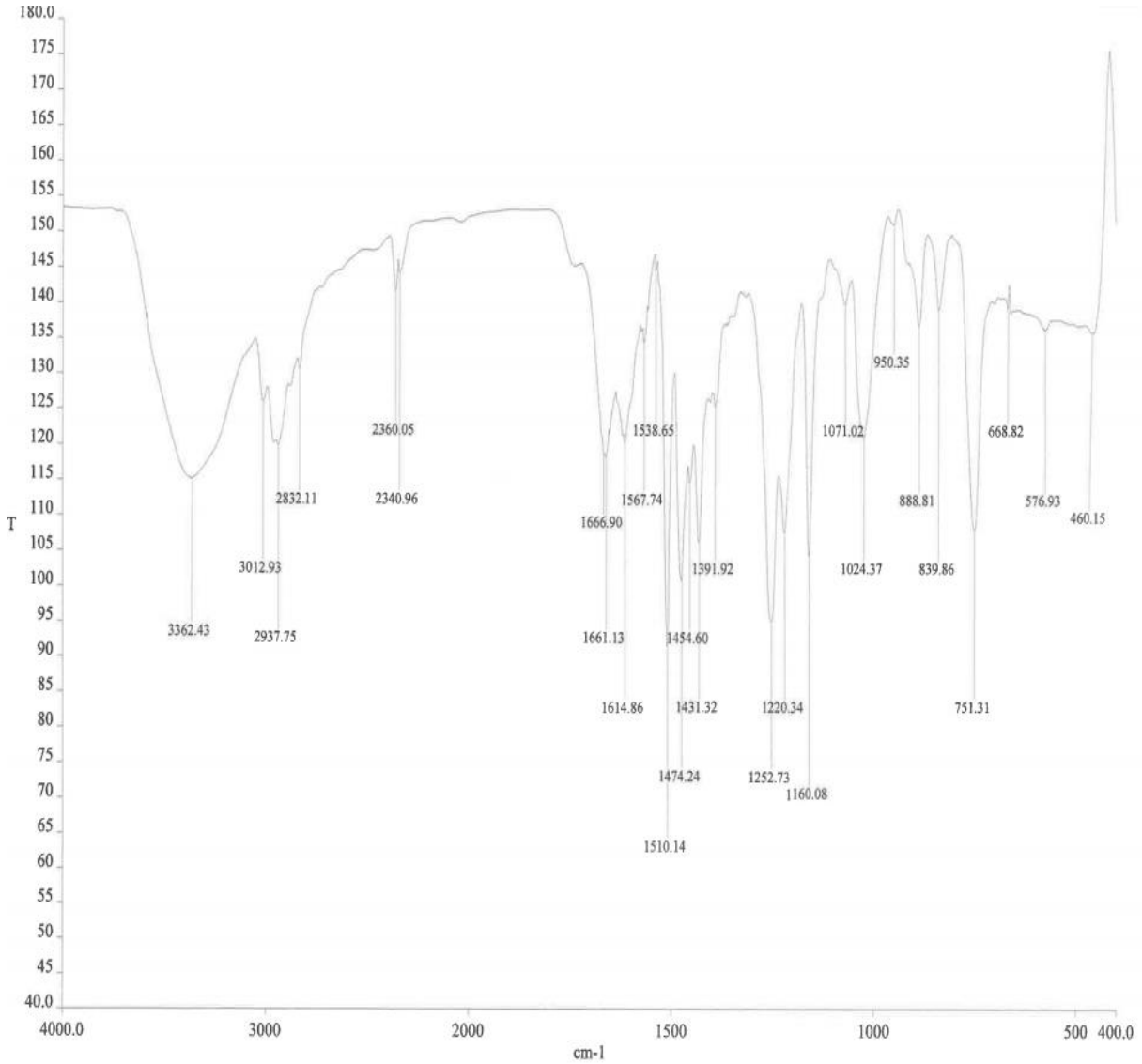

APPENDIX D

^{1}H NMR of antofine (4)

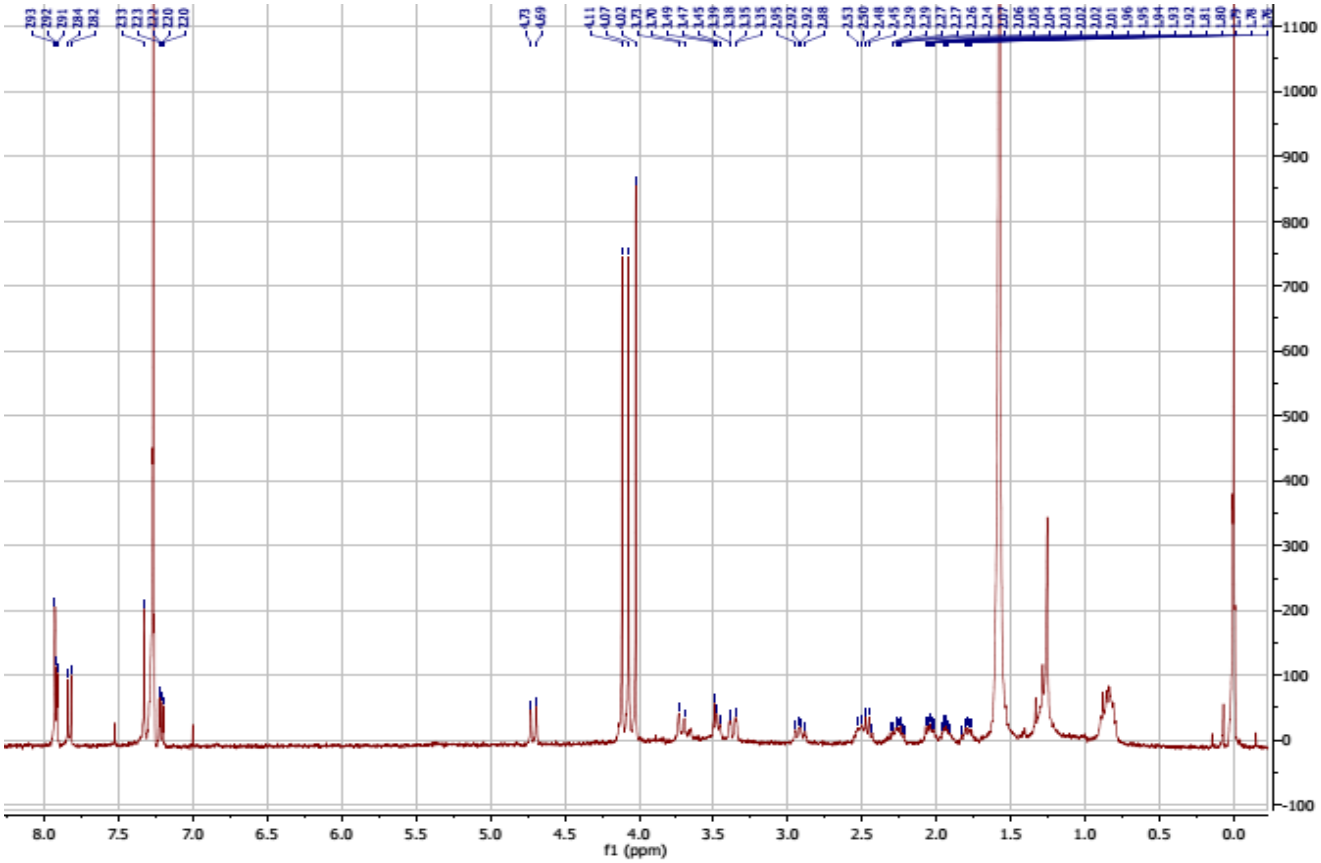

HRESIMS of antofine (4)

Data:FTL4_291116
Sample Name:
Description:
Ionization Mode:ESI+
History:Determine m/z[Peak Detect[Centroid,30,Area];Correct Base[0.5%]];Correct Ba...

Acquired:11/29/2016 11:21:18 AM
Operator:AccuTOF
Mass Calibration data:Int Calib 291116
Created:11/29/2016 2:16:02 PM
Created by:AccuTOF

Charge number:1 Tolerance:30.00(ppm), 5.00 .. 15.00(mmu) Unsaturation Number:0.0 .. 25.0 (Fractio...
Element:^{12}C:0 .. 30, ^{1}H:0 .. 30, ^{14}N:0 .. 3, ^{16}O:0 .. 5

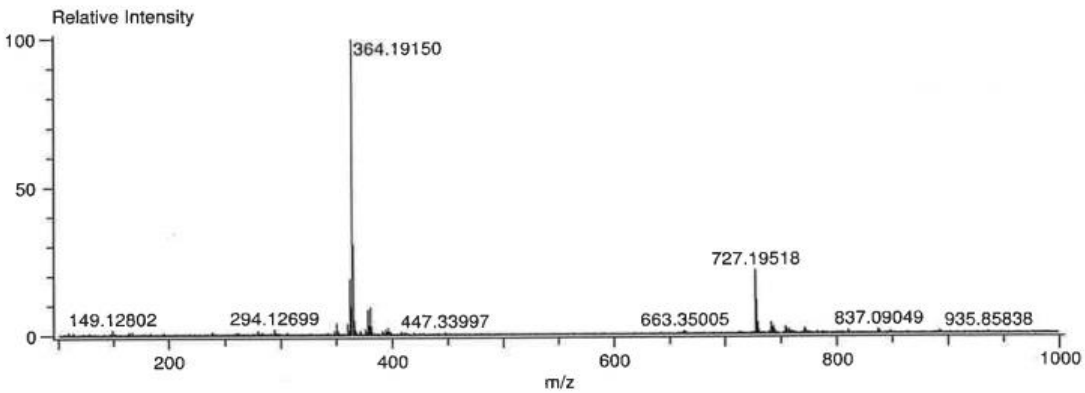

FT-IR spectrum of antofine (4)

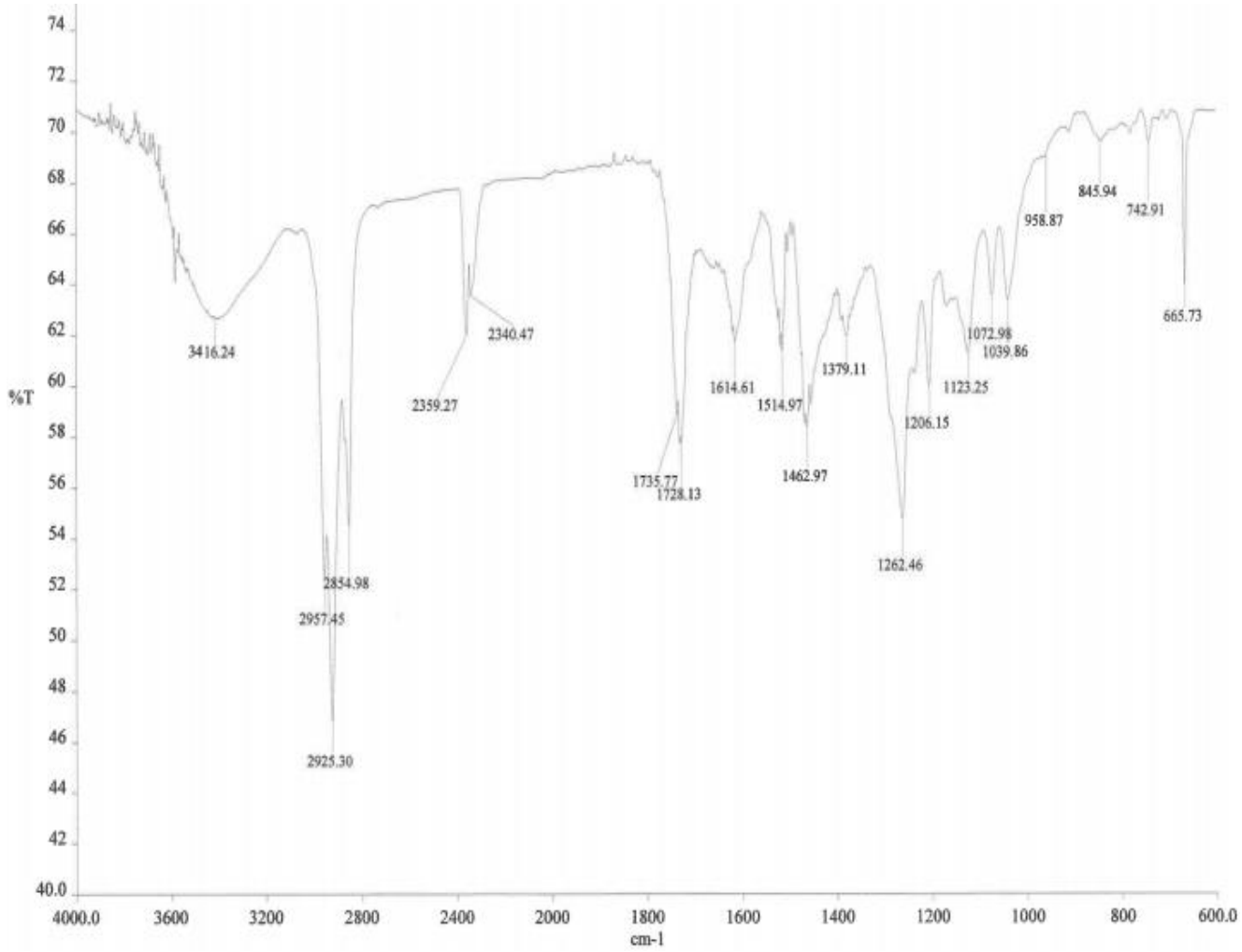

APPENDIX E

NMR spectra of *seco*antofine (5)

^{1}H NMR

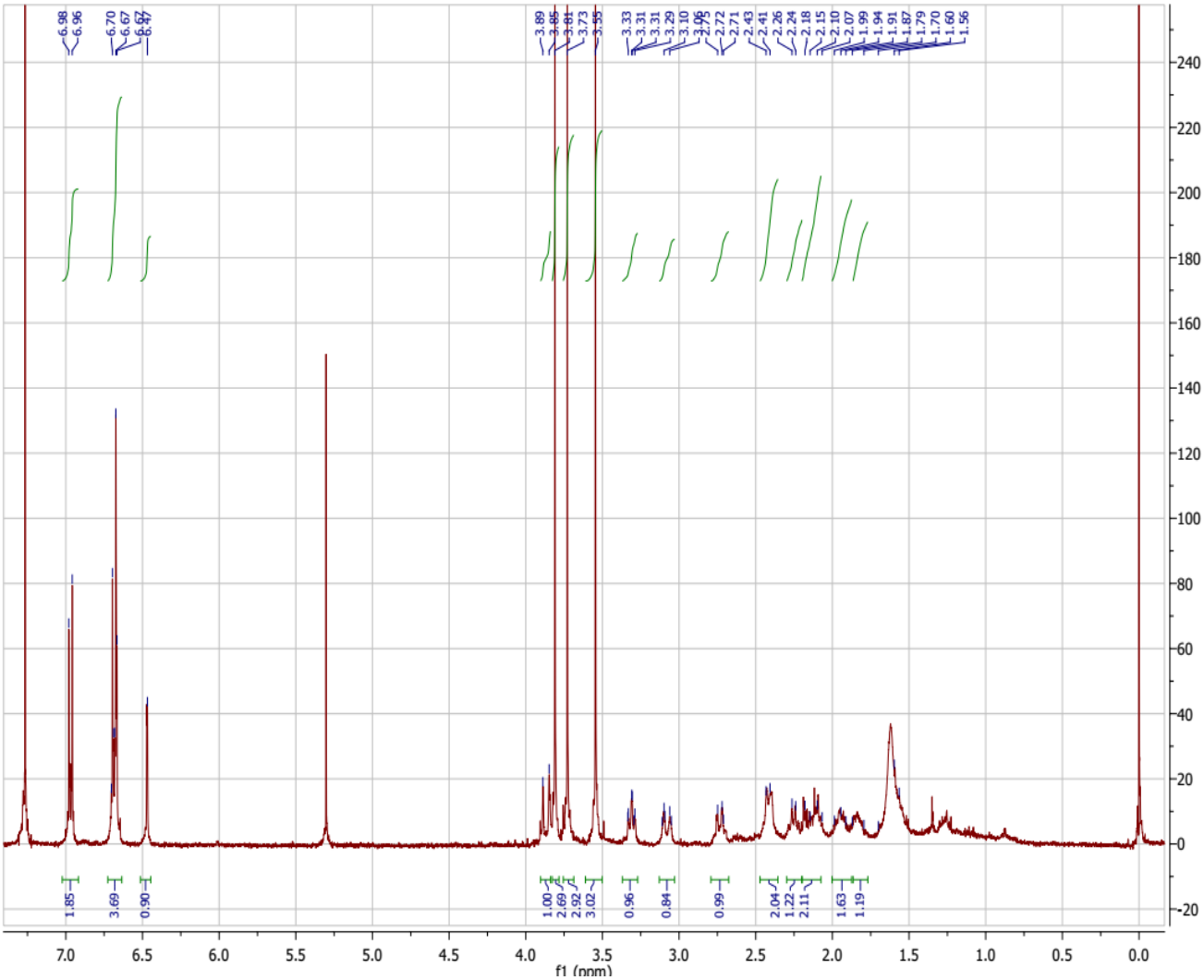

^{13}C NMR

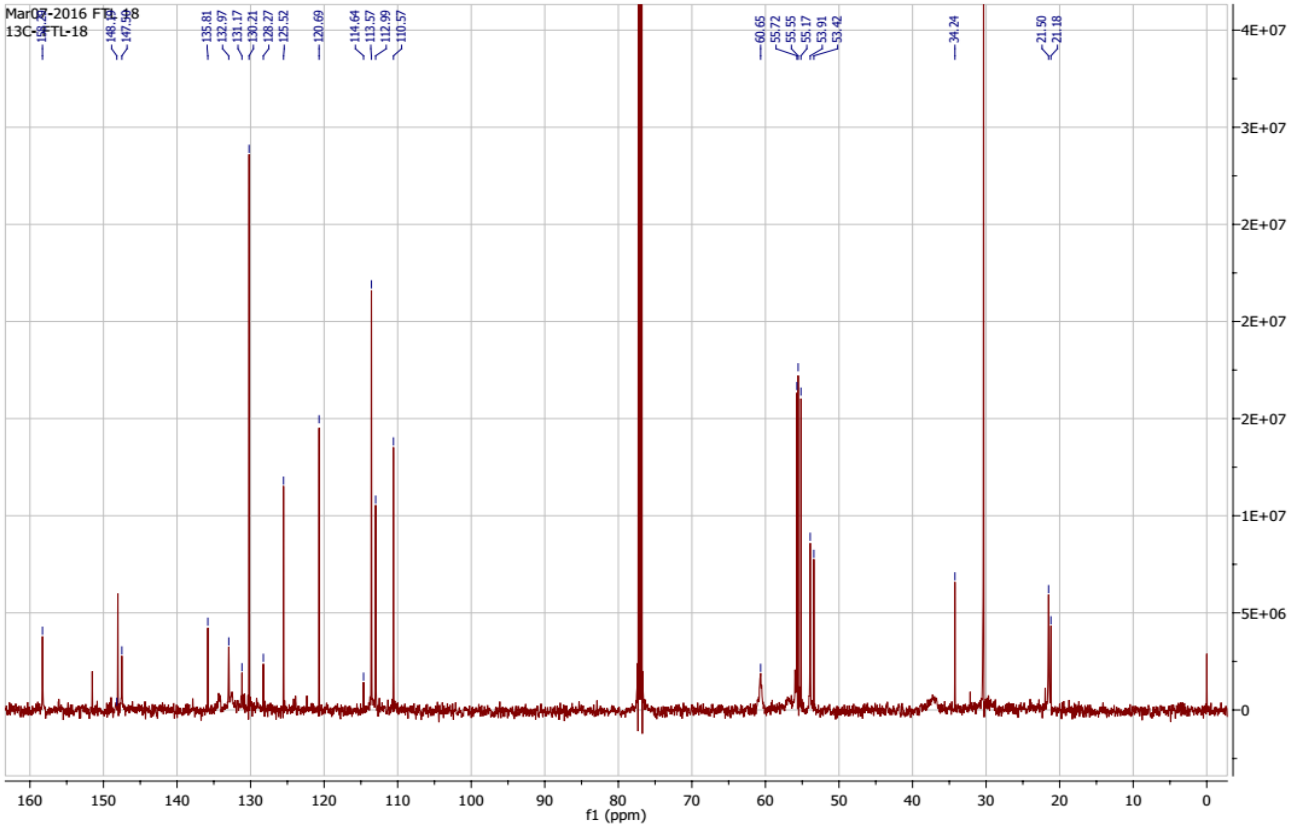
Mar07-2016 FTL-18
13C-FTL-18
135.81
132.97
131.17
130.21
128.27
125.52
120.69
114.64
113.57
112.99
110.57
60.65
55.72
55.55
55.17
53.91
53.42
34.24
21.50
21.18
4E+07
3E+07
2E+07
2E+07
2E+07
1E+07
5E+06
0
160 150 140 130 120 110 100 90 80 70 60 50 40 30 20 10 0
f1 (ppm)

COSY

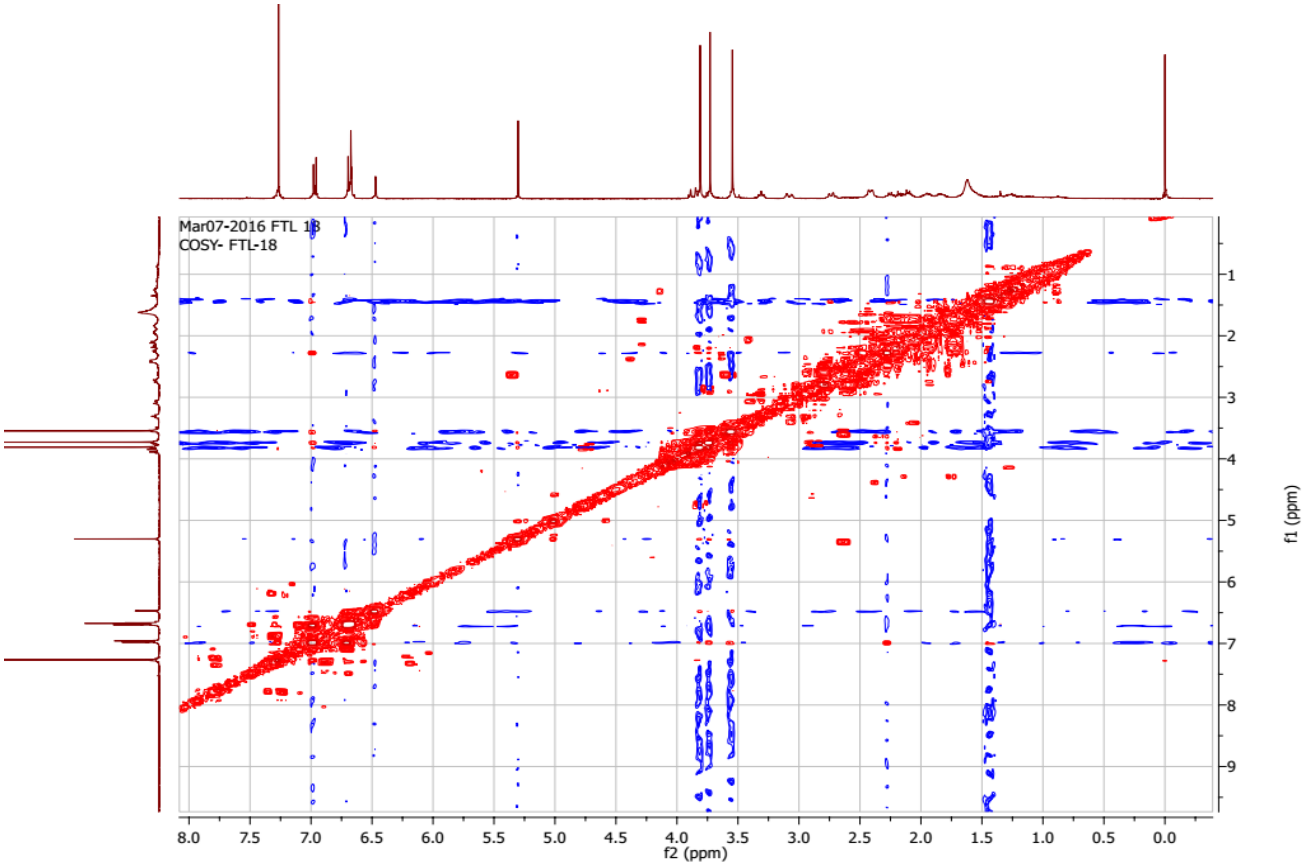
Mar07-2016 FTL 18
COSY- FTL-18
1 2 3 4 5 6 7 8 9
f1 (ppm)
8.0 7.5 7.0 6.5 6.0 5.5 5.0 4.5 4.0 3.5 3.0 2.5 2.0 1.5 1.0 0.5 0.0
f2 (ppm)

HSQC

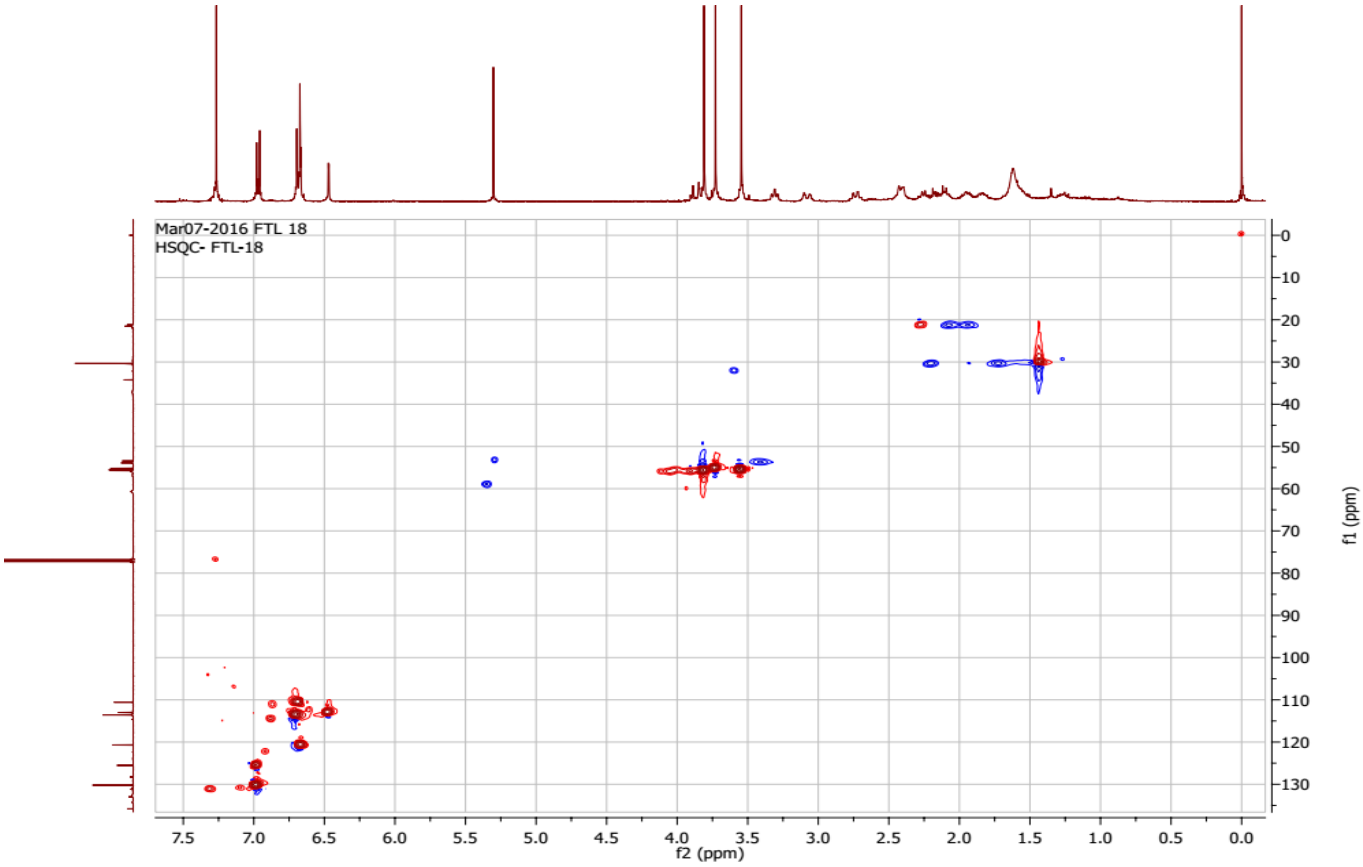
Mar07-2016 FTL 18
HSQC- FTL-18
f2 (ppm)
f1 (ppm)

HMBC

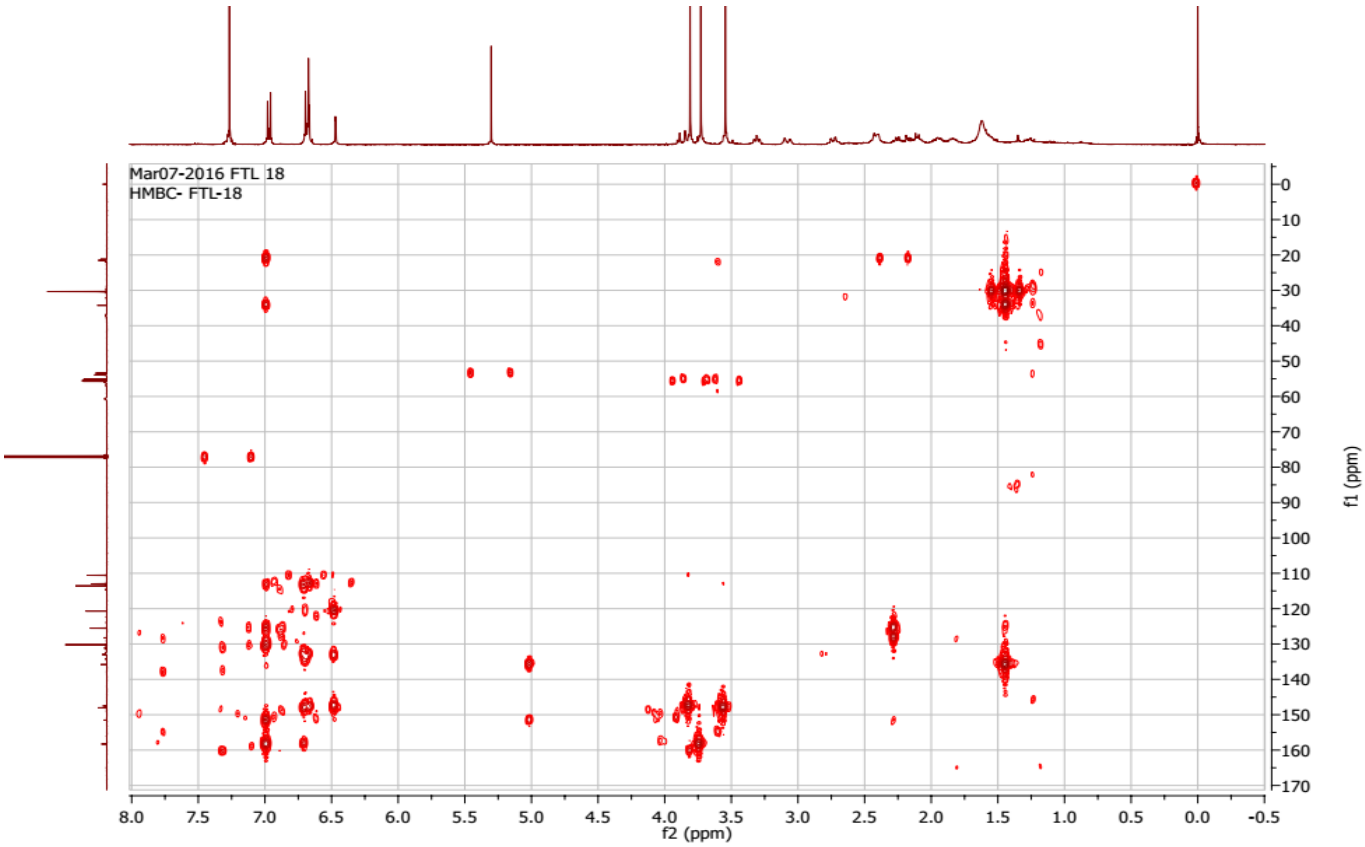
Mar07-2016 FTL 18
HMBC- FTL-18
f2 (ppm)
f1 (ppm)

NOESY

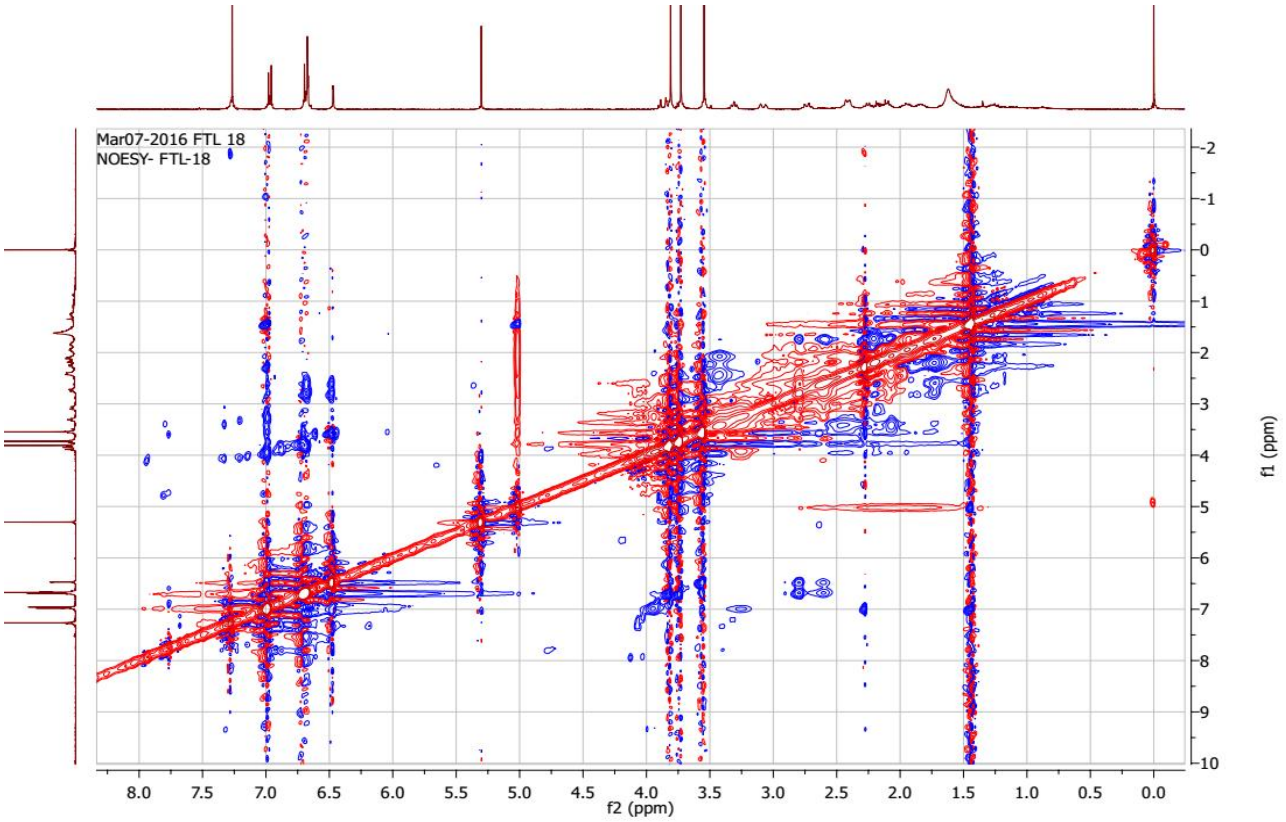

HRESMIS of *seco*antofine (5)

Data:FTL18_291116
Sample Name:
Description:
Ionization Mode:ESI+
History:Determine m/z[Peak Detect[Centroid,30,Area];Correct Base[0.5%]];Correct Ba...

Acquired:11/29/2016 11:24:21 AM
Operator:AccuTOF
Mass Calibration data:Int Calib 291116
Created:11/29/2016 2:49:10 PM
Created by:AccuTOF

Charge number:1 Tolerance:30.00(ppm), 5.00 .. 15.00(mmu) Unsaturation Number:0.0 .. 25.0 (Fractio...
Element:^{12}C:0 .. 30, ^{1}H:0 .. 30, ^{14}N:0 .. 3, ^{16}O:0 .. 5

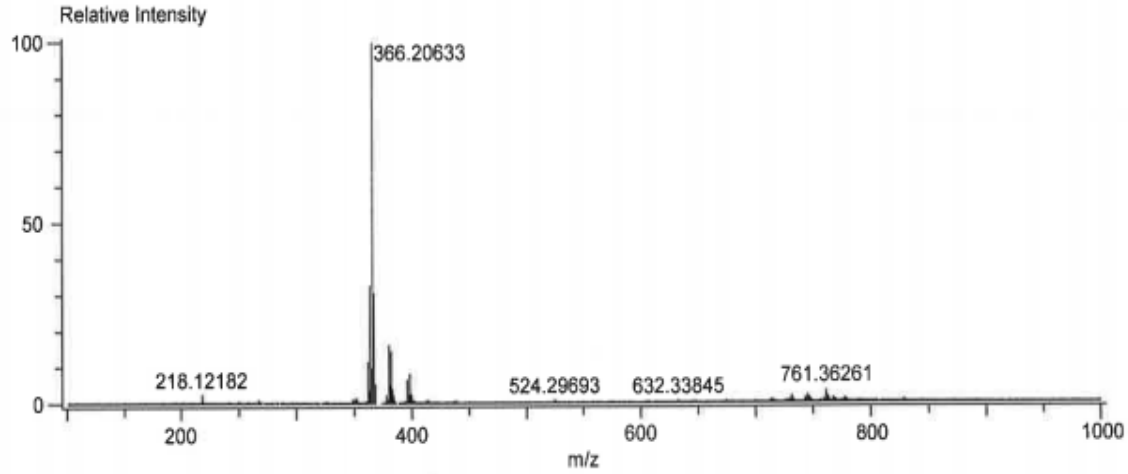

FT-IR spectrum of *seco*antofine (5)